The stability and transitions of coherent structures on excitable and oscillatory media.

A THESIS
SUBMITTED TO THE FACULTY OF THE GRADUATE SCHOOL
OF THE UNIVERSITY OF MINNESOTA
BY

Jeremy Charles Bellay

IN PARTIAL FULFILLMENT OF THE REQUIREMENTS
FOR THE DEGREE OF
Doctor Of Philosophy

February, 2009

The stability and transitions of coherent structures on excitable and oscillatory media.

by Jeremy Charles Bellay

ABSTRACT

We investigate reaction-diffusion systems near parameter values that mark the transition from an excitable to an oscillatory medium. We analyze existence and stability of traveling waves near a steep pulse that arises as the limit of excitation pulses as parameters cross into the oscillatory regime. Traveling waves near this limiting profile are obtained by studying a codimension-two homoclinic saddle-node/orbit-flip bifurcation as considered in [1]. The main result shows that there are precisely two generic scenarios for such a transition, distinguished by the sign of an interaction coefficient between pulses. Among others, we find stable fast fronts and unstable slow fronts in all scenarios, stable excitation pulses, trigger and phase waves. Trigger *and* phase waves are stable for repulsive interaction and unstable for attractive interaction. Finally, we study this transition numerically in the modified FitzHugh-Nagumo equations studied by Or-Guil et. al. [2].

Acknowledgements

I would like to extend my thanks and appreciation to Arnd Scheel, whose help and patience were truly essential for completion of this thesis.

Dedication

To my parents, Brooke and all those who have shared with me secrets of the world.

Contents

List of Figures

Chapter 1

Introduction

1.1 Background

Chemical and biological systems far from equilibrium are often characterized as oscillatory or excitable. While there are a number of ways the terms "excitable" and "oscillatory" are used and defined in the literature, we will use the following intuitive description. By an excitable medium we refer to a system in which the kinetics show threshold behavior with respect to sufficient perturbation: small perturbations decay to a resting equilibrium while larger perturbations grow and then slowly "recover" to the equilibria. In contrast, the kinetics of an oscillatory medium support asymptotically stable limit cycles. Intuitively, the smallest units of an excitable system are quiescent until perturbed while units in oscillatory media oscillate at some native frequency.

The simplest scalar model of such phenomena describes nonlinear phase dynamics only,

$$\theta' = f(\theta), \qquad f(\theta) = f(\theta + 2\pi), \tag{1.1}$$

where we think of $\theta \in S^1 = \mathbb{R}/2\pi\mathbb{Z}$. If $f > 0$ everywhere, the system is oscillatory. If f possesses two nondegenerate zeros, the system is excitable and the distance between the two equilibria on S^1 can be taken as one possible measure for the degree of excitability. A simple specific example is $f(\theta) = \cos\theta + \mu$, so that the system is oscillatory for $|\mu| > 1$; see Figure 1.2.

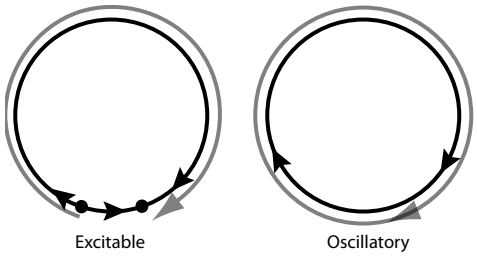

Figure 1.1: Here we have examples of excitable and oscillatory kinetics. In the excitable case, if we perturb away from the stable equilibrium past unstable equilibrium the solution travels around the loop before slowly approaching the rest state again. The oscillatory case has no equilibria and simply oscillates at some native frequency without outside perturbation.

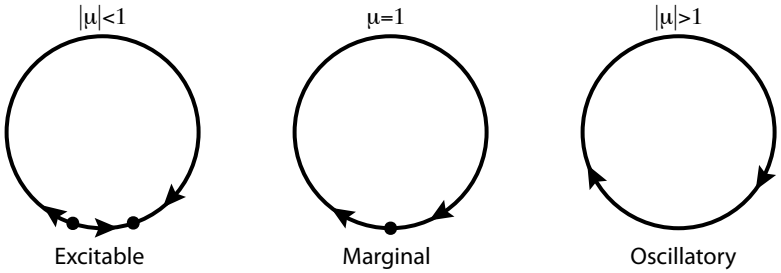

Figure 1.2: The transition between excitable and oscillatory kinetics can be simply modeled by a saddle-node homoclinic bifurcation.

A more complicated model results from activator-inhibitor dynamics, such as those of the FitzHugh-Nagumo equations:

$$u_t = f(u) - v \qquad v_t = \varepsilon(u - v + \rho). \tag{1.2}$$

Here, f has bistable characteristics, e.g. $f(u) = u(1-u)(u-a)$, and ε is typically small. For $\rho = 0$, the system is excitable; that is, perturbing from the equilibrium $u = v = 0$ results in a loop excursion that returns to the equilibrium. For $\rho = -1/2$ and $a = 1/2$, we find the van der Pol oscillator with a stable limit cycle, so the system is oscillatory; see Figure 1.3.

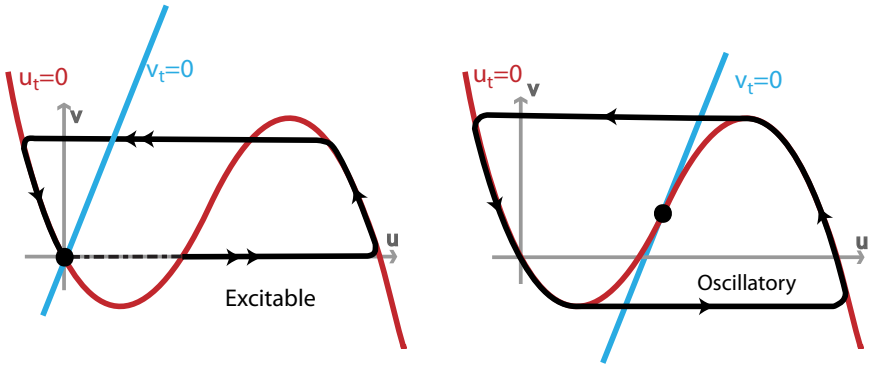

Figure 1.3: Excitable and oscillatory dynamics in activator-inhibitor kinetics.

In the first example (1.1), the dynamics are simple to describe for all nonlinearities f, and the transition from excitable to oscillatory happens as equilibria emerge on a limit cycle through a saddle-node bifurcation. At the boundary of oscillatory behavior, we find a homoclinic orbit to a saddle-node equilibrium, a typical codimension one phenomenon. In the second example (1.2), the transition from oscillatory to excitable behavior can be notably more complicated, possibly involving canards; see for example [3].

In spatially extended systems, both oscillatory and excitable kinetics can give rise to interesting patterns. Most notably, oscillatory media support *phase waves* $u(kx-\omega t;k)$, $u(\xi)=u(\xi+2\pi)$, which may nucleate at inhomogeneities or boundaries; see for instance [4]. Wave numbers vary in an admissible band, where the frequency is a function of the wave number, called the dispersion relation $\omega=\omega(k)$ [5, 6]. The limit $k=0$ corresponds to the spatially homogeneous oscillation. Excitable media support excitation pulses, which are emitted by wave sources such as spiral waves in two-dimensional media. Chains of excitation pulses are typically referred to as *trigger waves* and can be similarly described by a nonlinear dispersion relation $\omega=\omega(k)$, where now $k=0$ corresponds to the single excitation pulse. A notable difference between excitable and oscillatory media is the stability of long-wavelength waves. Phase waves are always stable whenever the homogeneous oscillation is PDE stable [7, 8, 6], while trigger waves are typically either stable or unstable, depending on the sign of an interaction force between individual

excitation pulses [9].

It is important to keep in mind that the terms excitable and oscillatory only refer to the local kinetics of the "units" of the media. The large scale behavior of excitable or oscillatory media may vary greatly and may not obviously reflect the underlying kinetics. In the one-dimensional case we will see that both excitable and oscillatory systems support wave trains, a behavior one might naively (and wrongly) associate only with oscillatory media.

In physical examples the line between oscillatory and excitable media is often blurred. For example, in certain regions of the brain neurons tend to only fire after sufficient exterior stimulation (excitable media) [10] [11]. Other neurons regularly and vary frequency in response to exterior perturbation (oscillatory media.) Additionally, there is evidence for systems that transition from oscillatory to excitable and back again! [10] [11] To investigate this transition, one would like to understand what coherent structures are stable in each regime and what happens to these structures as the systems transition from an excitable to oscillatory regime. To this end we consider the saddle-node (SN) bifurcation of a homoclinic orbit as the simplest model of the transition from an excitable to an oscillatory regime.

1.2 Outline

In chapter 2, we begin by examining an analytically tractable scalar example similar to one described by Ermentrout and Rinzel [12]. They previously have showed the existence of bifurcating traveling waves and fronts. We extend their results by first analyzing the bifurcation from the excitable state to the oscillatory state through the saddle-node. This is achieved by analyzing the fibrations of the center manifold under perturbation of the bifurcation parameter. In addition, we consider the PDE stability of the pulses, wavetrains and fronts. In the case of the fronts, we employ exponentially weighted spaces to shift away "transient" instabilities caused by essential spectra (see [13] for a discussion of transient and convective instabilities.) The spectral stability of the pulse (and fronts in appropriately weighted spaces) can be determined by an extension of Sturm-Liouville Theory to the real line. For the stability of the wave trains we rely on the more recent results of Sandstede and Scheel [13].

We then proceed in chapter 3 to consider a generalization of the scalar example. We assume the existence of a "steep pulse" that is the boundary pulse between excitable and oscillatory regimes. We make a number of assumptions regarding the unfolding of the equilibrium, and the spectral stability of the pulse. These assumptions are model independent in the sense that they are concerned with the physical properties of the pulses, rather than specifics assumptions on the kinetics.

In chapter 4 we show that the assumptions made on the steep pulse are enough to utilize the results of Chow, Lin and Deng ([1] [14]) to determine the local bifurcation diagram of the homoclinic that corresponds to the steep pulse in the traveling wave ODE. This result mirrors the proof given in chapter 2, however their approach is more sophisticated and uses a Melnikov type bifurcation function on weighted spaces.

The stability of the structures determined by the bifurcation diagram is considered in chapter 5. We show that there are *only two possible stability diagrams.* Which diagram is choosen depends on the relative orientation of the kernel and adjoint solutions of the linearization about the steep pulse. In both of these diagrams, the faster fronts are stable and the slow fronts are unstable. In addition, these fronts are separated by a "steep front" in validation of the conjectures of Saarloos [15].

Finally, in chapter 6 we consider our results in relation to the modified FitzHugh-Nagumo equations proposed by Or-Guil et. al. [2]. After verifying our assumptions numerically, we find that the dispersion relation is as predicted in both normal and anomalous regimes. We also discuss their interpretation of the transition between normal and anomalous dispersion in relation to the orientation flip described in our results.

Chapter 2

A Scalar Example

2.1 Main results

We begin by considering a scalar equation with explicit kinetics that exhibit a saddle-node bifurcation. This model is a special case of a class of scalar models considered in Ermentrout and Rinzel [12]. Many of our results here have been stated and proved there regarding the existence of the pulses, fronts and wave trains. However, we extend their existence results by considering the bifurcation through the critical case of the saddle-node homoclinic which allows the explicit statement of the bifurcation diagram. In addition, we consider the PDE stability of the various coherent structures, as well as the dispersion curves of various wave trains. This will provide a basic and tangible example for more general results that will be stated later.

To be specific, let us consider the following reaction diffusion system,

$$u_t = u_{xx} - 1 + \cos(u) - \mu, \qquad x \in \mathbb{R},\ u, \mu \in \mathbb{R}. \tag{2.1}$$

Consider this equation with u taking values on the circle. That is, identify u and $u + 2\pi$. However, we will generally look at solutions in the covering space $u \in \mathbb{R}$ and then later project to values on the circle. We emphasize that this projection takes place in the range and is completely independent of a possible choice of periodic boundary conditions in space x.

Spatially homogeneous solutions $u(t, x) \equiv u(t)$ solve the scalar ordinary differential

equation (ODE),

$$u_t = \cos(u) - 1 - \mu. \tag{2.2}$$

One can easily see that it is sufficient to restrict to $\mu \geq -1$ after a change of the sign of u. We are particularly interested in the parameter regime $\mu \sim 0$ where the ODE undergoes a saddle-node bifurcation. A saddle-node bifurcation can be described as follows: two equilibria collide and disappear as μ increases through $\mu = 0$. That is, there are:

- two equilibria $0 < s_0 < n_0 < 2\pi$ for $-1 \leq \mu < 0$;
- one equilibrium $sn_0 = 0$ for $\mu = 0$;
- no equilibria for $\mu > 0$.

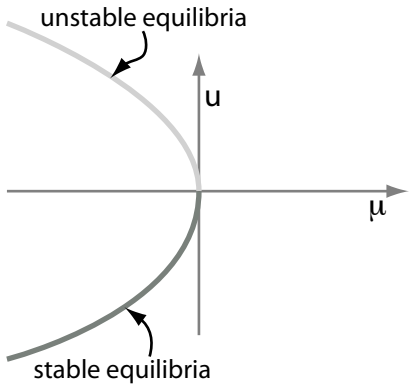

Figure 2.1: The bifurcating equilibria of a saddle-node. There are two equilibria, one stable and one unstable for any $\mu < 0$. There is one equilibrium for $\mu = 0$ and none for $\mu > 0$.

We are concerned with traveling wave solutions $u(x - ct)$ for some $c \geq 0$ as an interesting class of non-homogeneous solutions to the reaction-diffusion equation. Traveling waves are time invariant solutions to (2.1) after rescaling the spatial coordinate as $\xi = x - ct$. This change of coordinates can be thought of as moving along the x axis

at wave speed c and is commonly referred to as a "co-moving" frame. Equation (2.1) becomes:

$$u_t = u_{\xi\xi} + cu_\xi - 1 + \cos(u) - \mu. \tag{2.3}$$

Equilibrium solutions in time solve the following planar ordinary differential equation,

$$\begin{aligned} u' =& v \\ v' =& -cv + 1 - \cos u + \mu. \end{aligned} \tag{2.4}$$

Again, note that (u, v) here takes values on the cylinder $S^1 \times \mathbb{R}$, but we sometimes consider the equation in the covering space $\mathbb{R}^2$.

The traveling-wave equation (2.4) exhibits a saddle-node bifurcation at $\mu = 0$. For definiteness, we label equilibria,

$$S_0 = \begin{pmatrix} s_0 \\ 0 \end{pmatrix} = \begin{pmatrix} \arccos(1+\mu) \\ 0 \end{pmatrix}, \qquad N_0 = \begin{pmatrix} n_0 \\ 0 \end{pmatrix} = \begin{pmatrix} -\arccos(1+\mu) \\ 0 \end{pmatrix}, \tag{2.5}$$

where $0 \leq \arccos(1+\mu) < \pi$ so that $0 \leq s_0 < n_0 < 2\pi$ when $-1 \leq \mu < 0$. We also set

$$SN_0 = \begin{pmatrix} 0 \\ 0 \end{pmatrix},$$

the equilibrium at $\mu = 0$. In the covering space, $u \in \mathbb{R}$, we label the equivalent equilibria with indices k, so that

$$S_k = S_0 + \begin{pmatrix} 2\pi k \\ 0 \end{pmatrix}, \quad N_k = N_0 + \begin{pmatrix} 2\pi k \\ 0 \end{pmatrix}, \quad SN_k = SN_0 + \begin{pmatrix} 2\pi k \\ 0 \end{pmatrix}.$$

The equilibria $S_0 = S_0(\mu)$ and $N_0 = N_0(\mu)$ depend on μ and we suppress the dependence in the notation whenever convenient. Also note that $S_0(0) = N_0(0) = SN_0$ for $\mu = 0$. Finally, we will use the notation $SN_k(\mu)$ to refer to the group of bifurcating equilibria for various values of μ.

Several types of traveling wave phenomena can be observed in this setting. The three major categories are pulses, fronts and wave trains. Pulses are solutions that approach the same equilibrium as the spatial variable ξ goes to $\pm\infty$ (for instance connecting s_0 and s_k), while fronts are solutions that approach different equilibria as ξ goes to $\pm\infty$ (connecting s_0 to n_k). Wave trains are periodic solutions with respect to ξ.

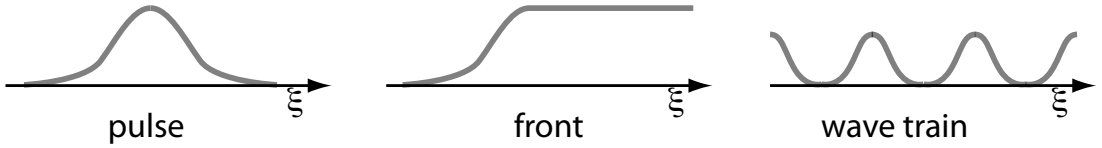

In terms of the planar system (2.4), fronts are heteroclinic solutions, pulses are homoclincs and wave trains are periodic orbits — all after identification of u with $u + 2\pi$. A heteroclinic trajectory in the covering space, connecting S_j to S_k, therefore becomes a pulse. We refer to the the winding number on the cylinder $k - j$ as the *index of the pulse*. Analogously, a heteroclinic from S_j to N_k becomes a front with index $k - j$. Lastly, for a periodic orbit, we can define a minimal period L on the cylinder and we can then define the index of the periodic solution as $(u(L) - u(0))/(2\pi)$.

There are a variety of types of pulse and front solutions possible in this setting.

- The "Steep Pulse" decays exponentially in forward time but only algebraically in backward time.
- "Excitation Pulses" are pulses that decay exponentially to an equilibrium as ξ goes to $\pm\infty$.
- "Steep Fronts" are fronts that decay exponentially to an equilibirum as ξ goes to ∞.
- "Algebraic Pulses" are pulses that decay algebraically to an equilibirum as ξ goes to $\pm\infty$.
- "Slow Fronts" and "Fast Fronts" both decay exponentially to an equilibirum, while "Slow" and "Fast" refer to their relative wave speeds.

Our main results in this scalar case classify all traveling wave solutions and their stability for parameter values $c > 0$ and $-1 < \mu \leq 0$.

Theorem 1 (Existence of fronts and pulses)**.** *There exist a $c_* > 0$ and a smooth curve $\gamma(c)$, defined for $c \sim c_*$, such that $\gamma(c_*) = 0$, $\gamma(c) < 0$ for all $c \neq c_*$, $\gamma'(c)(c - c*) > 0$, and $\gamma''(c_*) < 0$. For $\mu \sim 0$, we have the following pulse- and front solutions:*

- *there exist a steep pulse solution at* $\mu = 0$ *and* $c = c_*$*;*
- *there exist excitation pulse solutions at* $\mu = \gamma(c)$, $c < c_*$*;*
- *there exist an algebraic pulse for* $\mu = 0$, $0 < c \leq c_*$
- *there exist "slow" fronts for* $\mu < \gamma(c)$ *and "fast" fronts for* $\gamma(c) < \mu < 0$, $c > c_*$*;*
- *there exists a steep front solution at* $\mu = \gamma(c)$, $c > c_*$.

All pulses listed are index 1, all fronts listed are index 0. There are no other pulse or front solutions with $c > 0$ *and* $\mu \sim 0$.

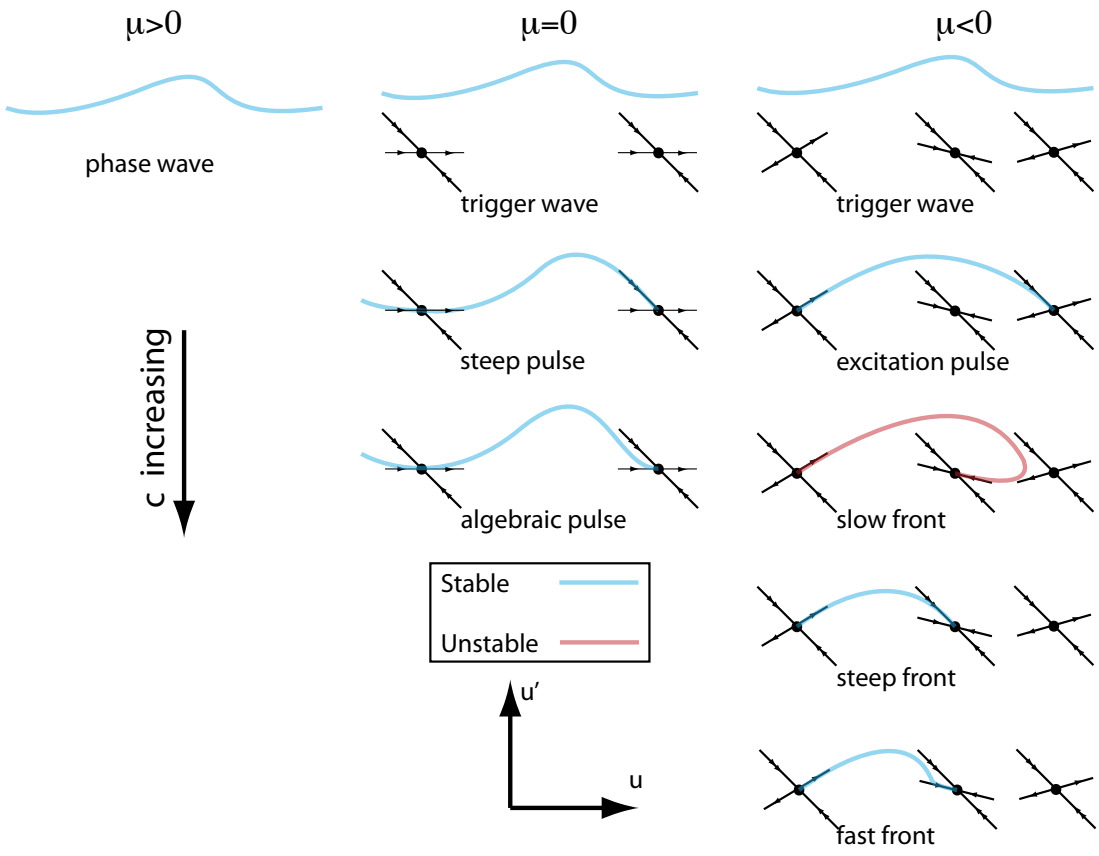

Figure 2.2: The various fronts, pulses and wave trains on the covering space.

The structures we wish to consider are all equilibrium solutions of (2.3). The next natural question for such equilibrium solutions is whether they will actually be observed in simulations or experiments. We therefore investigate their stability by studying perturbations $v(\xi)$ of the equilibrium solution $u_*(\xi)$ and investigating the asymptotics of $u(t,\xi)$ with $u(0,\xi) = u_*(\xi) + v(\xi)$. A natural choice for a function space is $v \in Y = H^1(\mathbb{R})$, but our results remain true for other choices such as $BC^0_{\text{unif}}(\mathbb{R})$.

The stability of the various coherent structures can be most easily studied by considering the spectrum of the linearized operator around these structures. The spectrum depends on the base space on which the operator is defined. We will make explicit use of this property when we consider exponentially weighted spaces that allow for more precise analysis of instabilities due to the presence of essential spectrum.

Definition 2.1 (Spectrum)**.** *Let $\mathcal{L} : X \to X$ be a closed operator where X is a Banach space. Then the resolvent set* ($\text{res}(\mathcal{L})$) *is the set of values in $\lambda \in \mathbb{C}$ such that the operator $\lambda - \mathcal{L}$ has a well defined inverse. The spectrum of $\mathcal{L}$* ($\text{spec}(\mathcal{L})$) *is the compliment of resolvent set* ($\text{spec}(\mathcal{L})^c$).

There are many possible definitions of point and essential spectrum (see for example [16].) We take a conservative definition limiting the point spectrum to finite dimensional eigenvalues.

Definition 2.2 (Point and Essential Spectrum)**.** *The point spectrum of the operator $\mathcal{L}$ is the subset of the spectrum of $\mathcal{L}$ that contains only finite dimensional isolated eigenvalues, denoted as* $\text{spec}_{\text{pt}}(\mathcal{L})$*. The essential spectrum of the operator $\mathcal{L}$, denoted as* spec_{ess}*, is the* $\text{spec}(\mathcal{L})/\text{spec}_{\text{pt}}(\mathcal{L})$.

We now define what we mean by stability.

Definition 2.3 (Asymptotic orbital stability)**.** *We say u_* is asymptotically stable if for all $\varepsilon > 0$ there exists $\delta > 0$ such that for all v with $|v|_Y < \delta$, we have*

$$\inf_{\xi_0 \in \mathbb{R}} |u(t,\xi) - u_*(\xi+\xi_0)|_Y < \varepsilon, \text{ for all } t > 0, \quad \text{and} \quad \inf_{\xi_0 \in \mathbb{R}} |u(t,\xi) - u_*(\xi+\xi_0)|_Y \to 0 \text{ for } t \to \infty.$$

A weaker notion of stability is spectral stability. Consider the linearized equation

$$u_t = u_{\xi\xi} + c u_\xi - \sin(u_*(\xi))u =: \mathcal{L}u,$$

with closed operator $\mathcal{L}$ defined on $L^2(\mathbb{R})$ with domain $\mathcal{D}(\mathcal{L}) = H^2(\mathbb{R})$.

Definition 2.4 (Spectral stability)**.** *We say u_* is spectrally stable if the spectrum of $\mathcal{L}$ is contained in the closed left half plane,*

$$\operatorname{spec}\mathcal{L} \subset \{\operatorname{Re}\lambda \leq 0\}.$$

In fact, in most of our cases we will have even stronger notions of stability, so that perturbations v converge to zero exponentially when measured against an appropriately shifted $u_*(\cdot + \xi_0)$, with ξ_0 fixed. Actually, this type of stability is implied by spectral stability if $\operatorname{spec}\mathcal{L} \cap \{\operatorname{Re}\lambda \leq 0\} = \{0\}$, an algebraically simple, isolated eigenvalue [17].

Fronts are never stable in the above sense since they connect a stable and an unstable equilibrium. We therefore characterize stability for fronts as stability in an appropriate exponentially weighted function space. Define the weighted function spaces L^2_η and H^1_η for $\eta = (\eta_-, \eta_+)$ via the norms

$$|u|^2_{L^2_{\eta_-,\eta_+}} := \int_{-\infty}^{0} |\mathrm{e}^{\eta_-\xi}u(\xi)|^2\mathrm{d} + \int_0^\infty |\mathrm{e}^{\eta_+\xi}u(\xi)|^2\mathrm{d}\xi, \quad |u|^2_{H^1_{\eta_-,\eta_+}} := |u|^2_{L^2_{\eta_-,\eta_+}} + |u'|^2_{L^2_{\eta_-,\eta_+}}.$$

Definition 2.5 (Weighted stability)**.** *We say that a front is orbitally weighted stable if there exists weights η_-, η_+ such that it is orbitally asymptotically stable in H^1_η. We say it is spectrally weighted stable if there exist weights η_-, η_+ such that it is spectrally stable in $L^2_{\eta-,\eta_+}$.*

Remark 1.1 (L^2_η)**.** *We will use the following shorthand:*

$$\begin{aligned} L^2_\eta =& L^2_{\eta,\eta}; \\ L^2_{-\eta} =& L^2_{-\eta,-\eta}. \end{aligned}$$

We characterize instability for each of these classes as the complementary statement. For instance, a wave is weighted spectrally unstable if it is not spectrally stable in *any* weight of the above form.

Theorem 2 (Stability of fronts and pulses)**.** *We have the following stability information:*

- *the excitation pulses are AOS;*
- *the algebraic pulse is weighted AOS stable;*
- *the slow fronts are unstable; the fast fronts are weighted AOS stable;*

- *the steep fronts are weighted AOS stable.*

Remark 1.2. *We will actually have much more information on the stability. For instance, the position of steep fronts will typically shift after perturbation while the position of fast fronts remains unchanged. Of course, all fronts are unstable in translation-invariant norms since one of the asymptotic states n_0 is unstable.*

Theorem 3 (Existence and stability of wave trains)**.** *Suppose that $\mu \sim 0$. For each μ, c such that $\mu > 0$ or $\mu > \gamma(c)$ and $0 < c < c_*$, there exists a unique index-1 periodic with minimal period $L > 0$. There do not exist other periodic orbits with non-zero index. For each fixed μ, the dispersion relation the wave trains can be parameterized by wavenumber $k = 2\pi/L \in \mathbb{R}_+$, and their frequency $\omega = ck$ is smooth and satisfies $\omega' > 0$. Moreover, we have the asymptotics*

$$\begin{aligned}
\omega(k) &= 1 - \mu + \mathrm{O}(k^{-1}), \quad k \to \infty \\
\omega(k) &= c_{\mathrm{pulse}}(\mu)k + \mathrm{O}(k^2), \quad \mu \leq 0,\, k \to 0 \\
\omega(k) &= \omega_* k + \mathrm{O}(k^4), \quad \mu > 0,\, k \to 0,
\end{aligned}$$

where ω_* is the frequency of the periodic solution to the kinetics (2.2).

All wave trains are asymptotically orbitally stable with respect to spatially periodic perturbations and spectrally stable as a solution on the real line.

Remark 1.3. *There exists a family of periodic orbits with index 0 for $c = 0$ and $-1 \leq \mu \leq 1$. All those wave trains are (weighted) spectrally unstable as solutions to the PDE. Existence can be readily concluded from the Hamiltonian structure and a phase plane picture, the instability is a consequence of Sturm-Liouville properties of the linearization that we will discuss in the proof of Theorem 3.*

Remark 1.4. *For μ finite, $0 \geq \mu \geq -1$, the picture can be continued: pulses exist for all μ and their speed decreases to $c = 0$ at $\mu = -1$. Steep fronts exist for all $\mu \geq \mu_{\mathrm{pp}}$, where the steep fronts disappear and the slowest stable front is determined by the linear stability analysis at the PDE unstable equilibrium. The schematic bifurcation diagram is summarized in the figure below. Since most of the analysis for μ finite is similar to the Nagumo case, where the transision μ_{pp} is explicitly known, we chose to not include a detailed analysis, here.*

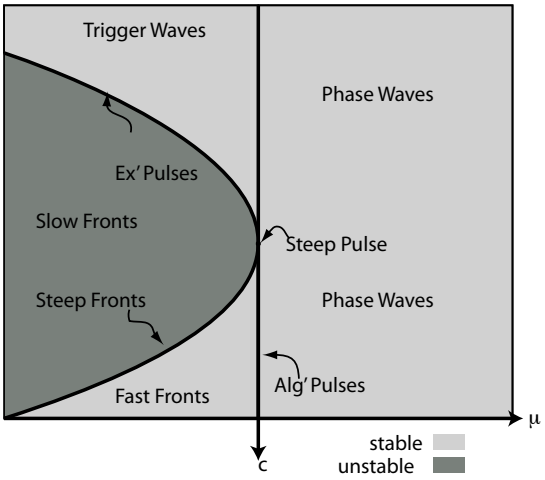

Figure 2.3: The bifurcation diagram and the stability of the various fronts pulses and wave-trains.

2.2 Existence of fronts and pulses

2.2.1 Local analysis

Linearization and invariant manifolds at equilibria We first consider the linearization around the equilibria S, N and SN. The eigenvalues and eigenvectors are summarized in the following tables.

Equilibrium	Larger e.v.	Smaller e.v.	Eq. Type
S	$\sigma_+ = \frac{-c+\sqrt{c+\sqrt{-\mu}}}{2}$	$\sigma_- = \frac{-c-\sqrt{c+\sqrt{-\mu}}}{2}$	Saddle
N	$\nu_+ = \frac{-c+\sqrt{c-\sqrt{-\mu}}}{2}$	$\nu_- = \frac{-c-\sqrt{c-\sqrt{-\mu}}}{2}$	Node
SN	0	$-c$	Saddle-Node

For $c > 0$ and $\mu \in [-1, 0)$ the equilibrium S has eigenvalues $\sigma_- < 0 < \sigma_+$ while for N both eigenvalues are negative and $\mathrm{Re}(\nu_-) < \mathrm{Re}(\nu_+) < 0$. For $c > \sqrt{-\mu}$, the eigenvalues ν_- and ν_+ are real, but for $c < \sqrt{-\mu}$ they are both imaginary. We will only be concerned with the case $c > \sqrt{-\mu}$. (The bifurcations away from $\mu = 0$ and $c = c_*$ are interesting, however, they are beyond the scope of the current paper.) The equilibria have the following eigenvectors with respect to the eigenvalues found above.

S	$\begin{pmatrix} 1 \\ \sigma_+ \end{pmatrix}$	$\begin{pmatrix} 1 \\ \sigma_- \end{pmatrix}$
N	$\begin{pmatrix} 1 \\ \nu_+ \end{pmatrix}$	$\begin{pmatrix} 1 \\ \nu_- \end{pmatrix}$
SN	$\begin{pmatrix} 1 \\ 0 \end{pmatrix}$	$\begin{pmatrix} 1 \\ -c \end{pmatrix}$

We now apply invariant manifold theory to find manifolds that are tangent to the eigenvectors and whose local dynamics are determined by the eigenvalue. In the cases of S and N we may distinguish the strong stable manifolds as the 1-d invariant manifolds that are tangent to the eigenvector corresponding to the eigenvalues σ_- and ν_-. Recall that while the stable and unstable manifolds are uniquely defined, this is not necessarily true of center manifolds. Additionally, in general center manifolds can only be defined locally. The following is a table of terminology we will use throughout to describe useful invariant manifolds. We will supress the dependence on the paramters when appropriate.

$W^{ss}(x_0;\mu,c)$	The strong stable manifold of a given equilibria x_0 depending on μ and c. equilibria x_0
$W^{cs}(x_0;\mu,c)$	The local center stable manifold of a given equilibria x_0 depending on c and μ
$W^{cu}(x_0;\mu,c)$	The local center unstable manifold of a given equilibria x_0 depending on c and μ
$W^{s}(x_0;\mu,c)$	The stable manifold of a given equilibria x_0 depending on c and μ
$W^{u}(x_0;\mu,c)$	The unstable manifold of a given equilibria x_0 depending on c and μ

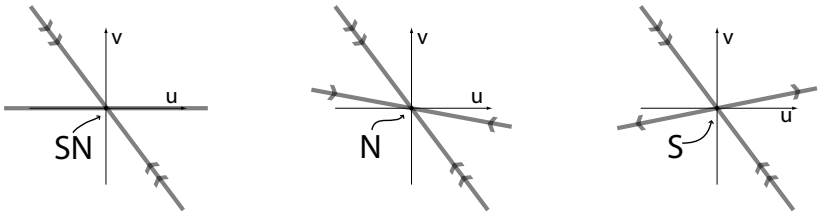

Figure 2.4: The positions of the eigenspaces with respect to the various equilibria.

Center manifold expansions at $\mu \sim 0$ We now analyze the behavior of the center manifold near $SN_0(\mu)$. It is clear from the linearization at SN that for $\mu = 0$ the equilibrium has a center eigenspace. However, we would like to understand how the center manifold behaves as we perturb μ away from zero. Therefore, we consider the parameter dependent center manifold for the following extended system:

$$\begin{aligned} u' &= v \\ v' &= -cv + 1 - \cos u + \mu \\ \mu' &= 0. \end{aligned} \tag{2.6}$$

The local center and stable manifolds are well defined for this system as can be seen in the review paper of Vanderbauwhede [18].

Lemma 2.5 (Center Manifold Dynamics)**.** *At $(u, v, \mu) = (0, 0, 0)$, the system (2.6) has a parameter dependent center manifold $W^c(\mu)$ which is tangent to the vector $(1, 0, 0)^T$ for $\mu = 0$. Locally, the graph of $W^c(\mu)$ is given by $\left(u, \frac{\mu}{c} + \frac{u^2}{2c} + O(x^3)\right)$ with the dynamics $u' = \frac{\mu}{c} + \frac{u^2}{2c} + O(x^3)$, $\mu' = 0$.*

Proof. By applying the center manifold theorem (see [18] for complete proofs and historical references) there exists a manifold tangent to the center eigenspace. Moreover, there is a function $h(u, \mu)$ so that the center manifold can be represented as the graph $\{u, h(u, \mu)\}$. In the following we will determine the beginning of a Taylor expansion for the center manifold. For a given value of μ the function $h(u, \mu)$ can be expressed as the following:

$$h(u, \mu) = a\mu + bu^2 + O(|\mu u| + |u|^2 + |\mu|^2). \tag{2.7}$$

Plugging this in for v in (2.6) we have:

$$v' = 2bu(a\mu + bu^2) = \frac{u^2}{2} + \mu - ca\mu - cbu^2 + \text{HOT} \tag{2.8}$$

Now solving both sides for the $O(\mu)$ and $O(u^2)$ terms we find have the following:

$$a = \frac{1}{c} \qquad\qquad b = \frac{1}{2c}. \tag{2.9}$$

Thus, for $|\mu| << 1$ we can express the center manifold as the graph in (u, v) coordinates:

$$\left(u, \frac{\mu}{c} + \frac{u^2}{2c} + \text{HOT}\right). \tag{2.10}$$

The dyanmics on a center manifold can be described by the system:

$$\begin{aligned} u' &= \frac{\mu}{c} + \frac{u^2}{2c} \\ \mu' &= 0. \end{aligned} \tag{2.11}$$

■

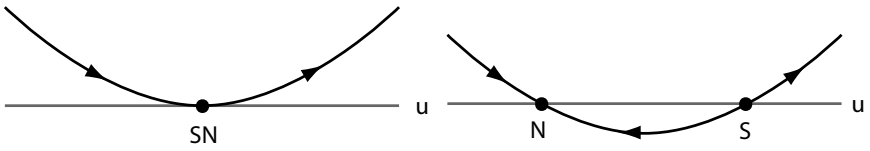

Figure 2.5: The left hand figure shows the local center manifold for $\mu = 0$, while the right hand figure shows it for small μ less than zero.

Fibrations In order to study the bifurcation of the heteroclinics with the change of the parameter μ, we consider the extended system (2.6). Using the center manifold expansion devised in (2.11), locally, we may rewrite (2.6)as the following:

$$u' = \frac{\mu}{c} + \frac{u^2}{c} \tag{2.12}$$

$$v' = -cv + O(|u|^2 + |v|^2). \tag{2.13}$$

The center manifold $W^c(SN_0(\mu))$ is attracting since the only spectrum outside a neighborhood of zero is negative. In fact each point y_0 contained in a local center manifold has a fibration. This means that for any point x_0 in the center stable manifold W^{cs} there is a point y_0 in W^c so that x_0 contracts exponentially towards y_0 as $t \to \infty$. That is, there is is a C^k function:

$$\phi(x) : W^{cs} \to W^c(\mu))$$

such that for any point $x_0 \in W^{cs}$ and some $\eta > 0$ so that:

$$e^{\eta t}|T(t,\mu)x_0 - T(t,\mu)\phi(x_0)| < \infty \qquad t > 0$$

Here $T(t,x)$ is the flow generated by (2.4.)

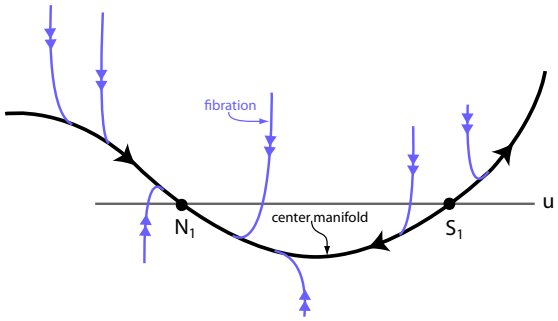

Figure 2.6: Fibrations on the center manifold.

The fibrations of the center manifold allow us to describe all solutions in a neighborhood of the equilibria $SN(\mu)$. For a given time, $t = t_0$, assume that the solutions $\mathbf{u}(t)$ is within a small neighborhood of $SN(\mu)$. Then $\mathbf{u}(t_0)$ can be associated with it's fibration point on the center manifold $\mathbf{y}(t_0)$ and $\mathbf{u}(t)$ exponentially approaches $\mathbf{y}(t)$ as $t \to \infty$. Therefore, we can roughly determine the evolution of such solutions by their positions with respect to the strong stable manifolds W_N^{ss} and W_S^{ss}. We call the region to the left of W_N^{ss} as I, the region between W_N^{ss} and W_S^{ss} as II and the region to the left of W_S^{ss} as III. Solutions in region I and II will tend to N_1, while solutions in region III will grow with the unstable center manifold.

2.2.2 Global analysis

Monotonicity in c We now analyze the properties of the direction field between the equilibria $SN_0(\mu)$ and $SN_1(\mu)$ in the covering space. The following lemma tells us about the monotonicity of various manifolds with respect to the parameter c.

Lemma 2.6. *We have the follow assertions regarding system* (2.4) *for* $\mu = 0$.

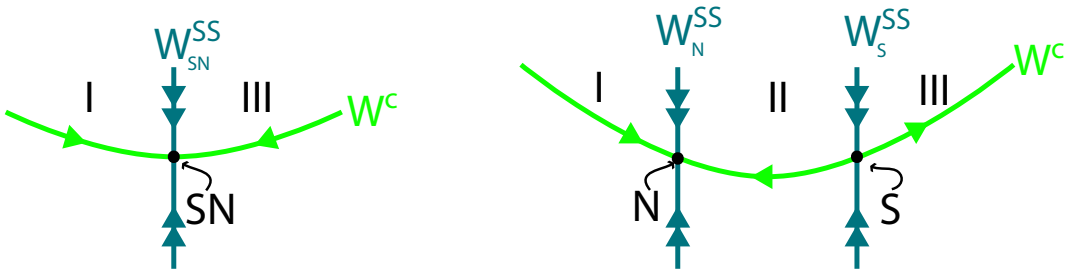

Figure 2.7: The three regions defined by the strong stable manifolds. The figure to the left is the $\mu = 0$ case while the right hand figure is for $\mu < 0$.

1. *Let* $W^{cu}_{SN_0}(c_1)$ *and* $W^{cu}_{SN_0}(c_2)$ *be the center unstable manifolds for two values of* c *where* $c_1 > c_2$. *Let* $(u, v_1) \in W^c_{A_0}(c_1)$ *and* $(u, v_2) \in W^u_{A_0}(c_2)$. *Then* $v_2 > v_1$ *for* $v \geq 0$ *and* $u \in (0, 2\pi)$.

2. *Let* $W^{ss}_{SN_1}(c_1)$ *and* $W^{ss}_{SN_1}(c_2)$ *be the strong stable manifolds for two values of* c *where* $c_1 > c_2$. *Let* $(u, v_1) \in W^{ss}_{A_1}(c_1)$ *and* $(u, v_2) \in W^{ss}_{A_2}(c_2)$. *Then* $v_1 > v_2$ *for* $v \geq 0$ *and* $u \in (0, 2\pi)$.

Proof. If we consider the graph of the center manifold near SN_0 we can see that the v component decreases as c increases. Thus for $0 < u << 1$ we have that $v_2 > v_1$. Now assume that at some value of $u_0 \in (0, 2\pi)$, $W^c_{SN_0}(c_1)$ intersects $W^c_{SN_0}(c_2)$. The slope of the tangent field at (u_0, v_0) can be expressed as follows:

$$m_c(u_0, v_0) = \frac{v'}{u'} = \frac{-cv + 1 - \cos u}{v}. \tag{2.14}$$

It is clear that $m_{c_1}(u_0, v_0) < m_{c_2}(u_0, v_0)$ and therefore $W^c_{SN_0}(c_1)$ cannot cross $W^c_{SN_0}(c_2)$ at (u_0, v_0). This shows 1. of the above assertions.

To show 2. we look at the eigenvectors computed above. The strong stable manifold $W^{ss}_{SN_1}$ is tangent to $(1, -c)^T$ as it enters SN_0. Since the slope of the eigenvector decreases as c increases $W^{ss}_{SN_1(c_2)}$ will be above $W^{ss}_{SN_1(c_1)}$ in the v direction close to SN_1. Appealing again to the slope of the direction field shows that this holds for the interval (SN_0, SN_1).

■

Behavior for large and small values of c. Continuing with the standard form of a shooting argument we now consider the behavior of $W^c_{SN_0}$ for large and small values of c in the following two lemmas. For $c = 0$, the system (2.4) becomes Hamiltonian so solutions can be found explicitly. However, the case $c \gg 1$ requires more serious machinery.

Lemma 2.7. *For $c = 0$ the manifold $W^c_{SN_0}$ is increasing as a graph over u and intersects the line $u = SN_1$ at $v = (2\pi, \sqrt{\pi})$.*

Proof. For $c = 0$ system (2.4) is Hamiltonian and hence integrable. This allows us to find the center manifold explicitly as a graph of v over u.

$$\begin{pmatrix} u \\ v \end{pmatrix}' = \begin{pmatrix} v \\ 1 - \cos(u) \end{pmatrix} \tag{2.15}$$

This system has the Hamiltonian:

$$E(u, v) = \frac{v^2}{2} - u + \sin(u) \tag{2.16}$$

At SN_0 we have $E(0, 0) = 0$ and we can find v as a function of u.

$$v(u) = \sqrt{2(u - sin(u))} \tag{2.17}$$

We plainly see that $W^c_{SN_0}$ intersects the line $u = 2\pi$ at the point $(2\pi, 2\sqrt{\pi})$. ∎

Lemma 2.8. *For $c \gg 1$ the point SN_1 is in the closure of the center manifold, $\overline{W^c_{SN_0}}$.*

Proof. In this proof we resort to the Geometric Singular Perturbation Theory (GSP) of Fenichel [19]. A useful review article can be found in Jones 1995 [20]. We begin by recalling the system (2.4.) Setting $c = \frac{1}{\epsilon}$, (2.4) can be rewritten as the following.

$$\begin{pmatrix} u \\ \epsilon v \end{pmatrix}' = \begin{pmatrix} v \\ -v + \epsilon(1 - \cos(u) + \mu) \end{pmatrix} \tag{2.18}$$

If we let $\epsilon = 0$ we obtain:

$$\begin{pmatrix} u \\ 0 \end{pmatrix}' = \begin{pmatrix} v \\ -v \end{pmatrix} \tag{2.19}$$

This is the "slow time" equation and $v = 0$ is the slow manifold $\mathbf{M_0}$. We can write down the fast system by re-parameterizing time $\epsilon t = \tau$ and $\frac{d}{dt} = \frac{d}{\epsilon\tau}$;

$$\begin{pmatrix} \dot{u} \\ v \end{pmatrix} = \begin{pmatrix} \epsilon v \\ -v + \epsilon(1 - \cos(u) + \mu) \end{pmatrix}. \tag{2.20}$$

Here letting $\epsilon = 0$ results in the following:

$$\begin{pmatrix} \dot{u} \\ v \end{pmatrix} = \begin{pmatrix} 0 \\ -v \end{pmatrix} \tag{2.21}$$

To apply GSP $\mathcal{M}_0$ needs to be normally hyperbolic. This means that if we linearize around any point in $\mathcal{M}_0$ in the "fast" system (2.20), there is exactly one eigenvalue on the imaginary axis. This is obvious here since the matrix in question is constant:

$$\begin{pmatrix} 0 & 0 \\ 0 & -1 \end{pmatrix}. \tag{2.22}$$

Obviously the eigenvalues are 0 and -1 so $\mathcal{M}_0$ is in fact normally hyperbolic. The slow manifold is simply the u-axis, and by the first theorem of GSP there is a manifold $\mathcal{M}_\epsilon$ diffeomorphic to and within $O(\epsilon)$ of $\mathbf{M_0}$ and is a graph over the "slow" variable. Thus we can write v as an expansion of u on $\mathcal{M}_\epsilon$.

$$v = \epsilon\phi_1(u) + \epsilon^2\phi_2(u) + O(\epsilon^3) \tag{2.23}$$

Differentiating with respect to t give us:

$$\dot{v} = \epsilon\dot{\phi_1}(u)\dot{u} + \epsilon^2\dot{\phi_2}(u)\dot{u} + O(\epsilon^3) \tag{2.24}$$

We already know an expansion for $\dot{v}$ (2.20).

$$-(\epsilon\phi_1(u) + \epsilon^2\phi_2(u) + O(\epsilon^3)) + \epsilon(1 - \cos u - \mu) = (\epsilon)^2\dot{\phi_1}(u)v + \epsilon^3\dot{\phi_2}(u)v + O(\epsilon^3) \tag{2.25}$$

Since the RHS has only $O(\epsilon^2)$ and higher terms we are left with the following equation.

$$-\epsilon\phi_1(u) + \epsilon(1 - \cos(u) + \mu) = 0 \tag{2.26}$$

$$\phi_1(u) = 1 - \cos(u) + \mu \tag{2.27}$$

So up to first order of ϵ we have the expansion for v in terms of u.

$$v = \epsilon(1 - \cos(u) + \mu) + O(\epsilon^2) \tag{2.28}$$

Finally the order ϵ dynamics $\mathcal{M}_\epsilon$ can be written as:

$$u' = \epsilon(1 - \cos(u) + \mu) + O(\epsilon^2) \tag{2.29}$$

This gives us two different pictures for the $\mu = 0$ and the $\mu \in (-1, 0)$ cases.

For $\mu = 0$ the dynamics on $\mathcal{M}_\epsilon$ are given by:

$$u' = \epsilon(1 - \cos(u)) + O(\epsilon^2) \tag{2.30}$$

Thus for $u \in (0, 2\pi)$ and $v > 0$, u is strictly increasing on $\mathcal{M}_\epsilon$ to the next equilibria SN_1.

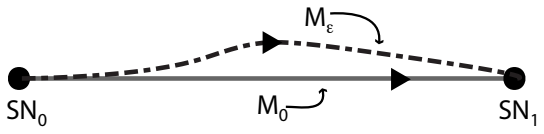

Figure 2.8: $\mathcal{M}_\epsilon$ dynamics for $\mu = 0$

The center manifold $W^c_{SN_0}$ begins on $\mathcal{M}_\epsilon$ from SN_0 and by the invariance property of the ϵ manifold it continues on $\mathcal{M}_\epsilon$ until reaching an equilibrium. Thus for large enough c, $W^c_{SN_0}$ follows $\mathcal{M}_\epsilon$ and connects SN_0 and SN_1. ■

Existence of a unique pulse for $\mu = 0$. We can now prove the existence of homoclinic connections from SN_0 to SN_1.

Proposition 2.9. *For $\mu = 0$ there exists $c = c_*$ such that the system (2.4) has a unique heteroclinic connection $\mathbf{q}(\xi)$ from SN_0 to SN_1 such that $\mathbf{q}(\xi) \in W^c_{SN_0} \cap W^{ss}_{SN_1}$. If $c > c_*$ then $\mathbf{q}(\xi)$ terminates in SN_1 but does not intersect the strong stable manifold.*

Proof. First notice that in the region $u \in (0, 2\pi)$ and $v > 0$ we have that $v' > 0$. In addition, $v' > 0$ along the u axis for $u \in (0, 2\pi)$.

Let $\mathcal{V}(c)$ be the value of v such that the manifold $W^c_{SN_0}$ intersects the line $u = sn_1$. In the previous lemma it was shown that $\mathcal{V}(0) > 0$ and for $c >> 1$ $\nu(c) = 0$. Additionally, from the comparison lemma $\nu(c)$ is a strictly decreasing function in c. The strong stable manifold $W^{SS}_{SN_1}$ is strictly increasing in the v direction as c increases. Hence there is a unique value of $c = c^*$ such that for this value $W^c_{SN_0} \cap W^{ss}_{SN_1} \neq \emptyset$. For larger values of c, $W^c_{SN_0}$ terminates in SN_1 but does not enter through the strong stable manifold. ∎

$\mu = 0$**: transversality** Unfortunately we cannot simply employ the standard Melnikov theory in the case $\mu = 0$. A modified Melnikov method is developed in ([1]) and we will use their results, later. The difficultly lies in the non-hyperbolicity of the equilibrium SN, and therefore the lack of an exponential dichotomy. Therefore, the linearization at the homoclinic is not a Fredholm operator in spaces of bounded functions and the Lyapunov-Schmidt reduction can not be used in the standard fashion to establish the bifurcating structures under changes in parameters (see [21] for an illustration of this method). In this scalar example, we can replace the Melnikov integral by an adhoc construction, exploiting center manifold fibrations (Lemma 2.5) and global monotonicity (Lemma 2.6) in order to analyze the bifurcations of connecting orbits near $\mu = 0, c = c_*$.

From the proof of existence of the homoclinic solution $\mathbf{q}$ we know that the v value can be considered as a function of u. We begin by considering the value $v(u = \delta; c)$ where $0 < \delta \ll 1$. From the local expansion of the center manifold (2.10), for $|u| \ll 1$ we have:

$$v(u : c, \mu) = \frac{\mu}{c} + \frac{u^2}{2c} + \mathrm{O}(\mu^2 + |\mu u| + u^3)$$

This allows one to find the partial derivative with respect to c for small u and $\mu = 0$.

$$\partial_c v(\delta; c, 0) = -\frac{\delta^2}{2c^2} < 0. \tag{2.31}$$

Now consider the v value where the center manifold intersects the line $u = 2\pi - \delta$, refer to this value as $v_-(\delta)$. Since we've already established that in the region of interest $v = v(u)$ the flow $\Phi(u, v_0(c), c)$

$$\Phi(\delta, v(\delta; c), c) = v(\delta; c)$$
$$\Phi(2\pi - \delta, v(\delta; c), c) = v_-$$

This can be used to determine the derivative of v_- with respect to c.

$$\partial_c v_- = \partial_c \Phi(2\pi - \delta, v(\delta; c), c) = \frac{\partial \Phi(2\pi - \delta, c)}{\partial c} + \frac{\partial \Phi(2\pi - \delta, v(\delta), c)}{\partial v(\delta)} \frac{\partial v(\delta; c)}{\partial c}$$

We know from Lemma (2.6) that $v(2\pi - \delta)$ is strictly decreasing in c so that the first term of (2.2.2), $\partial \Phi(2\pi - \delta, c)/\partial c \leq 0$. The fact that we are dealing with a planar system ensures that the ordering of solutions on the line $u = 2\pi - \delta$ is the same as on the line $u = \delta$. Therefore, $\partial \Phi(2\pi - \delta)/\partial v > 0$ (note that the derivative cannot be zero since the Wronskian of a flow cannot vanish). Finally, we have already found $\partial_c v(\delta) < 0$ in (2.31). This allows us to conclude that

$$v_-(\mu, c) = v_-^* + \partial_c v_-(c - c_*) + \mathrm{O}(|\mu| + |c - c_*|^2), \qquad \partial_c v_- < 0 \text{ when } c_* < 0$$

Now let us consider the intersection of $W^{ss}_{SN_1}$ with the line $u = 2\pi - \delta$ and refer to this value as v_+. The expansion of the local strong stable manifold around SN leads to the following graph of v in terms of u:

$$(u, g(u, c)) = \quad \left(u, -c(u - 2\pi) + \frac{(u - 2\pi)^2}{8c} + \mathrm{HOT} \right).$$

It is easy to see that for $u = 2\pi - \delta$, $v_+ \approx c\delta + \delta^2/8c$. Therefore,

$$v_+(\mu = 0, c) = v_+^* + \partial_c v_+(c - c_*) + \mathrm{O}(|c - c_*|^2), \qquad \partial_c v_- > 0 \text{ when } c_* < 0.$$

This shows transverse crossing of the shooting manifold and the strong stable fiber of SN_1.

However, this shows more when combined with the fibrations of the center manifold. For $c \sim c_*$, we appeal to the fibration of a neighborhood of SN_1 (Fig 2.2.1). If $v_- < v_+$ then $\mathbf{q}$ intersects a strong stable fiber associated with a base point in region I that is attracted to N_1. If $v_- > v_+$ then $\mathbf{q}$ intersects a strong stable fiber associated with a base point in region III and the trajectory will leave a neighborhood of SN_1.

In the next step, we will unfold this crossing in μ in order to find connecting orbits for $\mu \lesseqgtr 0$. Our goal is to show existence and smoothness of the curve $\gamma(\mu)$ and the quadradic tangency. We begin by expanding the locations of strong stable fibers of S_1 and N_1 in $u = 2\pi - \delta$, which we refer to as $v_+^{S/N}$. The strong stable manifold is tangent

to the eigenvector corresponding to the smallest eigenvalue:

$$S \to \left(1, \frac{-c - \sqrt{c + \sqrt{-\mu}}}{2}\right)^T$$
$$N \to \left(1, \frac{-c - \sqrt{c - \sqrt{-\mu}}}{2}\right)^T$$
$$SN \to (1, -c)^T .$$

To approximate the intersection of the strong stable manifold with $u = 2\pi - \delta$ we look at the intersection of the strong stable eigendirection and the line. We have the following expansions for $v_+^{S/N}(\mu, c; \delta)$:

$$v_+^N(\mu, c; \delta) = \frac{1}{2}(\delta - \sqrt{\mu})(-c - \sqrt{c - \sqrt{\mu}}) + O(|\mu| + c^2 + \delta^2) \tag{2.32}$$
$$v_+^S(\mu, c; \delta) = \frac{1}{2}(\delta + \sqrt{\mu})(-c - \sqrt{c + \sqrt{\mu}}) + O(|\mu| + c^2 + \delta^2).$$

We linearize around the parameters $(\mu = 0, c = c_*, \delta = \delta_*)$. Additionally, we replace $-\mu = \nu^2$ in order to smooth out the square root singularity. This gives us the following expansion for the strong stable manifold of N_1 (the expansions of S_1 are similar):

$$v_+^N(\nu, c, \delta) = \delta_* c_* - \frac{-\delta_* + c_* + \sqrt{c_*}}{2}(\nu) + \delta_*(c - c_*) + O(\nu^2 + (c - c_*)^2 + |c\nu| + |\delta - \delta_*|). \tag{2.33}$$

We would now like to match our expansion with that for v_-. Therefore we expand v_- as the following:

$$v_-(\nu, c, \delta) = v_-(0, c_*, \delta_*) + \partial_c v_-(\delta_*)(c - c_*) + O(\nu^2 + (c - c_*)^2), \tag{2.34}$$

with $\partial_c v_- < 0$. At $\mu = 0, c = c_*$, we have a homoclinic connection to the strong stable fiber as we saw before, hence $v_- = v_+$. Using the exansion for v_+ given in (2.32) we may write (2.34) as:

$$v_-(\nu, c, \delta) = \delta_* c_* + \partial_c v_-(\delta_*)(c - c_*) + O(\nu^2 + (c - c_*)^2). \tag{2.35}$$

Finally setting the expansions for v_- and v_+ equal we obtain:

$$0 = -\frac{-\delta_* + c_* + \sqrt{c_*}}{2}(\nu) + (\partial_c v_-(\delta_*) - \delta_*)(c - c_*) + O(\nu^2 + (c - c_*)^2). \tag{2.36}$$

We can now solve with the implicit function theorem for $c = c(\nu)$ and find $c = c_* + k_1\sqrt{-\mu} + \mathrm{O}(\mu)$, with $k_1 > 0$. We find a similar expansion for connecting orbits to the stong stable manifold of S_1, $c = c_* - k_1\sqrt{-\mu} + \mathrm{O}(\mu)$. Therefore, the curve γ is found by solving for $\sqrt{-\mu} = (c - c_*)/k_1 + \mathrm{O}((c - c_*)^2)$, which gives $\mu = -(c - c_*)^2/k_1^2 + \mathrm{O}(3)$, for both $c - c_* > 0$ and $c - c_* < 0$. This proves the expansion and C^2-smoothness of γ.

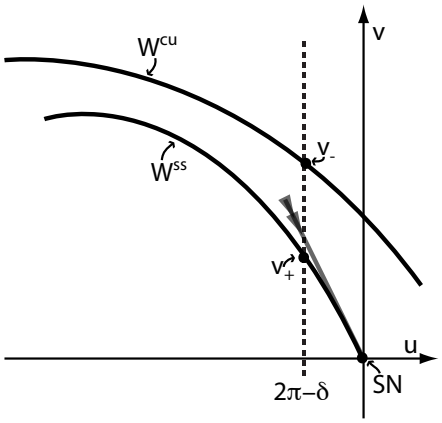

Figure 2.9: A diagram of the matching problem.

Examining the base point dynamics of strong stable fibers not associated with the equilibria S_1 and N_1, one can now complete the bifurcation diagram near $\mu = 0$ and $c = c_*$ and establish the existence of slow and fast fronts, as well as the absence of index-1 connecting orbits with speeds higher than the speed of the pulse. It remains to show that there are no connecting orbits of higher index.

If the unstable manifold $W^u_{S_0}$ does not connect to N_1 or S_1, then it must intersect the line $u = s_1$ at a value $v = v_0 > 0$. Therefore $W^u_{S_0} > W^u_{S_1}$ in the v direction. Since the phase plane is 2π periodic in the u direction, this precludes the possibility for $W^u_{S_0}$ to connect to S_2 since $W^u_{S_1}$ misses it. This argument extends inductively to show that for $W^u_{S_k}$ can connect at most to N_{k+1} or S_{k+1}. This concludes the proof of Theorem 1

2.3 Existence and stability of wave trains

2.3.1 Existence and uniqueness

This section is concerned with the proof of Theorem 3. We show the existence of index-one periodic orbits using a similar shooting argument as for heteroclinic orbits. Define $\Phi(v_0, c, \mu)$ be the map from the point (s_0, v_0) to the point (s_1, v_1) in the following way. Let $\phi(t)$ be the flow for (2.4) and define $\Phi(v_0, c, \mu) = \phi(t_0)(\alpha_0, v_0)$ such that $\phi(t_0)(s_0, v_0) = (s_1, v_1)$.

Lemma 3.10. *$\Phi(v_0, c, \mu)$ is well defined for the choices of μ and c in the theorem and $\Phi(v_0, c, \mu)$ is continuous with respect to v_0.*

Proof. We know that such a map is well defined for $\mu = -1$ and $c = 0$ since (2.4) is Hamiltonian in this case and we can find solutions explicitly as a graph $(u, v(u)$ (see Lemma 2.7.) Since the vector field at (s_1, v) is $(v, -cv)$ then for any $\mu > 0$, $c > 0$ the intersection is transverse. Moreover if $\mu > 0$ the flow must be above the u axis since the slope of the vector field is positive for $v = 0$. If $\mu \in [-1, 0)$ then any solution passing through the point (s_0, v_0) is above $W^u_{S_0}$ in the v direction. Hence the map $\Phi(v_0, c, \mu)$ is well defined for nearby values of c and μ. From the averaging argument below for $c > 0$, $\phi(t)(s_0, v_0)$ is decreasing for large v_0. Since $u' > 0$ for $v_0 > 0$ and the flow is bounded above and below in the v direction it must intersect line $u = \alpha_1$ at some time T_0. Thus Φ is well defined. Since the flow is continuous both with respect to initial conditions and parameters it follows that $\Phi(v_0, \mu, c)$ is continuous as well.

■

To complete the proof of existence we need to show that $\Phi(v, c, \mu)$ maps a closed interval to a closed interval. Let $w = \epsilon v$. This allows us to rewrite (2.4) in the following form:

$$\begin{pmatrix} \epsilon u \\ w \end{pmatrix}' = \begin{pmatrix} w \\ -cw + \epsilon(1 - \cos(u) - \mu) \end{pmatrix}. \tag{2.37}$$

Rescaling time $t = \frac{1}{\epsilon}\tau$ we have:

$$\begin{pmatrix} \dot{u} \\ \dot{w} \end{pmatrix} = \begin{pmatrix} w \\ -\epsilon cw + \epsilon^2(1 - \cos(u) - \mu) \end{pmatrix}. \tag{2.38}$$

We can rewrite this system as w as a function of u.

$$\frac{dw}{du} = -c\epsilon + \epsilon^2 \frac{1-\cos(u)-\mu}{w} = \epsilon\left(-c + \epsilon\frac{1-\cos(u)-\mu}{w}\right) \tag{2.39}$$

The right hand side is 2π periodic in u. Now we can use the averaging transformation (see [22]) $w = y + \epsilon h(y,t,\epsilon)$ where the dynamics of y are:

$$\dot{y} = -\epsilon c + \epsilon^2 F_2. \tag{2.40}$$

Thus for $0 < \epsilon << 1$ (or equivalently $v >> 0$,) $w \approx -c\tau$ (or in the original scaling $v \approx -ct$.) This implies that for v large $v(u)$ decreases monotonically. Let v_ω be sufficiently large so that $\Phi(v_\omega, c, \mu) < v_\omega$. Then Φ provides a map from the interval $(\alpha_0, v)|\ 0 \le v \le v_\omega$ to the interval $(\alpha_1, v)|\ 0 \le v \le v_\omega$ continuously. By the intermediate value theorem the function $\Phi(v_0) - v_0$ has at least one fixed point and is unique by the following argument. Assume there were two fixed points of Φ v_1 and v_2 such that $v_1 > v_2$. Since $v_i(t)$ are both assumed to be periodic with periods L_1 and L_2 then $\frac{v_i^2(t)}{2}$ is also periodic. Differentiating with respect to t gives us the following:

$$v\dot{v} = -cv^2 + (1-\cos(u)-\mu)\dot{u} \tag{2.41}$$

If we integrate both sides over the interval $[0, L_i]$ we get:

$$\int_0^{L_i} v_i\dot{v}_i dt = 0 = \int_0^{L_i} -cv_i^2 + (1-\cos(u_i)-\mu)\dot{u}_i dt \tag{2.42}$$

Notice that the second term of the RHS of (2.42) does not depend on i:

$$\int_0^{L_i} (1-\cos(u_i)-\mu)\dot{u}_i dt = (1-\mu)2\pi \tag{2.43}$$

For the first term of (2.42) we can rewrite it by substitution in terms of u.

$$\int_0^{L_i} -cv_i^2 = \int_0^{2\pi} -cv_i(u)du \tag{2.44}$$

But by assumption $v_1 > v_2$ so $\int_0^{2\pi} -cv_1(u)du < \int_0^{2\pi} -cv_2(u)du$. This contradicts our initial assumption that $\int_0^{T_i} v_i\dot{v}_i dt = 0$ for $i = 1, 2$. Hence the periodic must be unique.

2.3.2 Dispersion relations

Existence of $\Omega(k)$ and monotonicity. Showing that there is a function $\Omega(k)$ is not difficult. Assume for a given k there were two values of ω namely ω_1 and ω_2. Since $k = \frac{2\pi}{L}$ and $\omega = ck$ we could rephrase this question by asking if for a given period L can there be two periodics for c_1 and c_2 where $c_2 > c_1$. It is easy to see that $\Phi(v)$ is strictly decreasing as c increases. Thus the periodic orbit corresponding to c_2 should have initial point $v_2 < v_1$. This implies the periodic orbit P_1 corresponding to c_1 is strictly greater than P_2 (corresponding to c_2) in the v direction. However, $u' = v$ so P_1 necessarily has a shorter period than P_2. This contradicts our assumption that P_i have the same periods L. Therefore $\Omega(k)$ is a function of k.

The above argument has the useful corollary that the period L increases as the starting value v decreases. In fact for $v << 1$ the periodics approach the equilibria causing their periods to increase to infinity. This can be seen by linearizing around the equilibria and approximating the period (for example Wiggins [23]). This analysis gives $L \approx -\frac{1}{c}\ln(v_0)$.

Assympotics of $\Omega(k)$ as $k \to \infty$. When considering the quantity $\omega = c\frac{2\pi}{L}$, letting k go to infinity is equivalent to letting $L \to 0$ The question is what happens to c for large period L. To understand this relation it is convenient to employ the method of averaging. Recall the ODE system (2.4.) We are looking for solutions so that $v(0) = v(T)$ and $u(T) = u(0) + 2\pi$. For small values of L the orbit will have a large initial value v_0. Accordingly, define $w = \epsilon v$. Then (2.4) becomes:

$$\begin{pmatrix} \epsilon u \\ w \end{pmatrix}' = \begin{pmatrix} w \\ -cw + \epsilon(1 - \cos u - \mu) \end{pmatrix} \tag{2.45}$$

Rescaling time by $\tau = \frac{t}{\epsilon}$ allows the removal of ϵ from the right side of the equation. Also rescale $c = \epsilon\bar{c}$.

$$\begin{pmatrix} \dot{u} \\ w \end{pmatrix} = \begin{pmatrix} w \\ \epsilon^2(-\bar{c}w + 1 - \cos u - \mu) \end{pmatrix} \tag{2.46}$$

Notice that for $\epsilon = 0$ then (2.46) has a trivial periodic orbit for $w(0) > 0$. The question becomes can we find a periodic orbit for $\epsilon > 0$. We can slightly rephrase this question

by asking for solution $w(u)$ of the following:

$$\frac{dw}{du} = \epsilon^2 \frac{(-\bar{c}w + 1 - \cos u - \mu)}{w} \tag{2.47}$$

By considering w as a function of u we now seek a solution $w(0) = w(2\pi)$. Consider the following averaging transformation:

$$w(u, w_0, \epsilon) = w_0(w_0, t) + \epsilon^2 w_1(u, w_0) \tag{2.48}$$

where

$$w_1(u, w_0) = \int \left\{ \frac{(-\bar{c}w_0 + 1 - \cos u - \mu)}{w_0} - \frac{1}{2\pi} \int_0^{2\pi} \frac{(-\bar{c}w_0 + 1 - \cos u - \mu)}{w_0} du \right\} du. \tag{2.49}$$

For ϵ sufficiently small (2.47) has a unique periodic solution provided the following integral is zero (see [22]):

$$\int_0^{2\pi} \frac{(-\bar{c}w_0 + 1 - \cos u - \mu)}{w_0} du = 0. \tag{2.50}$$

Solving this integral leaves $\bar{c} = \frac{1-\mu}{w_0}$ and $c = \epsilon \frac{1-\mu}{w_0}$. Returning to the original variable gives us $c = \frac{1-\mu}{v_0}$. We can now rewrite ω as $\omega = \frac{2\pi(1-\mu)}{v_0 T}$. Now expand $u(L)$ as a Taylor series of (L, ϵ):

$$u(L) = u(0) + Lu'(0) + O(\epsilon) = u(0) + Lv(0) + O(\epsilon). \tag{2.51}$$

For small ϵ,we have that

$$u(L) - u(0) = \quad v(0)L = \quad 2\pi.$$

So finally we find:

$$\lim_{\epsilon \to 0^+} \omega = 1 - \mu.$$

Assymptotics as $k \to 0$ for $\mu \in [-1, 0]$. For $\mu \in [-1, 0]$ it is easy to see that as $k \to 0$ then $\omega \to 0$ since taking $k \to 0^+$ is equivalent to $T \to \infty$. We know that for $c = c^*$ we have a particular heteroclinic as described previously and no other periodics in for $v > 0$. From Lemma 2.6 we see that $\Phi(v_0, \mu, c)$ decreases as c increases which

disallows periodic orbits for $c > c^*$. Because c is bounded, this provides the following limit:

$$\lim_{T\to\infty} \omega = \lim_{T\to\infty} \frac{c2\pi}{T} = 0. \tag{2.52}$$

Notice this is not the case when $\mu > 0$.

We first begin by rescaling time so that the above theorem becomes a perturbation result. Recall the right hand side of (2.3), which is equal to zero for traveling wave solutions:

$$u_{\xi\xi} + cu_\xi + \cos(u) - 1 - \mu = 0. \tag{2.53}$$

We rescale time by taking $\tau = kt$, the equation (2.53) becomes:

$$k^2 u'' + \omega u' + f(u) = 0 \tag{2.54}$$

where $f(u) = \cos(u) + \mu - 1$. Notice that under the τ time scale the periodic solution u^* has period 2π. If $k^2 = 0$ we have the following first order ODE:

$$\omega_0 u' + \cos(u) - 1 + \mu = 0 \tag{2.55}$$

and we can solve explicitly for ω:

$$\omega_0 = \frac{2\pi}{\int_0^{2\pi} \frac{du}{1-\mu-\cos(u)}}. \tag{2.56}$$

This integral can be solved by the residue theorem (though not by mathematica evidentally).

$$\omega_0 = \frac{\sqrt{\mu^2 - 8\mu}}{2} \tag{2.57}$$

This proves the first part of the proposition.

Now we will change variables so we can consider periodic solutions $I = 1$. Letting $v = u - t$ we have the following equation:

$$k^2 v'' + \omega(v' + 1) + f(v + t) = 0 \tag{2.58}$$

We can rewrite this in to following convenient form:

$$\mathbf{F}(v, \omega, \mu, c) = v' + M^{-1}(\omega + f(v + t)) = 0 \tag{2.59}$$

$$M^{-1} = (k^2 \frac{d}{dt} + \omega)^{-1} \tag{2.60}$$

Here consider $\mathbf{F}$ as a map $\mathbf{F} : \mathbf{H}_1(\text{periodic on } [0,T]) \to L^2(2\pi \text{ periodic on } [0,T])$. M^{-1} is C^1 in k^2 for small values of k as long as $\omega \neq 0$. The smoothness can be seen by finding the inverse via the Fourier transform. Linearizing when $k = 0$ around the periodic solution $v^* = u^* - t$ gives the following familiar equation:

$$\mathbf{L}w = w' + \frac{f'(v_* + t)}{\omega} w \tag{2.61}$$

Comparing the linearization to $\mathbf{F}(v, \omega)$ notice that $v_*' + 1$ is in the kernel of the linearization. For ease of notation let $v_*' + 1 = \phi'$ and dual function be called e_1. Since e_1 satisfies the dual equation

$$-w' + \frac{f'(v_* + t)}{\omega} w = 0 \tag{2.62}$$

Then we have the following usual property:

$$(\phi' e_1)' = \phi'' e_1 + \phi' e_1' = v_*'' e_1 + v_*' e_1' = \frac{1}{\omega}(f'(v_*)(v_*' + 1)e_1 - (v_*' + 1) f(v_*) e_1) = 0. \tag{2.63}$$

So the product of $e_1 \phi'$ is constant and can be taken to be $e_1 \phi' = \frac{1}{2\pi}$. If we let $(v - v^*) = \hat{v}$, $(\omega - \omega_0) = \hat{\omega}$ then we are left with the following expansion.

$$\begin{aligned} \mathbf{F}(\hat{v}, k^2, \hat{\omega}) = \left(\frac{d}{dt} - \frac{f'(v^* + t)}{\omega_0} \right) \hat{v} - \left(\frac{\sin(v^* + t)}{\omega_0} \phi' \right) k^2 \\ - \left(\frac{f(v^* + t)}{(\omega_0)^2} \right) \hat{\omega} + o(k^2) + O(\hat{v}^2 + \hat{\omega}^2) = 0 \end{aligned}$$

Lyapunov-Schmidt Reduction Since $\mathbf{L}$ has compact resolvent, it is Fredholm of index 0. This means the domain can be decomposed as $M \oplus K$ where K is the kernel of $\mathbf{L}$. This allows us to write $\hat{v} = \nu + \eta\phi'$ where $\nu \in M$ and $\eta\phi' \in K$. Define the projection E as the L^2 projection against e_1. Consider the following equation:

$$(I - E)\mathbf{F}(\nu + \eta\phi', k^2, \hat{\omega}) = 0 \tag{2.64}$$

When restricted to M the projected linearization $(I - E)\mathbf{L}$ is invertible. Thus we can solve for ν by the implicit function theorem.

$$\nu(\eta\phi', k, \hat{\omega}) = O(\eta\phi' + k^2 + \hat{\omega}) \tag{2.65}$$

Now we will project onto the adjoint solution e_1 with E. The first $(\hat{v})$ term disappears since $e_1 \perp \text{Range}(\mathbf{L})$ and we are left with:

$$E\mathbf{F}(\eta\phi' + \nu, \hat{\omega}, k^2) = \tag{2.66}$$

$$= -\int_0^{2\pi} e_1 \frac{f'(v^*+t)}{\omega_0}\phi' \; k^2 dt - \int_0^{2\pi} e_1 \frac{f(v^*+t)}{(\omega_0)^2} \; \hat{\omega} dt \tag{2.67}$$

$$+\int_0^{2\pi} e_1(\phi')^2 \; \eta^2 dt + \int_0^{2\pi} e_1\phi' \; 2\eta \; \hat{\omega} dt + o(k^2) + O(\hat{\omega}^2 + \hat{v}^3) = 0 \tag{2.68}$$

The constant η corresponds to the shift in the direction of the periodic so we can set $\eta = 0$. This leaves us with the following:

$$= -\int_0^{2\pi} e_1 \frac{f'(v^*+t)}{\omega_0}\phi' \; k^2 dt - \int_0^{2\pi} e_1 \frac{f(v^*+t)}{(\omega_0)^2} \; \hat{\omega} dt + o(k^2) + O(\hat{\omega}^2 + |\omega| k^2) = 0 \tag{2.69}$$

We can calculate the k^2 term's coefficient easily also after projection. Letting $e_1 = \frac{1}{2\pi\phi'}$ and noting that $f'(v^*+x)\phi' = \phi''$ we can rewrite the k^2 coefficient as:

$$-\int_0^{2\pi} \frac{e_0'}{\phi'} dx = \ln(\phi')|_0^{2\pi} = 0 \tag{2.70}$$

On the other hand the $\hat{\omega}$ coefficient is not zero.

$$-A_\omega = \int_0^{2\pi} e_1 \frac{f(v^*+t)}{(\omega_0)^2} dt = \frac{1}{2\pi(\omega_0)^2} \int_0^{2\pi} \frac{\cos(v^*+t) - 1 + \mu^*}{\phi'} dt \tag{2.71}$$

We know $\phi' = v^{*'} + 1 > 0$ and for $\mu^* < 0$ then $\cos(v^*+t) - 1 + \mu^* < 0$. Since the integrand is strictly negative the integral (2.71) cannot be zero. This implies that $\partial_\omega F \neq 0$ and is invertible. Rewriting (2.67) with our calculations gives:

$$A_\omega \; \hat{\omega} + o(k^2) + O(\hat{\omega}^2) = 0 \tag{2.72}$$

Finally using the implicit function theorem we can now solve for ω in terms of k: $\Omega(k) = \omega_0 + o(k^2)$.

2.3.3 Stability of wave trains

The stability of wave trains with respect to the space $H^1_{\text{per}}([s_0, s_1])$ is a straight forward application of the Sturm-Liouville theory (for an extensive review see [24].) Let $\phi(\xi)$ be a particular periodic orbit of period L. To determine the stability of $\phi(\xi)$, we find the eigenvalues of the linearization around $\phi(\xi)$. This amounts to solving the following boundary value problem.

$$v'' + cv' + -\sin(\phi(\xi))v - \lambda v = 0 \tag{2.73}$$

$$v(0) = 0, \;\; v(L) = 2\pi$$

$$v'(0) = v_0, \;\; v'(L) = v_0$$

Notice $\phi'(t)$ is an eigenfunction for the linearized problem with eigenvalue $\lambda = 0$. It is easy to see that $\phi'(t)$ is strictly positive over the interval and thus by S-L theory we know that all other eigenvalues are smaller than zero. We now apply the stability theory available in Henry's book [17] which requires that the spectrum have at most one isolated simple zero and the rest of the spectrum contained in the left half plane. Thus the $\mathbf{I} = 1$ periodics are stable with respect to periodic perturbations.

If we consider instead perturbations in $H^1(\mathbb{R})$, this argument needs to be extended slighly. We use Theorem 2 of [13]. The theorem states that for there to be an eigenvalue λ of multiplicity l on the real line, then there is a period L^* such that for $L > L^*$ there are l eigenvalues in a neighborhood of λ. As we shewed in the above section on asymptotics, for any value L there is a unique solution $\phi(\xi)$ to the above system. Since ϕ' is a strictly positive eigenfunction of (2.73) then there is an isolated eigenvalue at zero and this is the largest (in absolute value) eigenvalue. Thus, applying Theorem 2 of [13], $\lambda = 0$ must be an isolated eigenvalue of (2.73) on $\mathbb{R}$.

To show the instability of the $\mathbf{I} = 0$ periodics we show that the linearization has a positive eigenvalue. This follows in the same way that stability was shown for the outer periodics. However, in this case the know eigenfunction $\phi'(t)$ crosses zero twice. The eigenvalue for $\phi'(t)$ is again zero, so by Sturm-Liouville theory there must be two eigenvalues greater than zero and hence the periodic orbit is unstable [17].

2.4 Stability of pulses and fronts

We will consider the stability of both fronts and pulses. Our approach is similar for both pulses and steep fronts, however, we will only show stability of steep fronts with respect to an appropriately weighted space. Therefore, we show the stability of pulses first and consider steep fronts as a modification of the argument for pulses.

2.4.1 The Essential Spectrum

We will determine the stability of the pulses and fronts through analysis of their spectra. We begin by considering the essential spectrum of each. The essential spectrum may be found by considering the dispersion curves corresponding to the linearized operator at the equilibria S_0 and S_1 (or N_1 in the case of the front.) The linearization around the

a pulse or front is a compact perturbation of the operators at the equilibria. Therefore, citing results in [16], the essential spectrum must lie between the dispersion curves determined by the linear operators at the equilibria.

Dispersion curves of Pulses and Steep Fronts From (2.3) travelling pulse $\phi_p(\xi)$ or steep front $\phi_f(\xi)$ is a solution to the following differential equation.

$$\phi'' - c\phi' + \cos(\phi) - 1 - \mu = 0 \tag{2.74}$$

Begin by linearizing around the solution $\phi(t)$:

$$\mathcal{L}(v) = v'' + cv - \sin(\phi(\xi))v$$

Then the dispersion curves are the following:

$$D_\pm = \left\{ \lambda | \left[-\tau^2 + i\tau c - \lim_{\xi \to \pm\infty} \sin(\phi_p(\xi)) - \lambda \right] = 0 \right\} \tag{2.75}$$

In the particular case for the pulse, $\lim_{\xi\to\pm\infty} \sin(\phi_p(\xi)) = \sqrt{1-(1-\mu)^2}$. So we have only one dispersion curve parametrized in the following way.

$$D_\pm = \begin{cases} \mathrm{Re}(\lambda) & -\tau^2 - \sqrt{2\mu - \mu^2} \\ \mathrm{Im}(\lambda) & c\tau \end{cases} \tag{2.76}$$

Notice that this is a parabola which surrounds part of the left half of the complex plane.

For the steep front the situation is different. We have the same equation for determining the dispersion curves:

$$D_\pm = \left\{ \lambda | \left[-\tau^2 + i\tau c - \lim_{\xi \to \pm\infty} \sin(\phi_f(\xi)) - \lambda \right] = 0 \right\}.$$

However, $\phi_f(\xi)$ approaches different values as $\xi \to \infty$:

$$\lim_{\xi\to\infty} \sin(\phi_f(\xi)) = -\sqrt{2\mu - \mu^2}$$
$$\lim_{\xi\to-\infty} \sin(\phi_f(\xi)) = \sqrt{2\mu - \mu^2}.$$

This gives us two dispersion curves:

$$D_+ = \begin{cases} \mathrm{Re}(\lambda) & -\tau^2 + \sqrt{2\mu - \mu^2} \\ \mathrm{Im}(\lambda) & c\tau \end{cases}, \qquad D_- = \begin{cases} \mathrm{Re}(\lambda) & -\tau^2 - \sqrt{2\mu - \mu^2} \\ \mathrm{Im}(\lambda) & c\tau \end{cases}. \tag{2.77}$$

Clearly the steep slopes are not asymptotically stable in the sense defined above since the essential spectrum extends into the left half plane!

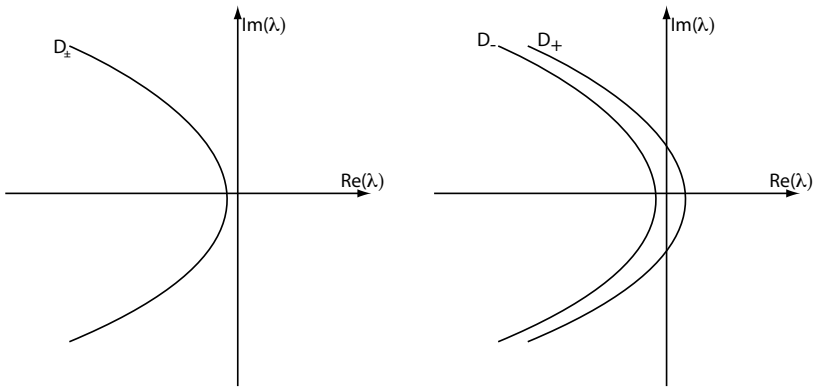

Figure 2.10: The figure to the left illustrates the essential spectrum for pulses, while the figure to the right is for the steep fronts.

Weighted Spaces While the spectrum of the steep fronts is not contained in the left half plane for solutions on $L^2(\mathbb{R})$, we would like to consider the essential spectrum on the weighted space $L^2_\eta(\mathbb{R})$ instead. Recall that a function u is in L^2_η if:

$$\int_{-\infty}^{\infty} |e^{\eta\xi}u(\xi)|^2 d\xi < \infty.$$

This means that only functions that decay faster than $e^{\eta\xi}$ are allowed, while some exponential growth is allowed in negative time. The operator $\mathcal{L} : L^2_\eta(\mathbb{R}) \to L^2_\eta(\mathbb{R})$ can be instead thought of the operator $\mathcal{L}_\eta : L^2(\mathbb{R}) \to L^2(\mathbb{R})$.

$$\mathcal{L}_\eta = (\partial_\xi - \eta)^2 - c(\partial_x i - \eta) - \sin(\phi(\xi). \tag{2.78}$$

We choose $\eta = c/2$ out of convenience because the operator is self-adjoint in this weighted space. This gives us the following:

$$\mathcal{L}_{\frac{c}{2}} = \partial_\xi^2 - \frac{c^2}{4} - \sin(\phi(\xi))$$

For ease of notation let us refer to $\mathcal{L}_{\frac{c}{2}}$ as $\tilde{\mathcal{L}}$

Since $\mathcal{L}_\eta$ is self-adjoint in $H^1(\mathbb{R})$, the spectrum is restricted to the real line. This makes computation of the dispersion curves easy:

$$D_\pm = \left\{ \lambda | \left[-\tau^2 - \frac{c^2}{4} - \lim_{\xi \to \pm\infty} \sin(\phi_f(\xi)) - \lambda \right] = 0 \right\}.$$

For $|\mu| \ll 1$ the u-value of the equilibrium N_1 is such that $0 < |\sin(n_1)| \ll 1$. Therefore we are assured that for μ near zero both dispersion curves are strictly contained in the negative real line. Finally, notice that for $\mu \lesssim 0$, steep fronts $\phi(\xi)$ are in the strong stable manifold and decay to the equilibrium like

$$e^{(\frac{-c-\sqrt{c}}{2})\xi}$$

and therefore $\phi'(\xi)$ is contained in the weighted space $L^2_{\frac{c}{2}}$. This will be important for our analysis of the discreet spectrum.

Asymptotic Stability of Pulses. The primary way to show asymptotic stability with reference to the spectrum of a linear operator is to determine the largest (or smallest depending on sign) eigenvalue and show that the essential spectrum is suitably bounded away from the imaginary axis and in such a way that the operator is sectorial. If the largest eigenvalue is negative or a simple zero one may appeal to the stability theorems of Henry [17].

We have showed above that the essential spectrum of the pulse lies strictly in the left hand plane. We are left to consider the positions of the point spectrum in order to apply the results from [17]. The following method is adapted from [17] though it may be found elsewhere.

Begin with the linear operator:

$$\mathcal{L}v = v'' - cv' - \sin(\phi(\xi))v \tag{2.79}$$

Since $\phi(\xi)$ is a solution of (2.4), $\phi(\xi)'$ is a solution of the linearized equation. Thus ϕ' is a eigenfunction of $\mathcal{L}$ with eigenvalue 0. We will use the known positivity of the solution ϕ' in showing that 0 is the largest eigenvalue and that it is simple.

$$\mathcal{L}v - \lambda v = v'' + cv' - \sin(\phi(\xi))v - \lambda v = 0 \tag{2.80}$$

$$0 = v'' - cv' - (\lambda + \sqrt{1-(1-\mu)^2})v \tag{2.81}$$

It is clear that in order to be bounded, $v(\xi) \to 0$ of at least order $e^{-c\xi}$. Therefore we may consider the operator on the previously mentioned weighted space $L^2_{\frac{c}{2}}$. Therefore

the eigenvalue problem on $H^1(\mathbb{R})$ becomes:

$$\mathcal{L}_{\text{wt}} v - \lambda v = v'' - \left(\frac{c^2}{4} + \sin(\phi) + \lambda \right) v = 0$$

Since we are assuming that the linearized solution v is bounded and decays exponentially we are considering only functions in the intersection of L^2 and $H^1(\mathbb{R})$. Thus the problem becomes one of solving a L^2 adjoint equation. Now consider the L^2 inner product $< \mathcal{A}v, v >$.

$$\int_{-\infty}^{\infty} \left(v'' - \left(\frac{c^2}{4} + \sin(\phi) + \lambda) \right) v \right) v \, d\xi$$

Solving for λ and integrating by parts gives us the following:

$$\lambda \int_{-\infty}^{\infty} v^2 d\xi = \int_{-\infty}^{\infty} v'' v - \left(\frac{c^2}{4} + \sin(\phi) \right) v^2 d\xi = \int_{-\infty}^{\infty} -(v')^2 - \left(\frac{c^2}{4} + \sin(\phi) \right) v^2 d\xi$$

Hence the following estimation for λ can be obtained.

$$\lambda \leq \max \left\{ \frac{\int_{-\infty}^{\infty} -(v')^2 - \left(\frac{c^2}{4} + \sin(\phi) \right) v^2 d\xi}{\int_{-\infty}^{\infty} |v|^2 d\xi} \;\middle|\; v \in \mathbf{H}^1 \right\}$$

Note that this estimation is the "Rayleigh" quotient [25] but can been seen by an application of Cauchy-Schwartz inequality. Now use the fact that a positive eigenfunction $\phi'(\xi)$ is already known. Let $\psi(\xi) = \phi'(\xi) e^{\frac{c}{2}\xi}$ and consider the resulting equation

$$0 = \int_{-\infty}^{\infty} -(v')^2 - \left(\frac{c^2}{4} + \sin(\phi) \right) v^2 d\xi$$

The following useful observation helps us to simplify the integral:

$$\psi'' - \left(\sin(\phi) + \frac{c^2}{4} \right) \psi = 0 \quad \rightarrow \quad \frac{\psi''}{\psi} = \left(\sin(\phi) + \frac{c^2}{4} \right)$$

Of course this relies on the fact that $\psi > 0$. Thus

$$\int_{-\infty}^{\infty} -(v')^2 - \left(\frac{c^2}{4} + \sin(\phi) \right) v^2 d\xi = \int_{-\infty}^{\infty} -(v')^2 - \frac{\psi''}{\psi} v^2 d\xi$$

This in turn is equal to the following simplification:

$$\lambda \leq -\max \int_{-\infty}^{\infty} \psi^2 \left(\left(\frac{v}{\psi} \right)' \right)^2 d\xi$$

To see this we expand the integral.

$$\int_{-\infty}^{\infty} \psi^2 \left(\left(\frac{v}{\psi} \right)' \right)^2 d\xi = \int_{-\infty}^{\infty} \psi^2 \left(\frac{v'\psi - v\psi'}{\psi^2} \right)^2 = \int_{-\infty}^{\infty} (v')^2 + v^2 \left(\frac{\psi'}{\psi} \right)^2 - (v^2)' \frac{\psi\psi'}{\psi^2} d\xi.$$

Now integrating by parts gives us:

$$\int_{-\infty}^{\infty} (v')^2 + v^2 \left(\left(\frac{\psi'}{\psi} \right)^2 - \left(\frac{\psi\psi'}{\psi^2} \right)' \right) d\xi = \int_{-\infty}^{\infty} \psi^2 \left(\left(\frac{v}{\psi} \right)' \right)^2 d\xi.$$

In order to integrate by parts we use the fact that ψ decays exponentially to 0 in both forward and backward time.

Thus $\lambda \leq 0$ and it will only equal zero provided $\left(\frac{v}{\psi}\right)' = 0$ This implies that ϕ' is the unique eigenfunction for zero so zero is a geometrically simple eigenvalue. Since the operator considered about is self-adjoint the dimension of the geometric eigenspace and algebraic eigenspace are equal [25]. This implies 0 is a simple eigenvalue. Since the essential spectrum lies within the boundary of the dispersion curve it is easy to see two important facts. First the real part of the essential spectrum is at most $-\sqrt{-2\mu + \mu^2}$, and second that the operator $\mathcal{L}$ is sectorial. These are precisely the conditions necessary to show asymptotic nonlinear stability from [17].

Stability of Steep Fronts The steep fronts are clearly not asymptotically stable since, as we showed previously, their essential spectrum in not confined to the left half plane. However, in the exponentially weighted space, the essential spectrum shifts to the left half plane. We can then apply the argument given above to show that the largest eigenvalue is at zero and is algebraically simple. Therefore we have the requirements for asymptotic stability, but only in the exponentially weighted space.

Stability of Slow and Fast Fronts There are several possibilities for showing stability of fast fronts. For instance, it is not difficult to see that fast fronts are stable in weighted spaces for large speeds c, see for example [26]. Then, the linearized operators, conjugated with the weight (make explicit) depened continuously on the parameter c as unbounded operators in L^2. Therefore, the only possibility for an instability is a zero eigenvalue for a particular value of $c = c_*$ — which would correspond to a steep front, since the decay would be with the smaller eigenvalue ν_-.This shows that all fast

fronts are weighted stable. A perturbation argument that we will carry out in much more generality in the next, main chapter, shows that the eigenvalue actually crosses the imaginary axis with non-vanishing speed, so that slow fronts always possess exactly one unstable eigenvalue.

In this scalar example, there is in fact a more direct, alternative proof, based on Sturm-Liouville theory [24, Chapter 9]. We know that eigenfunctions (above the essential spectrum) are ordered by the number of zeros. In fact, let u_λ^- denote the unique solution to the eigenvalue problem which is bounded at $\xi = -\infty$ and consider its asymptotics at $\xi = +\infty$. For $\lambda \gg 1$, u_λ^- converges to $+\infty$, while for $\lambda = 0$, u_λ^- is given by the derivative of the front and therefore converges to $+\infty$ for fast fronts, to 0 for steep fronts, and to $-\infty$ for slow fronts. This fact, together with monotonicity and continuity [24, Chapter 9, Sec 5] then gives the desired stability and instability results.

Other weights Without going into much detail, we note here that the point spectrum that we constructed in the weighted space with equal weight at both $+\infty$ and $-\infty$, is independent of the weight as long as the weight confines the essential spectrum to the left ot the point spectrum. This can easily be seen from decay properties of the ordinary differential equation; see also [13]. As a consequence, slow fronts are unstable in *any* weighted space. Also, the steep and fast fronts are stable in weighte spaces with trivial weight 0 at $-\infty$ and exponential weight $c/2$ at $+\infty$. Since such weights are bounded away from zero, the nonlinearity is a smooth operator on these function spaces and one can readily establish nonlinear stability in these weighted spaces [27].

Chapter 3

Unfolding the homoclinic saddle-node flip in general reaction-diffusion systems

We are interested in the transition from excitable to oscillatory media in reaction-diffusion *systems*, with species $u \in \mathbb{R}^N$. We will investigate existence and stability of coherent structures, that is, pulses, fronts, and wave trains, under robust assumptions at a bifurcations point. This analysis will show that the results in the scalar example are one out of two generic possible unfoldings of the excitable-oscillatory transition in a general reaction-diffusion system. In the present chapter, we will explain and interpret the assumptions on the bifurcation, section 3.1. We then state our main results, section 3.2. We conclude this chapter with a discussion of other codimension-one instabilities.

3.1 Assumptions on the pulse at the boundary of excitability.

Consider the reaction diffusion system,

$$u_t = Du_{xx} + f(u, \mu), \tag{3.1}$$

where $x \in \mathbb{R}$, $u \in \mathbb{R}^N$, $f : \mathbb{R}^N \times \mathbb{R} \to \mathbb{R}^N$, and $\mu \in \mathbb{R}$. Let D be a positive diagonal diffusion matrix, $D = \mathrm{diag}(d_j) > 0$. We assume that f is sufficiently smooth in u and

μ for our purposes here. If f is $C^3(\mathbb{R}^N)$ in u and $C^2(\mathbb{R})$ in μ, then f will be smooth enough for the results here. We have not determined whether these are the minimal smoothness conditions.

Local bifurcation. The following hypotheses guarantee that the ODE undergoes a generic saddle-node bifurcation with generic stable PDE spectrum.

Hypothesis 1.1 (Saddle-Node, S)**.** *The function $f(u,\mu)$ satisfies the conditions for a saddle node bifurcation in the ODE, $u' = f(u,\mu)$. Specifically that is:*

1. *simple kernel: $f(0,0) = 0$, $D_u f(0,0)\sigma_r = 0$, $D_u f(0,0)^T \sigma_l^T = 0$, $\sigma_l \sigma_r > 0$;*
2. *parameter unfolding: $\sigma_l \partial_\mu f(0,0) \neq 0$;*
3. *quadratic nonlinearity: $\sigma_l D_u^2 f(0,0)(\sigma_r, \sigma_r) \neq 0$.*

Hypothesis 1.2 (Stability)**.** *For D and $f(u,\mu)$ given in (3.1):*

1. *stable PDE spectrum:* $\operatorname{spec}(-Dk^2 + f'(0;0))$ *has negative real part for $k \neq 0$ and an algebraically simple eigenvalue $\lambda = 0$ for $k = 0$;*
2. *diffusive stability: $\sigma_l D \sigma_r > 0$.*

This guarantees that the linearization of the reaction-diffusion system at the saddle-node equilibrium does not have any non-decaying solutions other than the spatially homogeneous, constant solution σ_r, and that decay of localized perturbations in the linearization is diffusive. As a consequence, we find that for $k \approx 0$ the linearization $-Dk^2 + \partial_u f(0;0)$ possesses a single eigenvalue close to the imaginary axis, which can be expanded as $\lambda(k^2) = -dk^2 + \mathrm{O}(k^4)$ with $d = \sigma_l D \sigma_r > 0$.

Existence and stability of a excitation pulse at the boundary. In order to consider traveling waves of wave speed c we introduce the comoving frame coordinate $\xi = x - ct$. Then (3.1) can be rewritten as:

$$u_t = Du_{\xi\xi} + cu_\xi + f(u;\mu). \tag{3.2}$$

Traveling wave solutions of wave speed c are equilibria $u(t,\xi) \equiv u(\xi)$ in this traveling frame and thus satisfy the equation:

$$0 = Du_{\xi\xi} + cu_\xi + f(u;\mu). \tag{3.3}$$

The following hypothesis states that there is a pulse solution that decays exponentially to 0 in forward time but only decays algebraically in backward time.

Hypothesis 1.3 (Existence of a steep pulse, SP)**.** *For $\mu = 0$, there is $c = c_* > 0$ such that the equation (3.3) has a solution $u = q(\xi)$ with the following decay properties:*

1. $\lim_{\xi\to\infty} |q(\xi)|e^{\eta_0\xi} = 0$ *for some* $\eta_0 > 0$*;*
2. $\lim_{\xi\to-\infty} |q(\xi)| = 0$ *and* $|q(\xi)| \geq C(\epsilon)e^{-\xi\epsilon}$ *for any* $\epsilon > 0$ *and all* ξ *sufficiently large.*

In addition to existence, we need some robustness or transversality information, which we choose to encode in the physically meaningful way as information on the PDE linearization at the pulse. Consider therefore the operator,

$$\mathcal{L}v := Dv_{\xi\xi} + c_*v_\xi + f'(q)v, \tag{3.4}$$

which can be considered as a closed, densely defined operator on $L^2(\mathbb{R}, \mathbb{R}^N)$, or on exponentially weighted spaces $L^2_\eta(\mathbb{R}, \mathbb{R}^N)$, with norm,

$$|u|^2_{L^2_\eta} := \int_{-\infty}^{\infty} |e^{\eta\xi}u(\xi)|^2 d\xi.$$

We will see later (Lemma 7.12) that the essential spectrum of $\mathcal{L}$ has strictly negative real part for a small, positive value of η. In addition $\mathcal{L}$ is Fredholm of index 0 for $\eta < 0$, sufficiently small. The following hypothesis restricts our investigation to examples with isolated eigenvalues of finite multiplicity.

Hypothesis 1.4 (Stability of the steep pulse)**.** *Let $\mathcal{L}$ be as defined in (3.4).*

1. $\mathrm{spec}_{L^2_\eta}\mathcal{L} \cap \{\mathrm{Re}\,\lambda \geq 0\} = \{0\}$*, algebraically simple for $\eta > 0$ and sufficiently small;*
2. *$\mathcal{L}$ is invertible in L^2_η for $\eta < 0$ and sufficiently small.*

3.2 Main results on the unfoldings of the pulse

Our results for general reaction-diffusion systems closely mirror those of the scalar example above. The coherent structures we study are qualitatively the same: pulses, steep fronts, algebraic pulses, and slow and fast fronts. In the same fashion we will study the traveling waves, fronts, and wave trains by analyzing their equivalent structures in a system of first order ODEs.

Theorem 4 (Existence of fronts, pulses and wave trains)**.** *Assume hypotheses (1.1,1.2,1.3,1.4) hold for the reaction-diffusion system (3.2). Then there exists a value $c_* > 0$ and a at least C^2 curve $\gamma(c)$, defined for $c \sim c_*$, such that $\gamma(c_*) = 0$, $\gamma(c) < 0$ for all $c \neq c_*$, $\gamma'(c)(c - c*) > 0$, and $\gamma''(c_*) < 0$. For a neighborhood $\mathcal{N}$ of $(\mu, c) = (0, c_*)$ We have one of the two following bifurcation stuctures:*

Orientation-1

1. *there exist excitation pulse solutions at $\mu = \gamma(c)$, $c > c_*$;*
2. *there exist algebraic pulses for $\mu = 0$, $0 < c < c_*$*
3. *there exist "fast" fronts for $\mu < \gamma(c)$ and "slow" fronts for $\gamma(c) < \mu < 0$, $c < c_*$;*
4. *there exist steep front solutions at $\mu = \gamma(c)$, $c < c_*$;*
5. *there exist trigger waves for $\gamma(c) < \mu < 0$ and $c > c_*$;*
6. *there exist phase waves for $\mu > 0$ and any value of $c \sim c_*$.*

Orientation-2

1. *there exist excitation pulses at $\mu = \gamma(c)$, $c < c_*$;*
2. *there exist algebraic pulses for $\mu = 0$, $c > c_*$*
3. *there exist "slow" fronts for $\mu < \gamma(c)$ and "fast" fronts for $\gamma(c) < \mu < 0$, $c > c_*$;*
4. *there exist steep front solutions at $\mu = \gamma(c)$, $c > c_*$;*
5. *there exist trigger waves for $\gamma(c) < \mu < 0$ and $c < c_*$;*
6. *there exist phase waves for $\mu > 0$ and any value of $c \sim c_*$.*

We will use the concepts of stability that were developed in the scalar example, that is, asymptotic orbital stability (definition 2.3), spectral stability (definition 2.4) and weighted stability (definition 2.5). We find that the stability of the phenomena associated with the "excitable" regime (front, pulses and trigger waves) have fixed stabilities depending on whether orientation-1 or orientation-2 hold in theorem 4. This is stated in the following result.

Theorem 5 (Stability of fronts and pulses)**.** *Assume the conditions for Theorem 4 hold. We have the following stability information depending on the alternative cases given in Theorem 4:*

1. *the steep pulse solutions are weighted asymptotically orbitally stable (AOS);*
2. *the algebraic pulses are weighted AOS in orientation-2 and unstable in orientation-1;*
3. *the slow fronts are spectrally unstable;*
4. *the fast fronts are weighted AOS;*
5. *the steep front is weighted AOS;*
6. *the trigger waves near the excitation pulses are spectrally stable in orientation-2 and unstable in orientation-1.*
7. *the phase waves near the algebraic pulses are weighted spectrally stable in orientation-2 and unstable in orientation-1.*

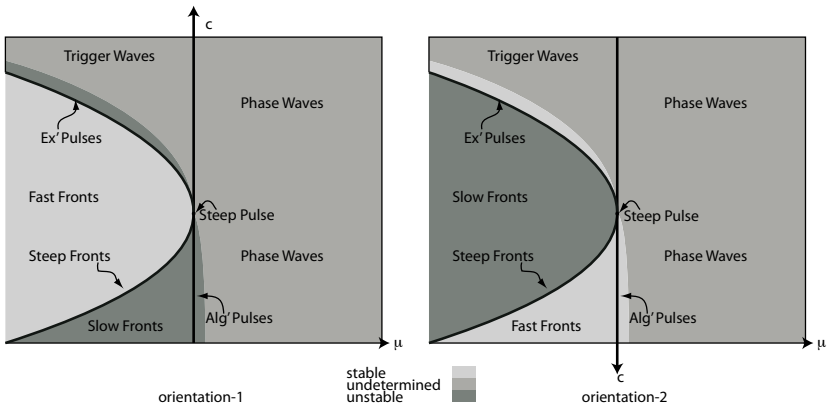

Figure 3.1: The two possible bifurcation and stability structure under the assumption of Theorem 4. The pulses are AOS and the steep fronts are WS in both cases. The stability of the algebraic pulses follows the stability of the nearby fronts. While we suspect the stability of the phase waves follows that of the trigger waves (as in the scalar example) this is an open problem.

Chapter 4

Bifurcation of pulses — existence

Pulses and fronts are solutions to the traveling wave equation (3.2), which can be viewed as a first-order differential equation in the phase space $\mathbb{R}^{2N}$. In this phase space description, pulses, fronts, and wave trains correspond to homoclinic, heteroclinic, and periodic orbits. This perspective allows our existence theorem, Theorem 4 to be viewed as a homoclinic bifurcation theorem. It turns out that such a homoclinic bifurcation has been analyzed by Chow and Lin [1], and, independently, by Deng [14]. However, the assumptions made in these articles are geometric assumptions on transversality of certain homoclinic intersections and unfoldings. Our contribution in this section is to show that our "PDE" spectral assumptions imply the "ODE" transversality assumptions in those articles.

4.1 The generic unfolding of Chow and Lin

We begin by describing the conditions stated in [1] that are necessary to completely describe the bifurcation of a particular homoclinic orbit. Let $\mathbf{q}$ be a solution to the following differential equation:

$$\mathbf{u}' = H(\mathbf{u}; (\mu_1, \mu_2)), \tag{4.1}$$

where $u \in \mathbb{R}^N$, $\xi \in \mathbb{R}$, and $(\mu_1, \mu_2) \in \mathbb{R}^2$. The function H is assumed to be at least C^3 in u, ξ and (μ_1, μ_2). Assume that equation (4.1) and $\mathbf{q}$ satisfy the following conditions.

Condition 1.1 (Saddle-Node Bifurcation)**.** *1. We assume that $H(0;0) = 0$, and that the derivative $D_{\mathbf{u}}H(0;0)$ has a simple eigenvalue $\nu_0 = 0$ with left and right eigenvectors Σ_l, Σ_r. We also assume that $D_{\mathbf{u}}F(0;0)$ does not have any other eigenvalues on the imaginary axis.*

2. $\Sigma_l D_{uu}H(0,0)(\Sigma_r, \Sigma_r) > 0$.

3. $\Sigma_l D_{\mu_1}H(0,0) > 0$, $\Sigma_l D_{\mu_2}H(0,0) = 0$.

One can therefore construct local invariant manifolds W^c and W^{ss} to the equilibrium $(0,0)$ in a fashion completely analogous to that described in the scalar example above.

Condition 1.2 (Existence of a Homoclinic)**.** *For $(\mu_1, \mu_2) = (0,0)$, equation (4.1) has a homoclinic solution $\Gamma_0 : (u,v) = \mathbf{q}(\xi)$ such that $\mathbf{q}(\xi) \in W^c(0)$ as $\xi \to \infty$ and $\mathbf{q}(\xi) \in W^{ss}(0)$ as $\xi \to -\infty$. Finally, $\frac{\mathbf{q}'}{|\mathbf{q}'|} \to \Sigma_r$ as $\xi \to \infty$.*

Condition 1.3 (A Transversality Condition)**.** *The manifolds $W^{cs}(0)$ and $W^{cu}(0)$ intersect transversely along the homoclinic $\mathbf{q}$.*

Condition 1.4 (Melnikov Condition)**.** *Assume the following, Melnikov-type integral is non-zero:*

$$\mathcal{M} := \int_{-\infty}^{\infty} \langle \Psi(\xi), \partial_{\mu_2} D_{\mathbf{u}} H(q,0)\mathbf{q} \rangle \, d\xi \quad \neq \quad 0 \tag{4.2}$$

where Ψ is a solution to the following adjoint equation:

$$\mathbf{u}' = -(D_{\mathbf{u}}H(\mathbf{q};\mu))^T \mathbf{u} \tag{4.3}$$

and contained in the weighted space $L^2_{-\eta}(\mathbb{R}^{2N})$.

If the above four conditions hold we have the following theorem regarding the homoclinic $\mathbf{q}$.

Theorem 6. *Assume that conditions 1.1, 1.2, 1.3 and 1.4 hold. Then there exists a C^1 change of parameters such that the bifurcation of phase flows of (4.1) in a neighborhood of $\mathbf{u} = 0$ is completely determined by the signs of $\mathcal{M}$, μ_1, μ_2 and a C^1 curve $\mu_1 = \gamma(\mu_2)$ which is quadratically tangent to the μ_2 axis and is contained in the half plane $\{\mu_1 | \mu_1 \leq 0\}$. The bifurcation diagram corresponding to $\mathcal{M} > 0$ will be referred to as orientation-1*

and the diagram for $\mathcal{M} < 0$ will be orientation-2. The bifurcation diagrams are depicted in (μ_1, μ_2)-space and the various cases are listed below.

Case 0: There exists a saddle node equilibrium and a homoclinic orbit $\mathbf{q}(\mu_1, \mu_2)$ such that hypothesis 1.3 holds.

Case 1: The homoclinic $\mathbf{q}(\mu_1, \mu_2)$ asymptotically approaches the equilibrium through W^{ss}.

Case 2: The homoclinic $\mathbf{q}(\mu_1, \mu_2)$ approaches the equilibrium through W^{cs}.

Case 3: The heteroclinic $\mathbf{q}(\mu_1, \mu_2)$ approaches the node through W^{ss}.

Case 4: The heteroclinic $\mathbf{q}(\mu_1, \mu_2)$ approaches the node through W^{cs}.

Case 5: There is a unique periodic solution with two equilibria.

Case 6: There is a unique periodic solution with one equilibrium.

Case 7: There is a unique periodic solution with no equilibria.

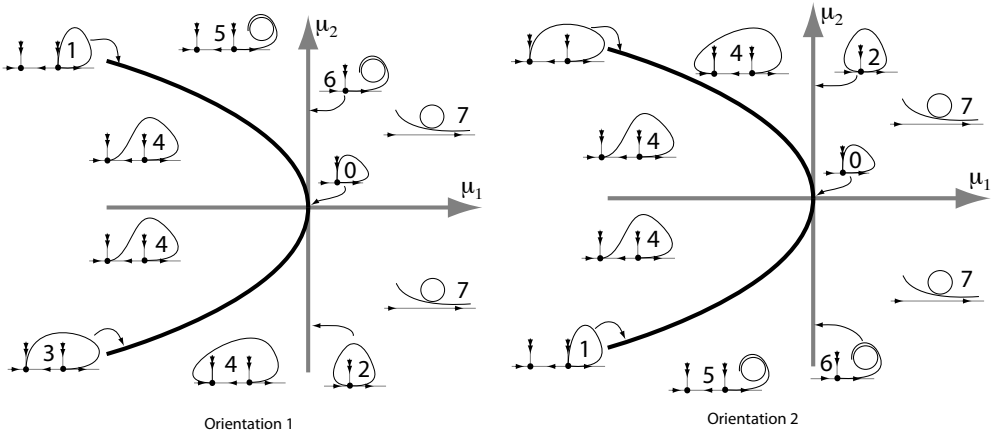

Figure 4.1: The two bifurcation diagrams corresponding to $\mathcal{M} > 0$ and $\mathcal{M} < 0$.

Remark 1.5. *As in the scalar example, let W^{ss}, W^{cs}, W^{cu} and W^c be the strong stable, center stable, center unstable and center manifolds as defined in the scalar example.*

In order to describe the decay of the various pulses and heteroclinic, we need to specify the spectrum at the equilibria at $\pm\infty$. Let the eigenvalues of the matrix

$D_{\mathbf{u}}H(q(\pm\infty), \mu_1, \mu_2)$ be $-\nu_{-N} \cdots - \nu_{-1}, \nu_0, \nu_1 \ldots \nu_M$ where:

$$-\operatorname{Re}(\nu_{-N}) \leq \cdots \leq -\operatorname{Re}(\nu_{-1}) < \operatorname{Re}(\nu_0) < \operatorname{Re}(\nu_1) \leq \cdots \leq \operatorname{Re}(\nu_M)$$

and $\nu_0 = 0$ when $\mu = \hat{c} = 0$. The eigenvalues (ν_i) are continuous functions of (μ_1, μ_2) provided the parameters are sufficiently small. This follows from spectral perturbation theorems given in classic texts such as [28]. Thus for small values of μ_1, μ_2 we have $-\operatorname{Re}(\nu_{-1}) < \operatorname{Re}(\nu_0) < \operatorname{Re}(\nu_1)$. The equilibrium splits into a stable (node) and unstable (saddle) equilibrium for $\mu < 0$. In the case of the node we refer to the eigenvalues ν_i as ν_i^n and in the case of the saddle we refer to the eigenvalues ν_i as ν_i^s. As indicated by the definition of a node and a saddle, $\operatorname{Re}(\nu_0^n) < 0$ and $\operatorname{Re}(\nu_0^s) > 0$. In terms of these decay rates, we can talk about the various manifolds more explicitly:

$W^{ss}(x_0)$	The strong stable manifold decays $\mathrm{O}(e^{-\nu_{-1}\xi})$ as $\xi \to \infty$ to x_0.
$W^{cs}(x_0)$	The center stable manifold decays $\mathrm{O}(e^{-\nu_0\xi})$ as $\xi \to \infty$ or algebraically if $\nu_0 = 0$ to x_0.
$W^{cu}(x_0)$	The center stable manifold decays $\mathrm{O}(e^{\nu_0\xi})$ as $\xi \to -\infty$ or algebraically if $\nu_0 = 0$ to x_0.

Remark 1.6 (Notation)**.** *We will primarily be concerned with the spectrum of the node, unless otherwise noted* $\nu_0 = \nu_0^n$*. Let* $\gamma_+(\mu)$ *be the upper half of the curve* $\gamma(\mu_2)$ *and* $\gamma_-(\mu)$ *the lower half.*

4.2 Existence of coherent structures from Chow and Lin

The bifurcations described in Theorem 6 directly implies our existence result, Theorem 4. We take μ_1 to be our bifurcation parameter μ, and μ_2 to be the wave speed recentered at 0, that is $c - c_*$. We proceed to relate the structures that are equilibria in the comoving frame equation (3.2) to coherent structures of the original PDE. This follows exactly the identifications made in the scalar example. Homoclinics and heteroclinics of (3.2) correspond to pulses and fronts respectively of (3.1). Similarly, periodic orbits of (3.2) can be interpreted as wave trains in (3.1). We refer to wave trains in the presence of equilibria as *trigger waves* and waves trains without equilibria as *phase waves.*

4.3 Interpretation in terms of the framework of Chow and Lin.

As noted above, the results of Chow and Lin directly infers the existence theorem, Theorem 4. Therefore, our task is to show that our hypotheses imply that their conditions 1.1, 1.2, 1.3 and 1.4 hold for our traveling-wave equation cast as a first-order differential equation with parameters $\mu_1 = \mu$ and $\mu_2 = c - c_* = \hat{c}$.

To begin, we rewrite equation (3.3) as the following $2N$ dimensional first order system:

$$\begin{aligned} u' &= v \\ v' &= -D^{-1} f(u;\mu) - cD^{-1} v. \end{aligned} \tag{4.4}$$

Our assumption on the existence of an excitation pulse implies that (4.4) possesses a homoclinic orbit to the origin for $\mu = 0$ and $c = c_*$. In order to state the conditions for the main theorem in [1], we introduce some notation and linearizations at the homoclinic orbit. Let $q(\xi)$ be the steep pulse, then $(q, q')^T =: \mathbf{q}$ is a homoclinic orbit to (4.4). We will consider solutions to the linearization at $\mathbf{q}$,

$$\begin{pmatrix} u \\ v \end{pmatrix}' = \begin{pmatrix} 0 & 1 \\ -D^{-1} f'(q(\xi), 0) & -cD^{-1} \end{pmatrix} \begin{pmatrix} u \\ v \end{pmatrix}. \tag{4.5}$$

Equations (4.4) and (4.5) can be written in a more compact notation as:

$$\mathbf{u}' = F(\mathbf{u};\mu,c), \tag{4.6}$$

$$\mathbf{v}' = D_{\mathbf{u}} F(\mathbf{q};\mu,c)\mathbf{v}. \tag{4.7}$$

Using equation (4.4) as the differential equation (4.1) in the conditions for Theorem 6, we can immediately see the consequences of Theorem 6 in terms of our existence Theorem 4. For any $\mathbf{u} = (u(\xi), u'(\xi))$ that is a solution of (4.4), the function $u(\xi)$ is a solution to (3.2). Therefore we can interpret the upper component of homoclinic, heteroclinic and periodic solutions of (4.4) as pulse, front and wave train solutions of (3.2) respectively. The particular decay rates provided by Theorem 6 will prove to be useful in our later stability analysis. We summarize the interpretation of the phase plane structures are PDE solutions in the following.

- The case 0 homoclinic implies the steeply decaying steep pulse.
- The case 1 homoclinics imply the steeply decaying excitation pulses.
- The case 2 homoclinics imply the weakly decaying algebraic pulses.
- The case 3 heteroclinics imply the quickly decaying steep fronts.
- The case 4 heteroclinics slowly decaying slow and fast fronts.
- The case 5 and 6 periodics imply the trigger waves.
- the case 7 periodics imply the phase waves.

In our existence theorem, we state that there is an alternative bifurcation and stability diagram where the orientation of the wave speed is reversed. The orientation of the bifurcation diagram depends on the sign of the Melnikov integral in Condition 1.4. This will play a major role in the stability analysis, but is unimportant in the confirmation of the conditions for Theorem 6.

4.4 ODE saddle-node

We begin by showing that the first order system (4.4) undergoes a saddle-node bifurcation at the equilibrium $(u, \mu) = (0, 0)$. Recall that we have assumed that the homoclinic $q(\xi)$ terminates at the equilibrium $(0, 0)$.

Lemma 4.7. *Assume Hypotheses 1.1 and 1.2. Then the traveling-wave ODE (3.3) undergoes a saddle-node bifurcation which satisfies condition 1.1 above.*

Proof.

Step 1: Linearization We claim that the traveling-wave ODE linearization at the equilibrium $(u, v) = 0$ possesses an algebraically simple eigenvalue $\nu = 0$, with eigenvector $(\sigma_r, 0) \in \mathbb{R}^{2N}$. Indeed, the ODE linearization is given by the block matrix

$$\begin{pmatrix} 0 & 1 \\ -D^{-1}f' & -cD^{-1} \end{pmatrix}.$$

The kernel of this matrix is given by vector of the form $(\sigma_r, 0)$, where σ_r lies in the kernel of $f'(0;0)$ as was assumed in Hypothesis 1.1. This shows that the eigenvalue $\nu = 0$ is geometrically simple and $\Sigma_r = (\sigma_r, 0)^T$ is the eigenvector. We next show that the eigenvalue is actually algebraically simple. Assume to the contrary that 0 is not algebraically simple and that equation for a principal vector (a, b) to Σ_r is given by

$$\begin{pmatrix} 0 & 1 \\ -D^{-1}f' & -cD^{-1} \end{pmatrix} \begin{pmatrix} a \\ b \end{pmatrix} = \begin{pmatrix} \sigma_r \\ 0 \end{pmatrix}.$$

Solving for a and b gives us:

$$b = \sigma_r, \quad -D^{-1}f'a - cD^{-1}b = 0.$$

There we have that,

$$\sigma_l f' u = \sigma_l c \sigma_r,$$

where the left hand side is zero since σ_l annihilates the range of f'. However, the right-hand side is assumed to be positive in Hypothesis 1.2 so there can be no principle eigenvectors.

Finally, we show that there are no purely imaginary eigenvalues of $D_{\mathbf{u}}F(0;0)$. Assume that (u, v) is an eigenvector to the imaginary eigenvalue $\mathrm{i}k \neq 0$. Then one readily sees that u is in the kernel of $-Dk^2 + c\mathrm{i}k + f'(0;0)$, which contradicts Hypothesis (1.2), part (1).

Step 2: Unfolding We have the following computation for $\partial_\mu F(0;0)$:

$$\partial_\mu F(0;0) = \begin{pmatrix} 0 & 0 \\ -D^{-1}\partial_\mu f(0;0) & 0 \end{pmatrix}.$$

To determine Σ_l we need to solve:

$$(a, b) \begin{pmatrix} 0 & 1 \\ D^{-1}f'(0;0) & -D^{-1}c \end{pmatrix} = 0.$$

Therefore $\Sigma_l = (bD^{-1}c, b)$ where $bD^{-1}f'(0;0) = 0$. Hence $bD^{-1} = \sigma_l$. The unfolding condition then can be expressed as follows:

$$\Sigma_l \partial_\mu F(0;0) = bD^{-1}\partial_\mu f(0;0) = \sigma_l \partial_\mu f(0;0) \neq 0,$$

Where $\sigma_l \partial_\mu f(0;0) \neq 0$ follows from (Hyp 1.1).

Step 3: Quadratic nonlinearity If we consider the second derivative $D_{\mathbf{uu}}F(0;0)$ the only non-zero mixed or second derivative is the $D_{uu}f(0;0)$ term. This gives us:

$$\Sigma_l D_{\mathbf{uu}}F(0;0)(\Sigma_r,\Sigma_r) = -bD^{-1}D_{uu}f(0;0)(\sigma_r,\sigma_r) = \sigma_l D_{uu}f(0;0)(\sigma_r,\sigma_r) \neq 0$$

where $\sigma_l D_{uu}f(0;0)(\sigma_r,\sigma_r) \neq 0$ is assumed in (Hyp 1.1).

■

4.5 Orbit-flip homoclinic

Our assumptions on the existence of a steep pulse guarantee that there exists a homoclinic connection to the origin in the traveling-wave ODE. In fact, using the dynamics on the center-manifold, one can readily see that the asymptotics of the steep pulse are algebraic as $\xi \to -\infty$ (see [18]),

$$|\mathbf{q}(\xi)| = \mathrm{O}(\frac{1}{\xi})$$

and exponential as $\xi \to +\infty$,

$$|\mathbf{q}(\xi)| \leq K(\epsilon)e^{-\xi(\eta_0-\epsilon)} \quad \text{for any } \epsilon > 0.$$

Since $\mathbf{q}$ decays weakly as $\xi \to -\infty$ it necessarily approaches 0 through a local center manifold $W^c(0)$. Because $\mathbf{q}$ decays exponentially as $\xi \to \infty$, it is necessarily contained in the strong stable manifold $W^{ss}(0)$.

4.6 ODE transverse intersection

We now show that our Hypothesis 1.4 implies Condition 1.3. Consider the linearized ODE at the homoclinic, $\mu = 0$, (4.5). This system is a linear ODE which possesses an exponential trichotomy. More precisely, there exist subspaces $E^{cs}_+ = E^{ss}_+ \oplus E^c_+$, and $E^{cu}_- = E^{uu}_- \oplus E^c_-$, such that E^{ss}_+ and E^{uu}_- consist precisely of the initial values (u,v) at $\xi = 0$ to solutions which decay exponentially as ξ goes to $+\infty$ and $-\infty$ respectively. Solutions in $E^c_\pm$ are those that decay algebraically. Note that $E^c_\pm$ are one-dimensional. Transversality of the intersection of W^{cu} and W^{cs} therefore is equivalent to the intersection $E^{cs}_+ \cap E^{cu}_-$ being one-dimensional. In the following we argue by contradiction. Assume that the intersection is more than one-dimensional. We will show that this

implies the existence of a solution (u_n, v_n) in the intersection of E_-^{uu} and E_+^{cs}. One can then readily see that the first component of this solution is contained in the kernel of $\mathcal{L}$ in L^2_η with $\eta < 0$, small enough, which contradicts our assumption hypothesis 1.4.

In order to exhibit this solution (u_n, v_n) in the intersection of E_-^{uu} and E_+^{cs}, we first consider the derivative of the pulse $\mathbf{q}'(\xi)$. By the decay assumptions on q, $\mathbf{q}'(\xi)$ is contained in $E_+^{ss} \cap E_-^{cu}$ but not in the intersection $E_+^{ss} \cap E_-^{uu}$. We can therefore choose E_-^c to be spanned by $\mathbf{q}'$, and span $(q') = E_-^c \cap E_+^{ss}$.

Since we assumed that the intersection $E_-^{cu} \cap E_+^{cs}$ is more than one-dimensional, there is $\mathbf{u} \in E_-^{cu} \cap E_+^{cs}$, linearly independent of $\mathbf{q}'$. Then we can decompose

$$\mathbf{u} = \mathbf{u}_-^{uu} + \mathbf{u}_-^c$$

where $\mathbf{u}_-^{uu} \in E_-^{uu}$ and $\mathbf{u}_-^c \in E_-^c$. However, E_-^c is spanned by $\mathbf{q}'$. Therefore we can write:

$$\mathbf{u} = \mathbf{u}_-^{uu} + \rho\mathbf{q}'.$$

Since $\mathbf{u}$ is in $E_-^{cu} \cap E_+^{cs}$, so is $\mathbf{u} - \rho\mathbf{q}' = \mathbf{u}_-^{uu}$. By construction, $\mathbf{u}_-^{uu} \in E_-^{uu}$ and we have found the desired nontrivial intersection of E_-^{uu} and E_+^{cs}. This contradicts the second part of hypothesis 1.4 and proves that condition 1.3 is implied by our original set of hypotheses.

4.7 ODE transverse unfolding

Here we wish to show that the hypothesized simplicity of the zero eigenvalue in a weighted space (hypothesis 1.4) is equivalent to the Melnikov condition 1.4. This argument is quite a bit more involved than the previous lemmas. The proof proceeds in several steps. We first show that the linearization at the pulse is actually Fredholm of index zero in the weighted spaces for small positive weights η. We will then readily see that the zero eigenvalue is geometrically simple. In the last step, we show that the kernel of the adjoint is not in the range if and only if the Melnikov integral does not vanish. We conclude this section with a remark on an alternative formulation of this hypothesis as used in [14].

The linearization is Fredholm of index 0. By hypothesis 1.4, we know $q \to 0$ as $\xi \to \pm\infty$. To understand the behavior of the essential spectrum it is useful to

consider the "background linearization," that is the operator $\mathcal{L}$ where q is replaced by the equilibria. Define:

$$\mathcal{L}_0 = D\partial_\xi^2 + c\partial_\xi + \partial_u f(0,0) \quad \mathcal{L}_0 : \mathcal{D}(\mathcal{L}_0) \subset L^2(\mathbb{R}, \mathbb{R}^N) \to L^2(\mathbb{R}, \mathbb{R}^N). \tag{4.8}$$

We begin by proving some results on the dispersion relation $d(k, \lambda)$.

Lemma 7.8. *A complex number λ belongs to the essential spectrum of $\mathcal{L}_0$ if and only if there is a $k \in \mathbb{R}$ such that*

$$d(k, \lambda) = det(-Dk^2 - cik + \partial_u f(0,0) - \lambda) = 0 \tag{4.9}$$

Proof. See lemma 2.1 of [29] for a complete proof. ∎

From hypothesis 1.1 we have the following lemma regarding $\mathcal{L}_0$.

Lemma 7.9. *We have the following expansions:*

1. $d(0,0) = 0$
2. $\frac{\partial d}{\partial \lambda}|_{\lambda=0,\nu=0} \neq 0$

For $k \sim 0$ there is a unique solution $\lambda(k) \sim 0$ to $d(\lambda, k) = 0$, and we have the expansion $\lambda(0) = 0$ and $\frac{d\lambda}{dk}|_{(\lambda=0,\nu=0)} = -ci$.

Proof. By the saddle-node assumption (1.1) the matrix $\partial_u f(0,0)$ has an algebraically simple zero eigenvalue. Therefore $\det(\partial_u f(0,0)) = 0$ and $\partial_\lambda \det(\partial_u f(0,0) - \lambda) \neq 0$. This proves (1) and (2). Also,

$$ci\partial_\lambda \det(\partial_u f(0,0) - \lambda) = \partial_k \det(-Dk^2 - cik + \partial_u f'(0,0) - \lambda),$$

so that $ci\partial_\lambda d(0,0) = \partial_k d(0,0)$. By the implicit function theorem, we have a unique solution $\lambda(k)$ with $\partial_k \lambda = ci\partial_k d(0,0)/\partial_\lambda d(0,0)$.

∎

Essential spectrum in exponentially weighted spaces. We are interested in considering stability of the traveling pulse, however, by assumption the essential spectrum touches the imaginary axis. The presence of essential spectrum on the imaginary axis does not necessarily imply "absolute instability." To investigate the stability we consider the operator $\mathcal{L}$ on the exponentially weighted space $L^2_\eta(\mathbb{R})$ defined as follows:

$$L^2_\eta(\mathbb{R}) = \{u | e^{\eta\xi} u \in L^2(\mathbb{R}, \mathbb{R}^N)\}. \tag{4.10}$$

First it is important to notice that by hypothesis (1.3), $q \in L^2_\eta$ provided that $\eta_0 > \eta$. Instead of considering $\mathcal{L}$ on $L^2_{0,\eta}(\mathbb{R})$ we can consider the operator $\mathcal{L}_\eta$ on $L^2(\mathbb{R})$ derived from the following diagram:

$$\begin{array}{ccc} & \mathcal{L} & \\ L^2_\eta & \longrightarrow & L^2_\eta \\ e^{-\eta\xi} \uparrow & & \uparrow e^{-\eta\xi} \\ L^2 & \longrightarrow & L^2 \\ & \mathcal{L}_\eta. & \end{array} \tag{4.11}$$

Thus $\mathcal{L}_\eta$ is given by the following:

$$\mathcal{L}_\eta = e^{\eta\xi}\mathcal{L}e^{-\eta\xi} = D(\partial_\xi - \eta)^2 + c(\partial_\xi - \eta) + \partial_u f(q, 0), \tag{4.12}$$

and $\mathcal{L}_{0,\eta}$ is given by

$$\mathcal{L}_{0,\eta} = e^{\eta\xi}\mathcal{L}e^{-\eta\xi} = D(\partial_\xi - \eta)^2 + c(\partial_\xi - \eta) + \partial_u f(0, 0). \tag{4.13}$$

We have the following regarding the effect of the exponential weights on the essential spectrum.

Lemma 7.10. *The essential spectrum of $\mathcal{L}_\eta$ is contained in the open left half of the complex plane for η such that $\eta > 0$ but sufficiently small.*

Proof. By hypothesis 1.4 the essential spectrum of $\mathcal{L}_\eta$ is contained strictly in the left half of the complex plane. Since $\mathcal{L}_0$ is a compact perturbation of $\mathcal{L}$, they share the same essential spectrum ([16].) Thus we calculate,

$$\frac{d\lambda}{d\eta}|_{\lambda=0,k=0,\eta=0}. \tag{4.14}$$

If we again consider the dispersion relation in terms of ν instead of ik we note that under the exponential weights the dispersion relation of $\mathcal{L}_0$ becomes:

$$\begin{aligned} d_\eta(k,\lambda) &= D(-k^2 - 2ik\eta + \eta^2) + c(-ik - \eta) + \partial_u f(0,0) - \lambda \\ &= D(-k\mathrm{i} + \eta)^2 + c(\mathrm{i}k + eta) + \partial_u f(0,0) - \lambda \end{aligned}$$

which is equal to:

$$d(k + \mathrm{i}\eta, \lambda). \tag{4.15}$$

The solution $\lambda_1(k)$ that we found above can be analytically continued to a solution $\lambda_1(k + i\eta)$. From our previous calculations in lemma 7.9

$$\frac{d\lambda}{d\eta}|_{\lambda=0,k=0} = i\frac{d\lambda}{dk}|_{\lambda=0,k=0} = -c < 0 \tag{4.16}$$

Thus the essential spectrum is moved locally into the left half of the complex plane ■

Lemma 7.11. *The operator $\mathcal{L}_0 : L^2_\eta \to L^2_\eta$ is invertible.*

Proof. From Lemma 7.10 we know that the essential spectrum of $\mathcal{L}_0$ is shifted into the left half of the complex plane on L^2_η for an appropriate value of η. Since $\mathcal{L}_0$ only has essential spectrum, the operator is in fact invertible on L^2_η. ■

This result can be extended from $\mathcal{L}_0$ to $\mathcal{L}$ by noticing that $\mathcal{L}$ is a relatively compact perturbation of $\mathcal{L}_0$. It is well known (for example see [16]) that the essential spectrum of the operator $\mathcal{L}$ is the same as $\mathcal{L}_0$ under compact perturbations and is bounded away from the imaginary axis in the left half of the complex plane. This gives us the following extension to the operator $\mathcal{L}$.

Lemma 7.12. *The operator $\mathcal{L} : L^2_\eta \to L^2_\eta$ is Fredholm of index zero.*

Unlike $\mathcal{L}_0$, $\mathcal{L}$ is not invertible because it necessarily possesses a zero eigenvalue, which we assumed to be algebraically simple. The eigenfunction is given by q', which is contained in L^2_η for η small as above since by the traveling pulse assumption q' decays exponentially in backward time and algebraically in forward time.

Remark 7.13. *The spectral assumptions also imply that the linearization at the equilibrium possesses precisely $N-1$ eigenvalues with positive real part and N eigenvalues*

with negative real part at $\mu = 0$. To see this, one notices that the dispersion relation does not possess any roots $\nu \in \mathrm{i}\mathbb{R}$ for $\lambda > 0$. This follows since for large λ the roots ν solve the equation:

$$\det(D\nu^2 - \lambda - \mathrm{O}(1)) = 0$$

and therefore $\frac{\nu_\pm}{\sqrt{\lambda}} = \pm\frac{1}{\sqrt{d_j}} + \mathrm{O}(1)$. Hence, for all $\lambda > 0$ we have N roots with positive real parts and N roots with negative real parts. For $\lambda = 0$, let $\nu_0 = 0$ and all other solutions non-zero. Since the 'group velocity' $\frac{\mathrm{d}\nu_0}{\mathrm{d}\lambda} = \frac{1}{c} > 0$, then the zero root must have come from the positive roots, thus proving the assertion.

Algebraic simplicity implies nonzero Melnikov. In order to construct the bifurcation diagram for the steep pulse, we need information about the transversality of the homoclinic connection that corresponds to the steep pulse. This is provided by the Melnikov integral $\mathcal{M}$. In terms of the first order system we define the Melnikov integral as the following function:

$$\mathcal{M} = \int_{-\infty}^{\infty} \langle \Psi, \partial_c (D_{\mathbf{u}} F(q;0)\mathbf{q}) \rangle \, d\xi$$

where Ψ is the unique (up to muliplication by a constant) solution to the adjoint linear equation:

$$\mathbf{u}' + D_{\mathbf{u}} F(q;0)^T \mathbf{u} = 0, \tag{4.17}$$

which belongs to $L^2_{-\eta}(\mathbb{R}^N)$. We know that such a solution exists because $\mathcal{L}$ is Fredholm of index zero in $L^2_\eta(\mathbb{R}^N)$. Therefore the L^2-adjoint $\mathcal{L}^*$ possesses an algebraically simple zero eigenvalue, as well. One then verifies easily that the kernel of $\mathcal{L}^*$ is isomorphic to the set of solutions to (4.17) in $L^2_{-\eta}(\mathbb{R}^N)$. Having defined the Melnikov integral, we can now state the main result of this section.

Lemma 7.14. *The eigenvalue $\lambda = 0$ is algebraically simple if and only if*

$$\mathcal{M} \neq 0. \tag{4.18}$$

Proof. Again we are are considering the differential equation

$$Dv_{\xi\xi} + cv_\xi + f'(q)v = 0. \tag{4.19}$$

This equation has the obvious bounded solution q' since we assume that (3.3). For ease of notation let $q' = \kappa$. Now we consider the algebraic multiplicity of the eigenvalue $\lambda = 0$ for the operator $\mathcal{L}$ on the exponentially weighted space $L^2_\eta(\mathbb{R}, \mathbb{R}^N)$ described above. If 0 is not algebraically simple then there is a bounded function e_1 so that:

$$D(e_1)_{\xi\xi} + c(e_1)_\xi + f'(q)e_1 = \kappa. \tag{4.20}$$

In other words $\mathcal{L}e_1 = \kappa$. In the previous section we showed that $\mathcal{L}$ is Fredholm of index zero in the weighted eigenspace. Thus $\text{Range}(\mathcal{L}) \perp \text{Ker}(\mathcal{L}^*)$ where $\mathcal{L}^*$ indicates the adjoint operator (see [16]). Of course it is preferable to work on L^2. So we again consider the operator $\mathcal{L}_\eta$ and the adjoint $\mathcal{L}^*_{-\eta}$. Notice that the adjoint operator can be written explicitly as:

$$D(\partial_\xi + \eta)^2 - c(\partial_\xi + \eta) + (\partial_u f(q, 0))^T. \tag{4.21}$$

Now note that $\kappa e^{\eta\xi}$ the unique bounded solution to $\mathcal{L}_\eta u = 0$. Likewise there exists a bounded solution $\kappa^* e^{-\eta\xi}$ to the adjoint weighted problem. In the end we have that κ is algebraically simple if and only if:

$$\int_{-\infty}^{\infty} \langle \kappa^*, \kappa \rangle \, d\xi \neq 0. \tag{4.22}$$

We find $\mathcal{M}$ explicitly.

$$\mathcal{M} = \int_{-\infty}^{\infty} \left\langle \Psi, \partial_c(A(\lambda)) \begin{pmatrix} q_0' \\ q_0'' \end{pmatrix} \right\rangle d\xi = \int_{-\infty}^{\infty} \left\langle \Psi(\xi), \begin{pmatrix} 0 \\ -D^{-1}q' \end{pmatrix} \right\rangle d\xi = \int_{-\infty}^{\infty} < \psi_2, -D^{-1}\kappa > d\xi \tag{4.23}$$

where we define the vector $\psi(\xi)$ as

$$\psi(\xi) = \begin{pmatrix} \psi_1 \\ \psi_2 \end{pmatrix}. \tag{4.24}$$

If $\psi(\xi)$ is a solution of the adjoint ODE then

$$\frac{d}{d\xi} \begin{pmatrix} \psi_1 \\ \psi_2 \end{pmatrix} = \begin{pmatrix} 0 & (\partial_u f(q, 0))^T D^{-1} \\ -\mathbb{I} & D^{-1}c \end{pmatrix} \begin{pmatrix} \psi_1 \\ \psi_2 \end{pmatrix}. \tag{4.25}$$

Considering only ψ_2' we see

$$\psi_2' = -\psi_1 + D^{-1}c\psi_2. \tag{4.26}$$

Differentiating both sides gives us

$$\psi_2'' = -\psi_1' + D^{-1}c\psi_2'. = -\partial_u f(q,0)^T D^{-1}\psi_2 + D^{-1}c\psi_2' \tag{4.27}$$

Thus ψ_2 is the unique bounded solution to (4.27) and

$$\psi_2 = D\kappa^* \tag{4.28}$$

The equation (4.23) reduces to:

$$\int_{-\infty}^{\infty} D\kappa^* \cdot D^{-1}\kappa d\xi = \int_{-\infty}^{\infty} \kappa^* \cdot \kappa d\xi \tag{4.29}$$

Thus $\mathcal{M} \neq 0$ if and only if $\lambda = 0$ is algebraically simple. ∎

4.7.1 Transversality of an extended system

In this section we prove that the transverse crossing can be interpreted as a transversality in an extended ODE. This is actually the condition used in [14] for the cases of pitchfork and transcritical bifurcations.

Lemma 7.15. *The integral condition (*4.18*) is also equivalent to the transversality of the center-unstable and strong stable manifold in the extended system where c is considered as a variable,*

$$(\cup_c W_c^{\mathrm{cu}}) \cap (\cup_c W_c^{\mathrm{ss}}) \text{ transversely along } (q, q')^T. \tag{4.30}$$

Proof. Consider the extended system where we treat c as a variable.

$$\begin{aligned} v' &= w \\ w' &= -D^{-1}f'(v) - D^{-1}cw \\ c' &= 0 \end{aligned} \tag{4.31}$$

For each c, there exist strong stable and center-unstable manifolds, which depend smoothly on c, so that the intersection in (4.30) is the intersection of two smooth manifolds. In order to investigate transversality of the intersection, we study the tangent

spaces, which are spanned by solutions to the linearize around the solution $(q_0, q_0', c^*)^T$:

$$\begin{aligned} \bar{u}' &= \bar{w} \\ \bar{w}' &= -D^{-1}f'(q_0)\bar{v} - D^{-1}c^*\bar{w} - D^{-1}q_0'\bar{c}. \\ \bar{c}' &= 0 \end{aligned} \tag{4.32}$$

The tangent space to the union of center-unstable manifolds consists of solutions that are bounded in negative time. The tangent space to the union of strong stable manifolds consists of solutions that are exponentially decaying in forward time in the $(\bar{u}, \bar{w})$-component, with some bounded $\bar{c}$.

Note that we still have the trivial solution $(q_0', q_0'', 0)^T$ to (4.32). Suppose that the intersection in (4.30) is non-transverse. Then there is another, linearly independent solution $(g_1, g_2, c^{**})^T$ with the prescribed growth conditions. Such a solution solves the equation:

$$\begin{aligned} \bar{u}' &= \bar{w} \\ \bar{w}' &= -D^{-1}f'(q_0)\bar{v} - D^{-1}c^*\bar{w} - D^{-1}q_0'c^{**} \end{aligned} \tag{4.33}$$

or

$$\begin{pmatrix} \bar{u} \\ \bar{w} \end{pmatrix}' = \begin{pmatrix} 0 & 1 \\ -D^{-1}f'(q_0) & -D^{-1}f'(q_0) \end{pmatrix} \begin{pmatrix} \bar{u} \\ \bar{w} \end{pmatrix} + \begin{pmatrix} 0 \\ -D^{-1}q_0'c^{**} \end{pmatrix}, \tag{4.34}$$

where $\bar{u}, \bar{w} \in L^2_\eta$ and c^{**} is an arbitrary constant. Now we take the L^2 inner product with the unique adjoint solution $\Psi \in L^2_{-\eta,0}(\mathbb{R})$, defined in the previous section and simplify

$$\int_{-\infty}^{\infty} \left\langle \Psi, \begin{pmatrix} \bar{u} \\ \bar{w} \end{pmatrix}' - \begin{pmatrix} 0 & 1 \\ -D^{-1}f'(q_0) & -D^{-1}f'(q_0) \end{pmatrix} \begin{pmatrix} \bar{u} \\ \bar{w} \end{pmatrix} \right\rangle d\xi \tag{4.35}$$

$$= \int_{-\infty}^{\infty} \left\langle \Psi, \begin{pmatrix} 0 \\ -D^{-1}q_0'c^{**} \end{pmatrix} \right\rangle d\xi \tag{4.36}$$

If we integrate (4.35) by parts we have the following:

$$\left\langle \Psi, \begin{pmatrix} \bar{u} \\ \bar{w} \end{pmatrix} \right\rangle \Bigg|_{-\infty}^{\infty} - \int_{-\infty}^{\infty} \left\langle \Psi' + \begin{pmatrix} 0 & -(D^{-1}f'(q_0))^T \\ 1 & -D^{-1}c^* \end{pmatrix}, \begin{pmatrix} \bar{u} \\ \bar{w} \end{pmatrix} \right\rangle \, d\xi = 0 \tag{4.37}$$

Therefore (4.36) is also zero and we have:

$$\int_{-\infty}^{\infty} \psi_2 D^{-1}q_0'c^{**} \, d\xi = c^{**} \int_{-\infty}^{\infty} \kappa^*\kappa d\xi = 0. \tag{4.38}$$

This contradicts (4.22) so we get that 0 is algebraically simple if and only if the manifolds intersect transversely. ■

4.8 Other codimension-one bifurcations

We are primarily interested in the case where the non-linearity has a saddle-node bifurcation. As was explained in the introduction, a saddle-node bifurcation is easily interpreted as the bifurcation between oscillatory and excitable dynamics. However, as it turns out, the following analysis can be extended to both pitchfork and transcritical bifurcations. We may use transcritical bifurcation hypotheses in place of the saddle-node hypothesis (1.1) and obtain similar stability results for the appropriate bifurcation diagrams. The exact results and difference will be addressed after the main result is proved.

Hypothesis 8.16 (Transcritical)**.** *The function $f(u,\mu)$ satisfies the conditions for transcritical bifurcation in the ODE $u' = f(u,\mu)$. Specifically that is:*

1. $f(0,\mu) = 0$ *for all* μ*;*
2. $\sigma_l D_u^2 f(0,0)(\sigma_r,\sigma_r) > 0$*;*
3. $\sigma_l D_{u\mu}^2 f(0,0)\sigma_r > 0$*;*
4. $\sigma_l D_{uc}^2 f(0,0)\sigma_r = 0$.

Similar results were given by Deng [14] regarding the case of transcritical and pitchfork bifurcations. The statement of the theorem in Deng's paper is virtually identical to Theorem 6 except the hypothesis that F satisfies the saddle-node conditions (hypothesis 1.1) is replaced with the condition for a transcritical (hypothesis 8.16). Additionally, Deng assumes a condition of the transversality of the unstable and stable manifolds in the extended system instead of the integral condition as in the paper of Lin and Chow. However, these conditions were shown to be equivalent in Lemma 7.14.

We may replace the saddle-node hypothesis with a transcritical hypothesis and obtain a similar stability result to Theorem 5. While the same is almost true of the pitchfork bifurcation, we would need to modify our assumptions regarding the existence of a steep pulse, so we do not pursue the result here.

Theorem 7 (Transcritical)**.** *There exists a C^1 change of variables such that the bifurcation of phase flows in a neighborhood of $x = 0$ is completely determined by the signs of μ and $\hat{c}$, and a C^1 curve $\mu = \gamma(\hat{c})$ which satisfies $\partial_c\gamma(0) < 0$. The bifurcation diagram is depicted in $(\mu, \hat{c})$-space. There various cases are listed below.*

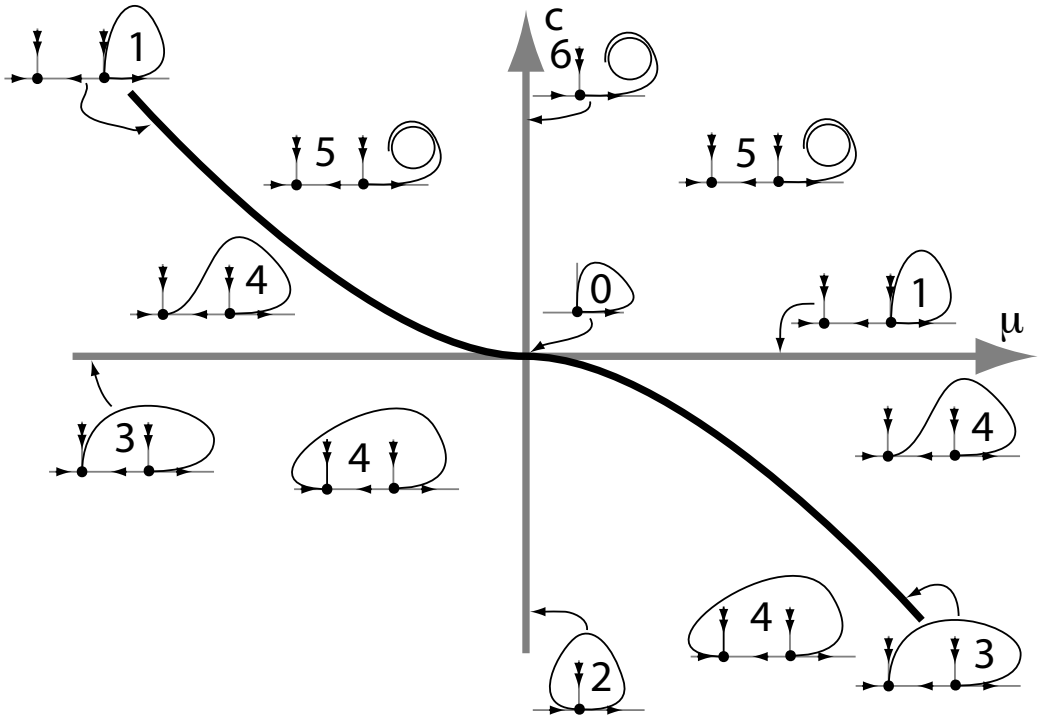

Figure 4.2: Bifurcation diagram in the transcritical case for $\mathcal{M} > 0$.

The asymptotics of the various homo/heteroclinics are described in the following list.

Case 0: There exists a saddle node equilibrium and a homoclinic orbit $\mathbf{q}(\mu_1, \mu_2)$ such that hypothesis 1.3 holds.

Case 1: The homoclinic $\mathbf{q}(\mu_1, \mu_2)$ asymptotically approaches the equilibrium through W^{ss}.

Case 2: The homoclinic $\mathbf{q}(\mu_1, \mu_2)$ approaches the equilibrium through W^{cs}.

Case 3: The heteroclinic $\mathbf{q}(\mu_1, \mu_2)$ approaches the node through W^{ss}.

Case 4: The heteroclinic $\mathbf{q}(\mu_1, \mu_2)$ approaches the node through W^{cs}.

Case 5: There is a unique periodic solution with two equilibria.

Case 6: There is a unique periodic solution with one equilibria.

Chapter 5

Stability of bifurcating coherent structures.

We now proceed to consider the PDE stability or instability of the pulses, fronts and wave trains. We will begin by considering the spectrum of the linearization at the steep pulse, excitation pulses and fronts for small parameter values μ and c. We will then appeal to the results in [17] to show non-linear stability. The spectrum of the linearization of the excitation pulses is sectorial and confined to the left half plane except for a single eigenvalue at zero, which is the requirement for asymptotic orbital stability (AOS). The fronts and excitation pulses have similar spectral qualities when considered in an appropriate exponentially weighted space. Therefore, these structures will be seen to be asymptotically stable in appropriately weighted spaces (WS.)

The spectrum of the steep fronts and excitation pulses will give us a framework from which to approach the other fronts, algebraic pulses and trigger waves. The fronts are at best stable in a weighted space because of destabilizing essential spectrum in the right half of the complex plane. Since the steep fronts divide the slow and fast fronts, and the essential spectrum is away from the imaginary axis in the weighted space, the spectral stability will be determined by a single eigenvalue in a neighborhood of zero. In the case of the steep fronts and pulses, q' was the eigenfunction for the zero eigenvalue. However, this eigenvalue is allowed to move in the weighted space because the fast and slow fronts decay slowly and subsequently their derivatives (q') are not included in the

weighted space. Therefore, we use perturbation theory to determine the movement of the zero eigenvalue as we cross the steep fronts in the $c - \mu$ plane. We will use the results of [30] to determine how the stability of the trigger waves with respect to the stability of the nearby fronts.

Finally, we discover that the same quantity that determines the stability of the triggers also controls the direction of the movement of the zero eigenvalue near the steep fronts. This result allows us four different stability diagrams depending on this quantity and the orientation of the wave speed (whether we are in case 1 or 2 of the existence theorem.) It turns out that only one stability diagram is possible for each of the two cases in accordance with the conjectures of van Saarloos.

5.1 Stability of excitation pulses and steep fronts

In this section we prove that the excitation pulses are asymptotically stable and that the steep fronts and algebraic pulses are only stable when considered on weighted spaces. We begin by considering how the spectrum is perturbed by changes in μ and $\hat{c}$. For this we define the following parameter dependent operators

$$\mathcal{L} = D\partial_{\xi\xi} + c\partial_{\xi} + f'(q(\xi), \mu); \tag{5.1}$$

$$\mathcal{L}_0^+ = D\partial_{\xi\xi} + c\partial_{\xi} + f'(q(\infty), \mu); \tag{5.2}$$

$$\mathcal{L}_0^- = D\partial_{\xi\xi} + c\partial_{\xi} + f'(q(-\infty), \mu); \tag{5.3}$$

where $q(\infty)$ and $q(-\infty)$ are the equilibria approached by $q(\xi)$ as $\xi \to \pm\infty$. For ease of notation in the following, let q^{s} be the steep front solution and q^{p} be the pulse solution. Finally we will use a subscript "spl" to designate the steep pulse, "fnt" to designate a front, "epl" to designate strongly decaying pulses away from the steep pulse and "algpl" to designate an algebraic pulse. Of course when linearizing around the pulses, the background linearizations agree in the forward and backward directions.

Lemma 1.1. *We have the following regarding the essential spectrum of $\mathcal{L}$ at pulses and*

fronts.

$$\operatorname{spec}_{\text{ess}}(\mathcal{L}_{\text{pl}}) \subset \{\lambda | \operatorname{Re}\lambda < 0\} \quad \text{for } \mathcal{L} : L^2(\mathbb{R}^N) \to L^2(\mathbb{R}^N); \tag{5.4}$$

$$\operatorname{spec}_{\text{ess}}(\mathcal{L}_{\text{fnt}}) \subset \{\lambda | \operatorname{Re}\lambda < 0\} \quad \text{for } \mathcal{L} : L^2_{0,\eta}(\mathbb{R}^N) \to L^2_{0,\eta}(\mathbb{R}^N); \tag{5.5}$$

$$\operatorname{spec}_{\text{ess}}(\mathcal{L}_{\text{spl}}) \subset \{\lambda | \operatorname{Re}\lambda < 0\} \quad \text{for } \mathcal{L} : L^2_{0,\eta}(\mathbb{R}^N) \to L^2_{0,\eta}(\mathbb{R}^N); \tag{5.6}$$

$$\operatorname{spec}_{\text{ess}}(\mathcal{L}_{\text{algpl}}) \subset \{\lambda | \operatorname{Re}\lambda < 0\} \quad \text{for } \mathcal{L} : L^2_{0,\eta}(\mathbb{R}^N) \to L^2_{0,\eta}(\mathbb{R}^N). \tag{5.7}$$

Proof. The essential spectrum is entirely determined by the dispersion curves of $\mathcal{L}_0^{\pm}$. We therefore need to expand $\mathcal{L}_0^{\pm}$ in the parameters μ and c. Since the critical dispersion curve is simple, and the dispersion relation is continuous in μ (actually smooth in $\sqrt{\mu}$) we can expand as follows.

For $d(\lambda, k; \mu) = 0$, we showed previously in Lemma 7.9 that there is a unique curve of essential spectrum $\lambda(k)$ that passes through a neighborhood of the origin. We expand this curve in terms of k and μ.

$$\begin{aligned}\lambda(k;\mu) =& ci k - d_1 k^2 + \mathrm{O}(k^3) \\ &+ a_1\sqrt{\mu} + a_2\mu + \mathrm{O}(\mu^{\frac{3}{2}}) \\ &+ b_1\sqrt{\mu}k + b_2\sqrt{\mu}k^2 + \mathrm{O}(\mu k)\end{aligned}$$

We are concerned with what happens to the tip of the dispersion curve, that is for $k = 0$:

$$\lambda(0;\mu) = a_1\sqrt{\mu} + a_2\mu + \mathrm{O}(\mu^{\frac{3}{2}}).$$

Recall from equation 7.10 that for $k = 0$, there exists u such that:

$$d(0,\lambda) = 0 \longleftrightarrow (f'(q(\pm\infty;\mu) - \lambda)u = 0.$$

Consider the ODE on the center eigendirection:

$$u_c' = \alpha_0\mu + \alpha_1 u_c^2 + \mathrm{O}(|\mu u_c| + u_c^3). \tag{5.8}$$

At the equilibria, $u_c' = 0$, we can solve for u_c:

$$u_c^* = \pm\sqrt{-\frac{\alpha_0}{\alpha_1}\mu} + \mathrm{O}(\mu).$$

Now linearize (5.8) around the equilibrium u_c^*:

$$v_c' = 2\alpha_1\left(\pm\sqrt{-\frac{\alpha_0}{\alpha_1}\mu}\right)v_c + \mathrm{O}(v_c^2).$$

Now matching the equation we find that:

$$a_1 = \pm 2\alpha_1 \sqrt{\frac{\alpha_0}{\alpha_1}}.$$

In the case of the pulse, the solution approaches the same equilibrium in forward and backward time. Therefore, the corresponding values of $\lambda(0;\mu)$ is the same in both directions. We claim it is in fact negative. Otherwise, the pulse would approach an equilibrium with exactly one unstable dispersion curve in the right half plane. Therefore, the Morse index of the equilibrium would be $N-1$. This however contradicts Remark 7.13.

In the case of the front we have:

$$a_1^+ > 0;$$
$$a_1^- < 0,$$

where a_1^+ is the value for a_1 at the equilibrium approached in positive time and a_1^- is the value of a_1 at the equilibrium approached in negative time. Recall the dispersion relation in the weighted space $L^2_{0,\eta}(\mathbb{R}^N)$:

$$d(k + \mathrm{i}\eta, \lambda).$$

Therefore we have the following for $\lambda(0;\mu)$ in $L^2_{0,\eta}(\mathbb{R}^N)$:

$$\lambda(0;\mu) = a_1^+ \sqrt{-\mu} - c\eta + \mathrm{O}(\eta^2 + |\mu\eta|).$$

Therefore for $0 < |\mu| << 1$, $\lambda(0;\mu) < 0$ for:

$$\eta > \frac{a_1^+}{c}\sqrt{-\mu}.$$

Thus we have showed that the dispersion curves for steep pulses are contained strictly in the left half of the complex plane, and that the same is true for the front in an appropriately weighted space. Since the operator $\mathcal{L}$ is a relatively compact perturbation of the background linearization operators $\mathcal{L}_0^{\pm}$, and essential spectrum is not shifted by compact perturbations, we may conclude that the essential spectrum is also contained in the left half plane for the appropriate space.

We use a similar approach when considering the essential spectrum of the steep pulse and the algebraic pulses. The situation is clearly simpler than for the steep pulses and

fronts when we look at the dispersion relation in Lemma 7.9, which does not depend on c. Therefore, for small values of c near c_*, the essential spectrum remains tangent to the imaginary axis. This spectrum can be stabilized by considering the linearization on the weighted space $L^2_{0,\eta}(\mathbb{R}^N)$, but not on $L^2(\mathbb{R}^N)$. This finishes the proof of the Lemma. ■

Now we show that there is a single algebraically simple eigenvalue in a neighborhood of zero.

Lemma 1.2. *We have the two following statements regarding the operator $\mathcal{L}$.*

1. *Around steep front solutions, the linearization $\mathcal{L}$ varies continuously on the parameters μ and c when considered as an operator from $H^2(\mathbb{R}^N) \to L^2(\mathbb{R}^N)$.*

2. *Around pulse solutions, the linearization $\mathcal{L}$ varies continuously on the parameters $c, \gamma(c)$ when considered as an operator from $H^2(\mathbb{R}^N) \to L^2(\mathbb{R}^N)$*

Proof. From the bifurcation result Theorem 6, the fronts vary continuously with respect to c and μ when considered as functions in the space $C^0(\mathbb{R}^N)$. We can see this because for any fixed initial condition, $x(0)$, solutions vary continuously in $C^0(\mathbb{R}^N)$ on any finite interval $(T, -T)$. Moreover, fronts converge asympotically to continuously varying equilibria in forward and backward time. Therefore, the variation on the intervals $(-\infty, -T]$ and $[T, \infty)$ can also be made arbitrarily small for small variations of μ and c. The proof of the second statement is the same as the first, except parameter values are restricted to the curve $c, \gamma(c)$. ■

This allows us to prove the following lemma regarding the number of eigenvalues in a neighborhood of the origin.

Lemma 1.3. *For μ and $c - c_*$ sufficiently small, there is a single eigenvalue of multiplicity 1 in a small neighborhood of the origin. Moreover, this eigenvalue, $\lambda(\mu, c)$, is continuous with respect to parameters.*

Proof. Let ω be a curve that contains the origin and only the simple eigenvalue at zero of the spectrum. Consider the following spectral projection:

$$\mathcal{P}(\mu, c) = -\frac{1}{2\pi \mathrm{i}} \int_\omega R(\lambda; \mu, c) d\lambda$$

where $R(\lambda;\mu,c)$ is the resolvent $(\mathcal{L}(\mu,c)-\lambda)^{-1}$. From Lemma 1.2 we know that $\mathcal{L}$ is continous with respect to μ and c. Therefore the resolvent $R(\lambda;\mu,c)$ is continuous for μ, c sufficiently close to 0 and c_*. For $(\mu,c)=(0,c_*)$ we have have by assumption:

$$\dim\mathcal{P}(0,0)=1.$$

By the continuity of the resolvent, for small values of $\mu, c-c_*$, the spectral projection is also continuous and therefore:

$$\dim\mathcal{P}(\mu,c)=1.$$

for (μ,c) in a neighborhood of $(0,c_*)$. Therefore, there is a single eigenvalue of multiplicity 1 in a neighborhood of 0. ∎

While we will use the convenience of the space $L^2_\eta(R^N)$ for most of our calculations regarding the spectrum, eventually, we will wish to consider perturbations on the space $L^2_{0,\eta}(R^N)$ so that we can apply the results from Henry [17] that relate spectral stability to asymptotic stability. The following lemma shows that the point spectrum in $L^2_\eta(R^N)$ is the same as the point spectrum in $L^2_{0,\eta}(R^N)$.

Lemma 1.4. *Let $\eta>0$ be such that the essential spectrum of $\mathcal{L}_{\text{front}}$ is contained strictly in the left half of the complex plane on $L^2_\eta(R^N)$. Then the point spectrum of the operator $\mathcal{L}_{\text{front}}$ on the space $L^2_{-\eta,\eta}(R^N)$ ($L^2_\eta(R^N)$) contains the point spectrum of the operator on $L^2_{0,\eta}(R^N)$. Moreover, they have the same point spectrum in a neighborhood of the origin.*

Proof. If we examine the dispersion curve as was calculated in Lemma 1.1, we see that the dispersion curves are confined to the left half of the complex plane in $L^2_{0,\eta}(R^N)$. This is because a_1^- (the value of the equilibrium as $\xi\to-\infty$) is necessary less than zero. We only need the exponential weight to control the dispersion curve of $\mathcal{L}_0^+$ since $a_1^+>0$. Therefore, the essential spectrum of $\mathcal{L}_{\text{front}}$ is contained in the left half of the complex plane on $L^2_{0,\eta}(R^N)$.

Now notice that the steep front q_*' is contained in $L^2_{0,\eta}(R^N)$. This is clear because q_*' decays exponentially in backward time from Theorem 6. Therefore λ is a zero eigenvalue with eigenvector q_*' on the space $L^2_{0,\eta}(R^N)$. However, it is also clear that $L^2_{0,\eta}(R^N)\subset L^2_\eta(R^N)$. Therefore any eigenfunction of $L^2_{0,\eta}(R^N)$ is also an eigenfunction of $L^2_\eta(R^N)$ and subsequently any eigenvalue of $\mathcal{L}_{\text{front}}$ in $L^2_{0,\eta}(R^N)$ is an eigenvalue of $L^2_\eta(R^N)$. ∎

We now state the relation between spectral stability and asymptotic stability in the pulses and various fronts. Recall the definitions of "asymptotically orbitally stable" and "asymptotically weighted stable" given in Definition 2.3 and following.

Lemma 1.5. *For (μ, c) in a neighborhood of $(0, c_*)$ we have the following:*

1. *The steep pulse is AWS (in $L^2_{0,\eta}(\mathbb{R}^N)$).*
2. *The excitation pulse solutions are AOS.*
3. *The steep front solutions are AWS (in $L^2_{0,\eta}(\mathbb{R}^N)$).*
4. *The fast fronts and slow fronts are AWS (in $L^2_{0,\eta}(\mathbb{R}^N)$) if the eigenvalue $\lambda(\mu, c) < 0$.*
5. *The algebraic pulses are AWS if the eigenvalue $\lambda(\mu, c) < 0$.*

Proof. These results depend primary on the well known results in Henry's book [17] on the stability of traveling waves. Another, perhaps more modern, approach can be found in Lunardi's book [31]. In either case, stability of traveling waves can be described as perturbation of the solution converges to a translate of the solution. In the language of dynamical systems, this is equivalent to the exponentially contracting fibrations of the center stable manifold when the manifold is one dimensional corresponding to a simple zero eigenvalue [21].

Thus, asymptotic orbital stability (see Definition 2.3) follows from the conditions necessary for constructing fibrations of the center unstable manifold (see proposition 9.2.4 [31].) Specifically, this means the spectrum of the operator $\mathcal{L}(q)$ is sectorial and strictly contained in the left half of the complex plane except for an algebraically simple eigenvalue at 0. That $\mathcal{L}$ is sectorial follows immediately from the stability of sectorial operators under perturbation [17] (for example consider $\mathcal{L}$ as a perturbation of the Laplacian operator.) From lemmas 1.1 and 1.3 we see that the excitation pulses satisfy the spectral conditions for the operator:

$$\mathcal{L}_{\text{pl}} : D(\mathcal{L}_{\text{pl}}) \subset L^2(\mathbb{R}^N) \to L^2(\mathbb{R}^N). \tag{5.9}$$

In lemma 1.1, we saw that considering the fronts and steep pulses in the weighted space $L^2_\eta(\mathbb{R}^N)$ stabilizes the essential spectrum. However, there is an added subtlety

when applying the stability results to an operator on a weighted space. Equation (3.1) can be written in terms of the linear operator $\mathcal{L}$ and a non-linear part $G(u)$:

$$u_t = \mathcal{L}u + G(u). \tag{5.10}$$

A necessary condition for the construction of fibrations of the center manifold is that the image of the domain of $\mathcal{L}$ in the base space with respect to G be contained in the base space. For the base space L^2_η this is clearly not the case since the square of a function in L^2_η is not necessarily contained in this space. We correct this problem by instead using the space $L^2_{0,\eta}(\mathbb{R}^N)$ since:

$$G : L^2_{0,\eta}(\mathbb{R}^N) \to L^2_{0,\eta}(\mathbb{R}^N). \tag{5.11}$$

Moreover, from lemma 1.4 the point spectrum is unchanged in $L^2_{0,\eta}$. This allows us to apply the stability theory of Henry to the fronts, steep pulse and algebraic pulses. ■

5.2 Stability and instability of slow and fast fronts

We now consider the stability of the slow and fast fronts. Like the steep fronts, the essential spectrum of the slow and fast fronts can be stabilized in the weighted space $L^2_{0,\eta}(R^N)$. However, unlike the steep fronts, the point spectrum of the slow and fast fronts is not necessarily located at the origin because the eigenfunction q' is not contained in the weighted space. Therefore the question of stability of these fronts depends on locating this eigenvalue.

Remark 2.6. *Let $\mathbb{N}_1$ be a neighborhood of $(\mu, c) = (0, c_*)$ so that Theorem 6 holds. Fix the weight η so that the essential spectrum is stabilized on a neighborhood $\mathbb{N} \subset \mathbb{N}_1$. In the following consider the linearization $\mathcal{L}$ at the fronts with parameters $(\mu, c) \in \mathbb{N}$.*

Lemma 2.7. *Let $\lambda(\mu, c)$ again represent the single eigenvalue in the neighborhood $\mathbb{N}$. Then $\lambda(\mu, c) = 0$ if and only if μ, c are such that we have a steep front or pulse.*

Proof. If the parameters (μ, c) are such that there is a steep front $q(\xi)$, then $q'(\xi) \in L^2_\eta$. Therefore q' is in the kernel of $\mathcal{L}$ and $\lambda(\mu, c) = 0$.

Now assume that $\lambda(\mu, c) = 0$. The intersection of the linear subspaces $E^{\text{cs}}_+ \cap E^{\text{cu}}_-$, corresponding to solutions bounded at $+\infty$ and $-\infty$ respectively, is one-dimensional

for all μ, c because the intersection of W^{cu} and W^{cs} is transverse. This intersection is spanned by the derivative of the front, $q'(\xi)$. We have $\lambda(\mu, c) = 0$ only if there is a kernel of the operator $\mathcal{L}$ on the space L^2_η, which corresponds to an intersection of E^{cu}_- and E^{ss}_+. Of course the intersection $E^{\mathrm{cu}}_- \cap E^{\mathrm{ss}}_+$ is contained in $E^{\mathrm{cs}}_+ \cap E^{\mathrm{cu}}_-$, which as stated is spanned by the derivative of the front $q'(\xi)$. However, the front only decays quickly enough to be included in L^2_η if it is the steep front. Therefore $\lambda(\mu, c) = 0$ only if the parameters correspond to a steep front solution. ∎

In a neighborhood of the origin, the eigenvalue $\lambda(\mu, c)$ can only be zero for steep front or excitation pulse solutions. Because there is only one such eigenvalue, it can only cross the imaginary axis through the value zero. Therefore the steep fronts form a stability boundary for the slow and fast fronts which we summarize in the following lemma.

Corollary 2.8. *The following two scenarios hold for parameter values (μ, c) in a neighborhood of $(0, c_*)$.*

1. *All fast fronts are spectrally stable in $L^2_{0,\eta}$ or all fast fronts are unstable.*
2. *All slow fronts are spectrally stable in $L^2_{0,\eta}$ or all slow fronts are unstable.*

Proof. In Lemma 1.1 we saw that on $L^2_{0,\eta}$, $\mathrm{spec}_{\mathrm{ess}}(\mathcal{L}) \in \{\lambda | \operatorname{Re}\lambda < 0\}$. Therefore the question of spectral stability depends entirely on the eigenvalue in a neighborhood of zero. From Lemma 1.3 we know that this eigenvalue, $\lambda(\mu, c)$, is continuous with respect to change of the parameters. Consider the fast fronts. Near the curve of steep fronts we know that the eigenvalue $\lambda(\mu, c)$ is either to the right or left of the imaginary axis. This eigenvalue can only cross the imaginary axis if there is a steep front solution to the linearized ODE by Lemma 2.7. However, by the Theorem 6, the only steep fronts exist on the curve separating the fast and slow fronts. Therefore if $\lambda(\mu, c)$ begins on $\mathbb{R}^-$, it must remain there for all the fast fronts, and it follows that the fast fronts are spectrally stable in the weighted space. Similarly, if it begins on $\mathbb{R}^+$ then all the fast fronts are unstable. The same argument holds in showing the analogous result for the slow fronts. ∎

We claim that the solution $u(\xi; c)$ of the linearized ODE is smooth in c when considered as an element of $L^\infty(\mathbb{R}^N)$. From this it follows immediately that the linearized

operator $\mathcal{L}$ when considered as an operator from $H^2_\eta(\mathbb{R}^N) \to L^2_\eta(\mathbb{R}^N)$ is smooth in c and therefore the isolated critical eigenvalue depends smoothly on c. We state and prove this in the following lemma.

Lemma 2.9. *The linearized operator, $\mathcal{L} : H^2_\eta(\mathbb{R}^N) \to L^2_\eta(\mathbb{R}^N)$, depends smoothly on c.*

Proof. Write the perturbed solution $u(\xi; c)$ as

$$u(\xi; c) = u(\xi; c_0) + v(\xi; c),$$

where $u(\xi; c)$ and $u(\xi; c_0)$ are solutions to the respective equations:

$$Du(\xi; c)'' + cu(\xi; c)' + f(u(\xi; c)) = 0;$$
$$Du(\xi; c_0)'' + cu(\xi; c_0)' + f(u(\xi; c_0)) = 0.$$

Substituting $u = u_{c_0} + v$ and subtracting the two equations results in the following:

$$Dv'' + c_0 v' + (c - c_0)u'_{c_0} + f(u_{c_0} + v) - f(u_{c_0}) = 0 \tag{5.12}$$

where we refer to the right hand side of (5.12) as $A(v; c)$. It is clear that A maps $H^2(\mathbb{R}^N)$ into $L^2(\mathbb{R}^N)$ since u'_{c_0} is contained in $L^2(\mathbb{R})$.

Now notice that the linear operator, $A'(0; c_0) = Dv'' + c_0 v' + f'(u_{c_0})$, is Fredholm of index 1 from $H^2(\mathbb{R}^N) \to L^2(\mathbb{R}^N)$. The Fredholm index is implied by the difference of of dimension of the stable and unstable subspaces (see Palmer's paper [32] for details) $E^s_\infty - E^u_{-\infty} = 1$. The kernel of the linearization $A'(0; c_0)$ is one dimensional and is spanned by the solution $v'(\xi)$. Therefore the linear operator is bijective and Fredholm index 0 provided that we project away the kernel, v'. This allows us to solve for $v(c)$ smoothly using the implicit function theorem. ∎

We also need to consider the smoothness on of the kernel of $\mathcal{L}$ with respect to c and μ.

Remark 2.10 (Notation)**.** *Let κ be the kernel of the operator $\mathcal{L}$ and κ_* the kernel of the adjoint operator $\mathcal{L}^*$ in the spaces L^2_η and $L^2_{-\eta}$ respectively. Recall that $\kappa = q'(\xi)$.*

Since the essential spectrum in the weighted space is bounded away from the imaginary axis, the spectral stability of the fast and slow fronts will be determined by the

location of the eigenvalue $\lambda = 0$. The eigenvalue was pinned at zero for parameter values that corresponded to steep fronts or pulses. Our strategy consists of computing the motion of this eigenvalue as c varies off the curve of steep fronts. Stability of all fast and slow fronts is then determined by the location of the small eigenvalue for c close to the speed of the steep front. Since the operators depend smoothly on c, we can in principle expand λ in c. The following lemma recalls this expansion procedure.

Lemma 2.11. *Let (μ^*, c^*) be such that $q(\xi)$ is a steep front solution and $|(\mu^*, c^* - c_*)| << 1$. Then the eigenvalue $\lambda(\mu^*, c - c^*) = \lambda(\hat{c})$ is determined by the following expansion:*

$$\lambda(\hat{c}) = \frac{\langle \kappa_*, (\partial_c \mathcal{L})\kappa \rangle_{L^2}}{\langle \kappa_*, \kappa \rangle_{L^2}}. \tag{5.13}$$

Where $\kappa = q'(\xi)$ and κ_* is a solution to the adjoint equation:

$$D\partial_{\xi\xi} w - c^* \partial_\xi w + f'(q_{p_*}, \mu^*)^T w = 0 \tag{5.14}$$

contained in the space $L^2_{-\eta}$.

Proof. Consider the following eigenvalue problem:

$$\lambda u - \mathcal{L} u = 0 \tag{5.15}$$

$$|u|^2 - 1 = 0 \tag{5.16}$$

Where λ, u and $\mathcal{L}$ are all C^1 functions of c. The derivative of (5.15)with respect to the vector variable (u, λ) gives us the matrix:

$$\begin{pmatrix} \mathcal{L}^0 & \kappa \\ 2\kappa & 0 \end{pmatrix} \tag{5.17}$$

The vector $(u_1, \lambda_1)^T$ is in the kernel of (5.17) only if κ is in the range of $\mathcal{L}$. However, we have shown previously that κ is algebraically simple. This allows the application of the implicit function theorem. For $\hat{c}$ sufficiently small there exists the following expansions satisfying (5.15):

$$\begin{aligned} \lambda =& 0 + \hat{c}\lambda_1 + o(\hat{c}) \\ u =& \kappa + \hat{c} u_1 + o(\hat{c}) \\ \mathcal{L} =& \mathcal{L}_0 + \hat{c}\mathcal{L}_1 + o(\hat{c}). \end{aligned} \tag{5.18}$$

Plugging these into (5.15) gives us the following equation:

$$(\hat{c}\lambda_1)(\kappa + \hat{c}u_1) = (\mathcal{L}_0 + \hat{c}\mathcal{L}_1)(\kappa + \hat{c}u_1) + o(\hat{c}). \tag{5.19}$$

Multiplying this out gives:

$$\hat{p}\lambda_1\kappa = \mathcal{L}_0\kappa + \hat{c}\mathcal{L}_0u_1 + \hat{c}\mathcal{L}_1\kappa + o(\hat{c}) \tag{5.20}$$

Notice that $\mathcal{L}_0\kappa = 0$. Now take the $L^2(\mathbb{R})$ inner product of both sides with κ_*. The term $< \kappa_*, \mathcal{L}u_1 >= 0$ since by the implicit function theorem $u(\hat{c})$ is c^1 and therefore $u_1 \in L^2_{0,\eta}(\mathbb{R})$. This leaves:

$$\hat{p}\left\langle \kappa_*, \kappa \right\rangle \lambda_1 = \hat{c}\left\langle \kappa_*, \mathcal{L}_1\kappa \right\rangle + o(\hat{c}) \tag{5.21}$$

or considering only order $\mathrm{O}(\hat{c})$ terms:

$$\lambda_1 = \frac{\langle \kappa_*, \mathcal{L}_1\kappa \rangle}{\langle \kappa_*, \kappa \rangle}. \tag{5.22}$$

This proves the proposition. ∎

Remark 2.12 (ODE notation)**.** *We consider the first order systems of ODE that correspond to the operators $\mathcal{L}$ and $\mathcal{L}^*$. Let us first clarify the notation required because we will need to consider both the operator $\mathcal{L}$ and the corresponding first order ODE which can be confusing.*

$$\begin{pmatrix} u \\ v \end{pmatrix}_\xi = \begin{pmatrix} 0 & \mathbf{I} \\ -D^{-1}f'(q;\mu) & -D^{-1}c \end{pmatrix} \begin{pmatrix} u \\ v \end{pmatrix} \quad \longrightarrow \quad \mathbf{u}' = D_{\mathbf{u}}F(q,\mu,c)\mathbf{u} \tag{5.23}$$

$$\begin{pmatrix} w_1 \\ w_2 \end{pmatrix}_\xi = \begin{pmatrix} 0 & (f'(q))^T D^{-1} \\ -\mathbf{I} & D^{-1}c \end{pmatrix} \begin{pmatrix} w_1 \\ w_2 \end{pmatrix} \quad \longrightarrow \quad \mathbf{w}' = -(D_{\mathbf{u}}F(q,\mu,c))^T\mathbf{w} \tag{5.24}$$

We define the $2N$ vectors Q' and Ψ as the following:

$$\begin{pmatrix} u \\ v \end{pmatrix} = \begin{pmatrix} \kappa \\ \kappa' \end{pmatrix} = Q'$$

$$\begin{pmatrix} w_1 \\ w_2 \end{pmatrix} = \begin{pmatrix} c\kappa_* - D\kappa_*' \\ D\kappa_* \end{pmatrix} = \Psi.$$

Notice that Q' is the unique solution up to multiplication by a scalar of (5.23) in L^2_η and Ψ is the unique solution up to multiplication by a scalar of (5.24) in $L^2_{-\eta}$.

Finally we have the eigenvectors of the matrix of the ODE and the adjoint ODE as we let $\xi \to \infty$ that correspond to the small spatial eigenvalue ν_0.

$$\mathcal{E}_r = \begin{pmatrix} e_r \\ 0 \end{pmatrix} + \mathrm{O}(\sqrt{\mu}) \tag{5.25}$$

$$\mathcal{E}_l = \begin{pmatrix} ce_l \\ De_l \end{pmatrix} + \mathrm{O}(\sqrt{\mu}). \tag{5.26}$$

Recall that e_r and e_l are the left and right eigenvectors of $f'(0,\mu)$ as defined in hypothesis 1.1. Of course the steep fronts have two sets of such eigenvectors, a pair corresponding to the equilibrium in forward time and a pair corresponding to the equilibrium in backward time. We will indicate this distinction with a $+$ or $-$ superscript for the respective linearizations.

Lemma 2.13 (Asymptotics)**.** *Let $\mu > 0$ be fixed and $\nu_0(\mu)$, $\delta(\mu)$ both depend on μ where ν_0 is the smallest eigenvalue of (5.23) as described previously and $\delta > 0$ is small. Then we have the following regarding the asymptotics.*

$$Q_p(\xi)e^{-\nu_0\xi} = Q_{(-\infty,p)}\mathcal{E}_r^- + \mathrm{O}(e^{-\delta|\xi|}), \qquad \xi \to -\infty \tag{5.27}$$

$$Q_p'(\xi)e^{-\nu_0\xi} = \nu_0 Q_{(-\infty,p)}\mathcal{E}_r^- + \mathrm{O}(e^{-\delta|\xi|}), \qquad \xi \to -\infty \tag{5.28}$$

$$\Psi_p(\xi)e^{\nu_0\xi} = \Psi_{(\infty,p)}\mathcal{E}_l^+ + \mathrm{O}(e^{-\delta|\xi|}), \qquad \xi \to \infty \tag{5.29}$$

$$\Psi_{sf}(\xi)e^{\nu_0^+\xi} = \Psi_{(\infty,sf)}\mathcal{E}_l^+ + \mathrm{O}(e^{-\delta|\xi|}), \qquad \xi \to \infty \tag{5.30}$$

$$\Psi_{sp}(\xi)e^{\nu_0\xi} = \Psi_{(\infty,sp)}\mathcal{E}_l^+ + \mathrm{O}(e^{-\delta|\xi|}), \qquad \xi \to \infty \tag{5.31}$$

where $Q_{(-\infty,P)}, \Psi_{(\infty,p)}, \Psi_{(\infty,sf)}$ are real numbers not equal to zero.

Proof.

Let $A(\xi) = D_{\mathbf{u}}F(q(\xi),\mu^*,\hat{c}^*)$ and the asymptotic matrices be defined as $A(\infty) = D_{\mathbf{u}}F(b,\mu^*,\hat{c}^*)$ and $A(-\infty) = D_{\mathbf{u}}F(a,\mu^*,\hat{c}^*)$, where "$a$"and "$b$" are the limiting equilibria as q goes to $-\infty$ and $+\infty$ respectively. Notice that $A(\xi) \to A(\pm\infty)$ in an exponential

fashion. The same is true for the matrices $B(\xi) = -D_{\mathbf{u}}F(q_p, \mu^*, \hat{c}^*)^T$ and $B(\pm\infty)$. Consider the corresponding homogenous ODE's:

$$\mathbf{u}' = A(-\infty)\mathbf{u} \tag{5.32}$$

$$\mathbf{w}' = B(\infty)\mathbf{w} \tag{5.33}$$

Since $|A(-|\xi|) - A(-\infty)|$ and $|B(\xi) - B(\infty)|$ go to zero exponentially as $\xi \to \infty$ we have that for any integer h:

$$\int_{\xi_0}^{\infty} |\xi|^h |A(\xi) - A(\infty)| d\xi < \infty, \qquad \int_{\xi_0}^{\infty} |\xi|^h |B(\xi) - B(\infty)| d\xi < \infty. \tag{5.34}$$

From theorem 10.13.2 of [33], for every nontrivial solution $\phi(\xi)$ ($\psi(\xi)$) of (5.23) (or (5.24)) there is a nontrivial solution $\phi_L(\xi)$ ($\psi_L(\xi)$) of (5.32) ((5.33)) such that:

$$|\phi(\xi) - \phi_L(\xi)| = o(\phi_L(\xi)), \qquad |\psi(\xi) - \psi_L(\xi)| = o(\psi_L(\xi)) \tag{5.35}$$

as $\xi \to +\infty$.

Now consider the solution of (5.23), Q_p. We know by assumption $q'(\xi)$ decays weakly in backward time. That is, $q'(\xi) \notin L^2_{-\eta}$ by hypothesis 1.4 which implies that $Q_p \notin L^2_{-\eta}(\mathbb{R}^{2N})$. However, $|A(\xi) - A(-\infty)|$ still decays in an exponential fashion. Therefore, Q_p must approach the equilibrium as the solution Q_L of the homogenous equation (5.32). Because of the slow decay of $Q_p(\xi)$, it necessarily approaches the linear solution that decays like $e^{\nu_0 \xi}$. This proves the first part of (2.13.) The second can be seen by differentiating Q_p.

We will now consider the asymptotics of the adjoint solution. If we consider the differential equation (5.23) as the operator $\mathcal{V}$ on the space L^2_η, the Fredholm index of $\mathcal{V}$ is zero as has been shown previously. Since $\dim(\text{Null}(\mathcal{V})) = 1$ and is spanned by Q' there exists a unique bounded solutions Ψ of (4.27) contained in the space $L^2_{-\eta}$. Therefore Ψ decays in a strong exponential fashion to zero as $\xi \to -\infty$. The kernel of $\mathcal{V}$ is empty considered on the space $L^2_{-\eta}$ by hypothesis 8.16. Thus $\Psi(\xi) \in (L^2_{-\eta}/L^2_\eta)$. Now using the properties of linear autonomous equations, $\Psi(\xi)$ must approach a solution $\Psi_L(\xi)$ to the homogenous equation (5.33). Therefore $\Psi(\xi)e^{-\nu_0\xi} \to \Psi_{(\infty,p/sf)}\mathcal{E}_l$ as $\xi \to \infty$ where $\Psi_{(\infty,p/sf)} \neq 0$ is some constant. This concludes the proof of the lemma. ∎

We would like to understand how the orientations of the adjoint solutions relate to each other on the steep front and pulse. This is determined in the following lemma.

Lemma 2.14. *Let $\Psi_{\infty,p}$ and $\Psi_{\infty,sf}$ be as in Lemma 2.13. Then we have the following:*

$$\Psi_{\infty,p}\Psi_{\infty,sf} > 0.$$

Proof. The solution Ψ lies in $E_-^{uu*} \cap E_+^{cs*}$, the intersection of the center stable and unstable subspaces of the adjoint equation. These subspaces vary continuously with respect to $\mu < 0$ up to $\mu = 0$. This follows from the continuity of the resolvent with respect to μ and therefore the continuity of the spectral projections. Since $\kappa_*(\xi)$ converges as $\mu \to 0$ in L^∞, so do Ψ_{sf} and Ψ_p:

$$\Psi_p, \Psi_f \to \Psi_{sp} \text{ as } \mu \to 0_-.$$

Since $\Psi_{sp} = \Psi_{sp,\infty} e_l + \mathrm{O}(e^{-\delta|\xi|})$, we may conclude that the coefficients $\Psi_p, \Psi_f \to \Psi_{sp}$ as $\mu \to 0_-$ from which the statement follows. ∎

We also need to know the asymptotic behavior of $\partial_c Q'(\xi)$ as $\xi \to \pm\infty$.

Lemma 2.15. *We have the following asymptotics for $\partial_c Q'(\xi)$.*

$$\lim_{\xi\to\infty} e^{\nu_o \xi} \partial_c Q'(\xi) = Q_{(\infty,c)} \mathcal{E}_r^+,$$

$$\lim_{\xi\to-\infty} \partial_c Q'(\xi) = 0.$$

Proof. This proof follows the general idea used in (2.13.) Let μ_* and c_* be such that $q(\xi)$ is a steep front solution. Then $q(\xi)$ satisfies the following differential equation:

$$Dq'' + c_* q' + f(q, \mu_*) = 0. \tag{5.36}$$

Thus $\partial_c q_{p_*}(\xi)$ is a solutions to:

$$D(\partial_c q)'' + c_*(\partial_c q)' + f'(q,\mu)\partial_c q = -q'. \tag{5.37}$$

This means that formally (without regard to the domain space of the operator):

$$\mathcal{L}\partial_c q = -\kappa. \tag{5.38}$$

However, we have showed previously that $\kappa(\xi)$ is an algebraically simple eigenfunction in the weighted space $L^2_{0,\eta}(\mathbb{R})$. Thus $\partial_c q \notin L^2_{0,\eta}(\mathbb{R})$. Because we know that $q'$is in $L^2_{0,\eta}(\mathbb{R})$, for some $\zeta > 0$ sufficiently small we have the following relation:

$$|q'| \le c(\xi_0) e^{-\zeta\xi} |\partial_c q| \qquad \xi \ge \xi_0. \tag{5.39}$$

Now rewrite (5.37) as a first order ODE

$$\partial_c Q' = A(\infty)\partial_c Q + (A(\xi) - A(\infty))\partial_c Q + \begin{pmatrix} 0 \\ D^- q' \end{pmatrix}. \tag{5.40}$$

Using our previous argument about the exponential decay of $|A(\xi)-A(\infty)|$ from Lemma 2.13 and (5.39) we have that for $\xi > \xi_0$:

$$\|(A(\xi) - A(\infty))\partial_c Q + \begin{pmatrix} 0 \\ D^- q' \end{pmatrix}\| \leq K(\xi_0)e^{-\zeta\xi}\partial_c Q. \tag{5.41}$$

This decay condition and the fact that $\partial_c Q$ decays to zero allow us again to appeal to Theorem 10.13.2 of [33] regarding the asymptotics of $\partial_c Q$. The result states that $\partial_c Q$ must decay like a solution of the linearized equation $\mathbf{u}' = A(\infty)\mathbf{u}$. However, we have shown above that $\partial_c Q \notin L^2_{0,\eta}$. Therefore it must decay with the eigenvalue ν_0. More precisely we have that:

$$\lim_{\xi\to\infty} e^{\nu_0\xi}\partial_c Q \to Q_{(\infty,c)}\mathcal{E}_r \tag{5.42}$$

for some constant $Q_{(\infty,c)} \neq 0$. This proves part (1) of the lemma. The second part is obvious since $Q(\xi)$ is bounded. ∎

Now we can calculate the first derivative of the critical eigenvalue with respect to c for a fixed $\mu < 0$. The sign of the derivative will determine how the critical eigenvalue moves as we cross the curve of steep fronts in the c direction.

Lemma 2.16. *We have the following regarding the derivative of the critical eigenvalue λ with respect to c for fixed $\mu < 0$:*

$$\partial_c\lambda = -\frac{\Psi_{\infty,sf}Q_{\infty,c}}{\langle\kappa_*,\kappa\rangle} + \mathrm{O}(\sqrt{\mu}).$$

Proof. From the previous Lemma 2.11, we have the following expansion for the critical eigenvalue:

$$\lambda'(c) = \frac{\langle\kappa_*, (\partial_c\mathcal{L})\kappa\rangle_{L^2}}{\langle\kappa_*,\kappa\rangle}. \tag{5.43}$$

Since κ is in the kernel of $\mathcal{L}$, it is trivial to see that:

$$\partial_c(\mathcal{L}\kappa) = 0.$$

This in turn implies that:

$$(\partial_c \mathcal{L})\kappa + \mathcal{L}(\partial_c \kappa) = 0.$$

This allows us to rewrite (5.43) as the following:

$$\partial_c \lambda = -\frac{\langle \kappa, \mathcal{L}\partial_c \kappa \rangle}{\langle \kappa_*, \kappa \rangle}. \tag{5.44}$$

Please notice that $\partial_c \kappa \notin L^2_\eta(\mathbb{R})$ from the asymptotic results of lemma 2.15; it decays too slowly in forward time. Therefore we consider $\mathcal{L}\partial_c \kappa$ simply as a differential operator acting on κ. Notice that if we take the adjoint formally we have the following:

$$\langle \mathcal{L}^* \kappa_*, \partial_c \kappa \rangle = 0.$$

Therefore we consider the following:

$$\partial_c \lambda = \frac{-\langle \kappa_*, \mathcal{L}\partial_c \kappa \rangle + \langle \mathcal{L}^* \kappa_*, \partial_c \kappa \rangle}{\langle \kappa_*, \kappa \rangle}. \tag{5.45}$$

We will address the sign of $\langle \kappa_*, \kappa \rangle$ later. For the time begin, consider the numerator of the right hand side of (5.45.)

$$\begin{aligned}\partial_c \lambda \langle \kappa_*, \kappa \rangle = &- \int_{-\infty}^{\infty} \langle \kappa_*, D\partial_{\xi\xi}\partial_c \kappa \rangle \, d\xi - \int_{-\infty}^{\infty} \langle \kappa_*, c\partial_\xi \partial_c \kappa \rangle \, d\xi - \int_{-\infty}^{\infty} \left\langle \kappa_*, f'(q,\mu)\partial_c \kappa \right\rangle d\xi \\ &+ \int_{-\infty}^{\infty} \langle D\partial_{\xi\xi}\kappa_*, \partial_c \kappa \rangle \, d\xi - \int_{-\infty}^{\infty} \langle c\partial_\xi \kappa_*, \partial_c \kappa \rangle \, d\xi + \int_{-\infty}^{\infty} \left\langle (f'(q,\mu))^T \kappa_*, \partial_c \kappa \right\rangle d\xi.\end{aligned}$$

It is clear that the terms $-\int_{-\infty}^{\infty} \langle \kappa_*, f'(q,\mu)\partial_c \kappa \rangle \, d\xi + \int_{-\infty}^{\infty} \left\langle (f'(q,\mu))^T \kappa_*, \partial_c \kappa \right\rangle d\xi = 0$. These two integrals actually converge because κ_* decays exponentially in backward time ($\partial_c \kappa$ is bounded in backward time) and $f'(q,\mu)$ converges to 0 exponentially in forward time (κ_* is bounded as $\xi \to \infty$.)

Now consider the terms with ∂_ξ and $\partial_{\xi\xi}$. These terms necessarily converge, so we may apply integration by parts:

$$\begin{aligned}\partial_c \lambda \langle \kappa_*, \kappa \rangle = &- [\kappa_*, D\partial_\xi \partial_c \kappa]_{-\infty}^{\infty} + \int_{-\infty}^{\infty} \langle \partial_\xi \kappa_*, D\partial_\xi \partial_c \kappa \rangle \, d\xi - \int_{-\infty}^{\infty} \langle \kappa_*, c\partial_\xi \partial_c \kappa \rangle \, d\xi \\ &+ [\partial_\xi \kappa_*, D\partial_c \kappa]_{-\infty}^{\infty} - \int_{-\infty}^{\infty} \langle \partial_\xi \kappa_*, D\partial_\xi \partial_c \kappa \rangle \, d\xi - [\kappa_*, c\partial_c \kappa]_{-\infty}^{\infty} + \int_{-\infty}^{\infty} \langle \kappa_*, c\partial_\xi \partial_c \kappa \rangle \, d\xi\end{aligned} \tag{5.46}$$

We can quickly see that the boundary terms are bounded. From the previous lemmas 2.13 and 2.15 we have:

$$\begin{aligned} -\left[\kappa_*, \partial_\xi \partial_c \kappa\right]_{-\infty}^{\infty} =& \nu_0 \left\langle \Psi_{(\infty,sf)} e_l, DQ_{(\infty,c)} e_r \right\rangle \\ \left[D^{-1}\partial_\xi \kappa_*, D\partial_c \kappa\right]_{-\infty}^{\infty} =& \nu_0 \left\langle \Psi_{(\infty,sf)} e_l, DQ_{(\infty,c)} e_r \right\rangle \\ -\left[\kappa_*, c\partial_c \kappa\right]_{-\infty}^{\infty} =& -c \left\langle \Psi_{(\infty,sf)} e_l, Q_{(\infty,c)} e_r \right\rangle \end{aligned} \tag{5.47}$$

Because the right hand side of (5.45) is convergent, the integrals of (5.46) must also converge and therefore can be cancelled with each other.

The small eigenvalue depend on μ as $\nu_0(\mu) = \mathrm{O}(\sqrt{\mu})$. Additionally, recall that we previously assumed that $\langle e_l, e_r \rangle = 1$. Therefore, for $0 < |\mu| \ll 1$ the first two quanties in 5.47 are $\mathrm{O}(\sqrt{\mu})$. This allows us to express $\partial_c \lambda$ as the following:

$$\partial_c \lambda = -c \frac{Q_{(\infty,c)} \Psi_{(\infty,sf)}}{\langle \kappa_*, \kappa \rangle} + \mathrm{O}(\sqrt{\mu}). \tag{5.48}$$

This proves the lemma. ∎

We now address the interpretation of the term $\langle \kappa_*, \kappa \rangle$ which has followed us throughout our calculations. In fact this quantity determines which of the two following bifurcation diagrams results after applying the result of Chow and Lin (Theorem 6.) Recall that this is in fact equivalent to the quantity $\mathcal{M}$ by Lemma 7.14.

For ease of understanding these results we will use the following notation:

$$\begin{aligned} Q_{(\infty,c)} \Psi_{(\infty,sf)} =& \Lambda \\ \langle \kappa_*, \kappa \rangle =& \mathbf{M}. \end{aligned}$$

The sign of $\partial_c \lambda$ and therefore the stability of the slow and fast fronts depends on quantities Λ and $\mathbf{M}$. At this point we have four possible cases of orientation of c and stability.

Lemma 2.17. *Assume that $\Lambda \neq 0$ and that $\mathbf{M} \neq 0$. Let "orientation 1" and "orientation 2" be as in figure 5.2. Then we have four possible cases:*

1. $\Lambda > 0, \mathbf{M} > 0$ *Orientation 1 – fast fronts stable, slow fronts unstable;*

2. $\Lambda < 0, \mathbf{M} > 0$ *Orientation 1 – slow fronts stable, fast fronts unstable;*

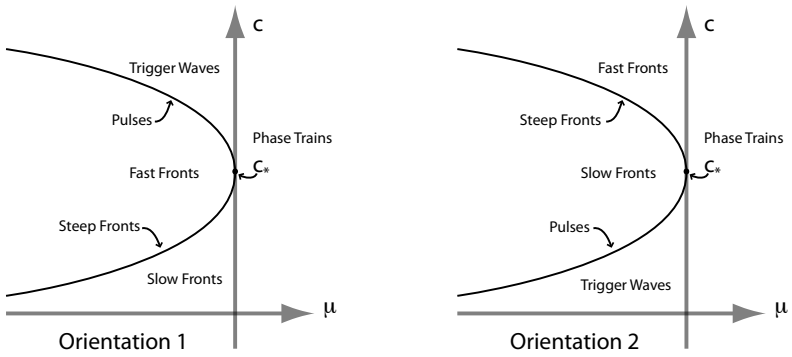

Figure 5.1: Orientation 1 corresponds to the case $\langle \kappa_*, \kappa \rangle > 0$ while orientation 2 corresponds to $\langle \kappa_*, \kappa \rangle < 0$.

3. $\Lambda > 0, \mathbf{M} < 0$ *Orientation 2 – slow fronts stable, fast fronts unstable;*

4. $\Lambda < 0, \mathbf{M} < 0$ *Orientation 2 – fast fronts stable, slow fronts unstable.*

Proof. From corollary 2.8 we know that all the fast fronts are either stable or unstable for parameter values near $(\mu, c) = (0, c_*)$. Moreover, the movement of the critical eigenvalue is determined by the sign of the ratio:

$$-\frac{\Lambda}{\mathbf{M}}.$$

In cases (2) and (3) above this ratio is positive indicating that the critical eigenvalue crosses to the positive real axis as c is varied to cross the curve of steep fronts. This indicates the fast fronts are unstable and the slow fronts are stable. Similarly, in cases (1) and (4) the ratio is negative and therefore we get the reverse stability situation. ■

5.3 Stability of trigger waves

We now know something about the stability of the fast fronts, slow fronts and steep fronts. We now ask if we can relate the stability these phenomena to that of the trigger trains. Happily the answer is yes. First we state theorem 5.2 from [30] in terms of our current framework.

Theorem 8. *Consider the ODE* (5.23). *Let* $Q_p(\xi) = (q, q')^T$ *be a homoclinic solution to* (5.23). *Assume that* $Q_p(\xi)$ *satisfies* $\mathcal{M} \neq 0$, $\mathbf{q}'(\xi)$ *is the unique solution of the variational equation and the following quantity is non-zero:*

$$\mathcal{N} = \int_{-\infty}^{\infty} \left\langle \psi(\xi), \begin{pmatrix} 0 & 0 \\ D^{-1} & 0 \end{pmatrix} q'(\xi) \right\rangle d\xi \neq 0. \tag{5.49}$$

Assume that the pulse $q(\xi)$ *has the simple leading eigenvalue* $\lambda = 0$. *Also assume that the eigenvalues of* $D_{\mathbf{u}}F(q, \mu^*, \hat{c}^*)$, ν_i*'s, are bounded by* ν_u *such that* $0 < \nu_u < |\nu_i|$. *Then there are positive constants* C *and* δ *and a function* $\lambda(\gamma)$ *that is analytic in* $\gamma \in \mathbb{R}/2\pi\mathbb{Z}$ *such there is a periodic solutions if and only if* $\lambda = \lambda(\gamma)$. *Furthermore we have the expansion:*

$$\lambda(\gamma) = (e^{i\gamma} - 1)e^{-2\nu_0 L}\left(\frac{< \Upsilon_l, \Upsilon_r >}{\mathcal{N}} + R(\gamma)\right) \tag{5.50}$$

for $\gamma \in \mathbb{R}/2\pi\mathbb{Z}$. *The remainder term is analytic in* γ *with*

$$|\partial_\gamma^l R(\gamma)| \leq Ce^{-\delta L}. \tag{5.51}$$

The vectors Υ_l *and* Υ_r *are the vectors defined in the following fashion.*

$$e^{-\nu_0 \xi} Q' = \Upsilon_r \quad \xi \to -\infty$$
$$e^{\nu_0 \xi} \Psi = \Upsilon_l \quad \xi \to \infty$$

Thus the stability of periodic orbits depends on $< \Upsilon_l, \Upsilon_r >$ and $\mathcal{N}$. Let us investigate these two quantities.

Lemma 3.18. *The quantity* $\mathcal{N}$ *defined in Theorem 8 is equal to* $\mathbf{M}$ *defined above. Additionally the sign of the inner product* $\langle \Upsilon_l, \Upsilon_r \rangle$ *is equal to the sign of* $Q_{(-\infty,p)}\Psi_{(\infty,p)}$.

Proof. The first part of the lemma follows from the fact that $\mathbf{\Psi} = (\psi_1, \psi_2)^T$ and we have seen (4.28) that $\psi_2 = D\kappa_*$. Then from (5.49):

$$\mathcal{N} = \int_{-\infty}^{\infty} \left\langle De_{p_*}^* d\xi D^{-1} e_{p_*} \right\rangle = \mathbf{M}. \tag{5.52}$$

As was shown in Lemma 2.13, we have that:

$$\mathcal{E}_l = \begin{pmatrix} ce_l \\ De_l \end{pmatrix} + \mathrm{O}(\sqrt{\mu}) \quad \mathcal{E}_r = \begin{pmatrix} e_r \\ 0 \end{pmatrix} + \mathrm{O}(\sqrt{\mu}).$$

Therefore the inner product of the vectors we have:

$$\langle \Upsilon_l, \Upsilon_r \rangle = Q_{(-\infty,p)}\Psi_{(\infty,p)} \langle \mathcal{E}_l, \mathcal{E}_r \rangle = Q_{(-\infty,p)}\Psi_{(\infty,p)} c \langle e_l, e_r \rangle$$

Because we assume that $\langle e_l, e_r \rangle = 1$ and that $c > 0$ we have the second part of the Lemma. ∎

The quantity $Q_{(-\infty,p)}\Psi_{(\infty,p)}$ looks familiar reminding us of $\Lambda = Q_{(\infty,c)}\Psi_{(\infty,sf)}$. From Lemma 2.14 we know that $\Psi_{(\infty,p)}$ and $\Psi_{(\infty,sf)}$ have the same sign. The question becomes how do $Q_{(\infty,c)}$ and $Q_{(-\infty,p)}$ relate. We address this in the following lemma.

Lemma 3.19. *The sign of $Q_{(\infty,c)}$ depends on the sign of $Q_{(-\infty,p)}$ in the following fashion:*

1. $Q_{(\infty,c)}Q_{(-\infty,p)} < 0$ *in the case of orientation 1;*
2. $Q_{(\infty,c)}Q_{(-\infty,p)} > 0$ *in the case of orientation 2.*

Proof. The quantity $Q_{(-\infty,p)}$ described the direction the pulse $Q_p(\xi)$ enters the equilibrium in backward time with respect to the eigenvector $\mathcal{E}_r$. This eigenvector lies in the direction of the center manifold since it corresponds to the small spatial eigenvalue ν_0. On the other hand $Q_{(\infty,c)}$ corresponds to the movement of the strong stable manifold as c is perturbed. Thus, if we examine the bifurcation diagram provided by Chow and Lin (Theorem 6) we see that in the case of orientation 1, as c increases , the strong stable manifold moves in the opposite direction of $Q_{(-\infty,p)}\mathcal{E}_r$. In the case of orientation 2, if c increases, the strong stable manifold moves in the same direction as $Q_{(-\infty,p)}\mathcal{E}_r$. This proves the lemma. ∎

5.4 The relation between trigger waves and fronts

Now we can consider the stability of the trigger waves with respect ot the slow and fast fronts. It appears that the same quantity determines the stability of the fast fronts, slow fronts, and trigger waves! We state the four possible stability situations in the following corollary.

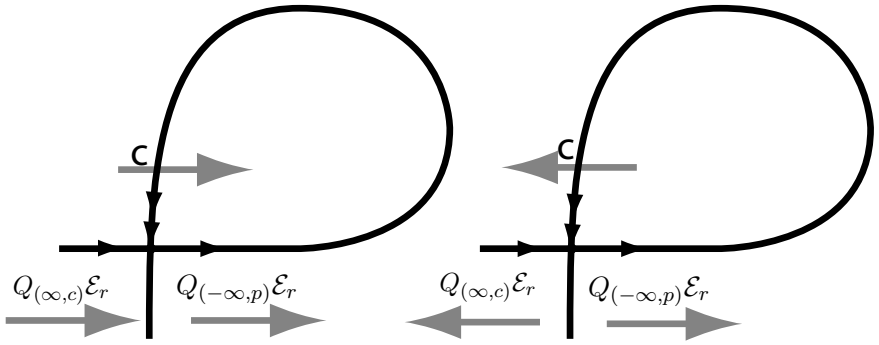

Figure 5.2: The diagram to the left shows the strong stable manifold moves in the same direction of $Q_{(-\infty,p)}\mathcal{E}_r$ as c increases in the case of $\langle \kappa_*, \kappa \rangle > 0$. The diagram on the left shows the movement of the strong stable manifold with respect to c $\langle \kappa_*, \kappa \rangle < 0$

Corollary 4.20. *There are four possible stability diagrams with respect to trigger waves, fast fronts and slow fronts.*

1. $\Lambda > 0, \mathbf{M} > 0$ *Orientation 1 – FF stable, SF unstable, TW unstable.*
2. $\Lambda < 0, \mathbf{M} > 0$ *Orientation 1 – FF unstable, SF stable, TW stable.*
3. $\Lambda > 0, \mathbf{M} < 0$ *Orientation 2 – FF unstable, SF stable, TW unstable.*
4. $\Lambda < 0, \mathbf{M} < 0$ *Orientation 2 – FF stable, SF unstable, TW stable.*

Proof. The stability of the fronts follows from corollary 2.17. The stability of the trigger waves follows from Theorem 8 and lemma 3.18. The stability of the triggers waves is determined in a similar fashion. From Lemma 3.18 we know that their stability depends on the following ratio:

$$\Lambda_t = \frac{Q_{(-\infty,p)}\Psi_{(\infty,p)}}{\mathbf{M}}. \tag{5.53}$$

From Lemma 3.19 we know that the sign of $Q_{(-\infty,p)}\Psi_{(\infty,p)}$ is opposite of Λ in the case of orientation 1 and the same as Λ in the case of orientation 2. Therefore if $\Lambda > 0$ and $\mathcal{M} > 0$, $\Lambda_t < 0$ and the trigger waves are unstable. We use the same reasoning to determine the other three cases. ∎

The question is whether or not all four diagrams are possible. It turns out that only two of the above four are possible. To prove this we need the following theorem from [30]. This theorem restricts the types of wave trains that can bifurcate from the curve of pulses for values of Λ and $\mathcal{M}$.

Theorem 9 (Sandstede and Scheel [30] Theorem 4.1)**.** *Given the system (5.23) with the hypotheses assumed for Theorem 6. Then there are positive constants C, δ and L_* with the following property. Let $L > L_*$, then system (5.23) has a periodic solution $p_L(x)$ with period $2L$ at $c = c^*$ such that*

$$\sup_{|x|\leq L} |p_L(\xi) - \mathbf{q}(\xi)| < \delta, \qquad |c - c^*| < \delta \tag{5.54}$$

if and only if

$$\langle \Psi(L), \mathbf{q}(-L)\rangle - \langle \Psi(-L), \mathbf{q}(L)\rangle - \hat{c}\int_{-\infty}^{\infty} \langle \Psi(\xi), D_c f(q,0)\rangle \, d\xi + R(c) = 0. \tag{5.55}$$

The remainder term $R(c)$ is such that $R(c) \leq C(e^{-\alpha L} + |c|)(|c| + e^{-2\alpha L})$.

This allows us to show the relationship between the stability of the trigger waves and that of the fronts.

Lemma 4.21. *There exists a solution $\tilde{\mathbf{q}}(x)$ of the linearized system (5.23) so that:*

$$|\mathbf{q}(t) - \tilde{\mathbf{q}}(t)| \leq o(|\tilde{\mathbf{q}}(t)|) \tag{5.56}$$

as $t \to -\infty$.

Proof. The proof is a straight forward application of theorem 10.13.2 of [33]. ∎

Lemma 4.22. *Of the four possible stability situation listed above in Corollary 4.20, only (1) and (4) are possible.*

Proof. We assumed the condition $\int_{-\infty}^{\infty} \langle \psi(x), D_c f(q,0)\rangle \, d\xi = \mathcal{M} \neq 0$ in hypothesis 1.4. Then we can use (5.55) to solve for $\hat{c}$ in terms of the period of the periodic:

$$\hat{c} = \frac{< \Psi(L), \mathbf{q}(-L) > - < \Psi(-L), \mathbf{q}(L) >}{\int_{-\infty}^{\infty} < \psi(\xi), D_c f(q,0) > d\xi} + R_2(c). \tag{5.57}$$

We have seen previously that $\Psi(\xi)$ decreases in a strong exponential fashion as $\xi \to -\infty$ and $\mathbf{q}(\xi)$ decreases similarly as $\xi \to \infty$. Therefore the term $\langle \Psi(-L), \mathbf{q}(L) \rangle$ goes to zero for L sufficiently large. We also know about the decay of $\Psi(\xi)$ and $\mathbf{q}(\xi)$ as $\xi \to \infty$ and $\xi \to -\infty$ respectively. From out results Lemmas 2.13, both decay more slowly in these directions. Therefore $\hat{c}$ is determined by the $\langle \Psi(L), \mathbf{q}(-L) \rangle$ term.

$$\text{sign}(\hat{c}) = \text{sign}\left(\frac{\langle \Psi(L), \mathbf{q}(-L) \rangle}{\int_{-\infty}^{\infty} \langle \Psi(\xi), D_c f(q,0) \rangle \, d\xi}. \right) \tag{5.58}$$

From lemmas 2.13 and 4.21, we have that for large L:

$$\text{sign}(\langle \Psi(L), \mathbf{q}(-L) \rangle) = \text{sign}(\Psi_{(\infty,p)} Q_{(-\infty,p)}) = \text{sign}(\Lambda). \tag{5.59}$$

The denominator of (5.58) is simply $\mathbf{M}$. Therefore we have that:

$$\text{sign}(\hat{c}) = \text{sign}\left(\frac{\Lambda}{\mathbf{M}} \right) \tag{5.60}$$

Now look at the diagrams corresponding to orientation 1 and orientation 2. In orientation 1 the trigger waves lie above the curve of pulses with respect to c, therefore $\hat{c}$ must be bigger than zero. Conversely, in orientation 2 the trigger waves lie below the curve of pulses and therefore $\hat{c} < 0$. Now consider the 4 stability cases in Corollary 4.20. The ratio $\Lambda/\mathcal{M} > 0$ for case (1) of Corollary 4.20 and negative for case (2). However, we know that $\hat{c} > 0$ for orientation 1. Therefore the stability diagram corresponding to case (2) is not possible. Similarly, for orientation 2, only case (4) is possible because $\hat{c} < 0$ here. ∎

5.5 Algebraic pulses and nearby phase waves

We now conclude the proof of Theorem 5. The algebraic pulses are limits of fronts in L^∞ in both bifurcation diagrams. Continuity of the point spectrum, Lemma 1.3, implies that in the weighted space $L^2_\eta(\mathbb{R}^N)$ the point spectrum of the algebraic pulses is the limit of point spectra of the fronts in a neighborhood of the origin. It therefore consists of precisely one eigenvalue, $\lambda \leq 0$ in the case of orientation 2, and $\lambda \geq 0$ in the case of orientation 2. However, as in the case of the slow and fast fronts, $\lambda = 0$ cannot be an eigenvalue in L^2_η, since the algebraic pulse is not exponentially decaying at $\xi = +\infty$.

This shows that the stability of the algebraic pulses follows that of the nearby fronts; that is, they are WS for orientation 2 and unstable for orientation 1.

Next, we consider the phase waves that border the algebraic pulses. Their stability can also be determined since their spectrum is closely related to the algebraic pulses, as was demonstrated by Gardner [34]. We restate this result in terms of our particular situation.

Theorem 10 (Gardner 1997, Theorem 1.2)**.** *Let q^{p} be a particular algebraic pulse. Let $\mathcal{K}$ be a simple closed curve disjoint from the spectrum of q^{p} and let m be the multiplicity of eigenvalues of q^{p} interior to $\mathcal{K}$. Then there exists a a wave length $L_0 >$ such that for phase waves of wave length $L > L_0$, the curve $\mathcal{K}$ encloses exactly m γ-eigenvalues of the phase wave for each γ on the unit circle of the complex plane.*

Lemma 5.23. *There is $L_0 > 0$ such that for all $L > L_0$, the spectrum of a phase wave in L^2_η near a fixed algebraic pulse with wavelength L consists precisely of a circle of essential spectrum in $\operatorname{Re}\lambda \geq -\delta$. The circle converges to the eigenvalue of the algebraic pulse as $L \to \infty$.*

Proof. This a direct consequence of Theorem 10. It is not difficult to see that the linearization at phase waves is invertible whenever the linearization at the algebraic pulse is invertible. So the stability of the phase waves (like the algebraic pulses) is determined by the point spectrum near the origin. By Theorem 10 this point spectrum must lie to the left or right of the imaginary as the single eigenvalue of the algebraic pulse. ∎

This concludes the proof of our main result Theorem 5.

5.6 Stability diagrams for other nonlinearities

While we will not discuss the details here, similar stability results hold when the saddle-node assumptions are replaced by a transcritical bifurcation. The argument is analogous to our main result in every aspect. We give the stability diagram for the transcritical case in the figure 5.6. Notice that the trends of the saddle-node bifurcation are continued

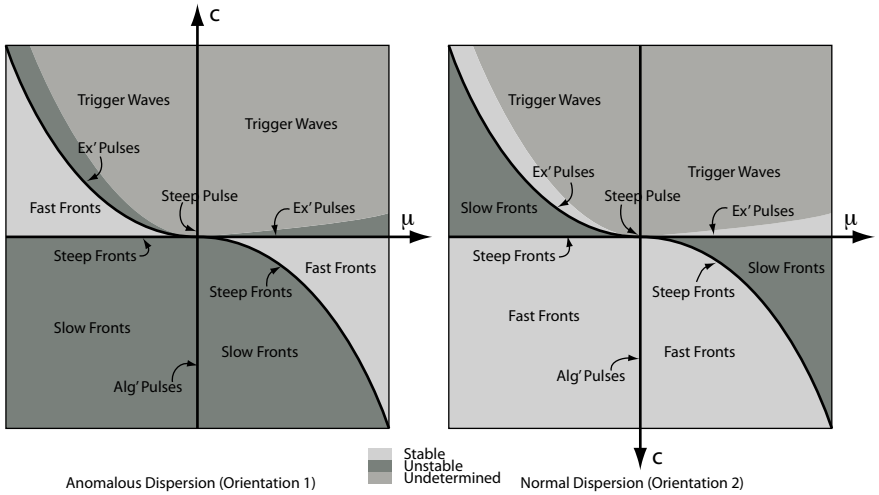

with a transcritical bifurcation: there are two possible diagrams, the fast fronts are always stable and the fast trigger waves are unstable.

Chapter 6

A numerical study of a FitzHugh-Nagumo like system.

We would like to illustrate the behaviors found in Theorem 5 in a more interesting system than the scalar equation we considered above. The Fitzhugh-Nagumo [35] equations are often considered as a simplification of the Hodgkin-Huxley [36] equations that were derived to model excitation in the squid axon. Indeed, one of the original motivating notions for the present research was an insight into locally connected networks of excitable units like neurons. We therefore investigate a modified FitzHugh-Nagumo type system of equations where a transcritical bifurcation has been introduced.

6.1 Bär's equations

The system of equations considered by Bär et. al. in [37] originally were derived to model pattern formation during CO oxidation on a Pt surface (the well known catalyzed reaction that takes place in your car's catalytic converter.) These equations modify the slow inhibitory kinetics of the equations of Barkley [38], which in turn are a numerically friendly variation of the FitzHugh-Nagumo equations. Bär's equations are as follows:

$$\begin{aligned} u_t &= \frac{1}{\epsilon}u(u-1)(u-\frac{b+v}{a}) + u_{xx} \\ v_t &= \epsilon(f(u)-v). \end{aligned} \tag{6.1}$$

The function $f(u)$ is defined as follows:

$$f(u) = \begin{cases} 0, & 0 \leq u < 1/3 \\ 1 - 6.75u(u-1)^2, & 1/3 \leq u < 1 \\ 1, & 1 < u. \end{cases} \tag{6.2}$$

Bär's equations reduce to Barkley's if we let $f(u) = u$.

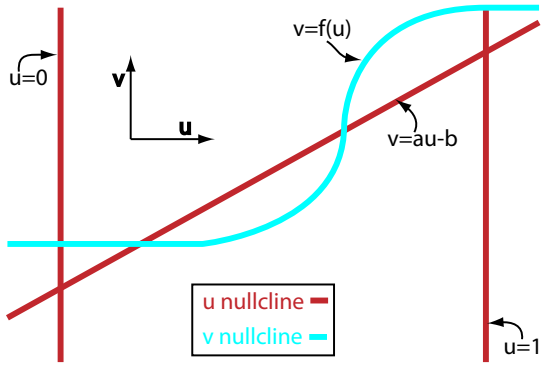

Figure 6.1: The u and v nullclines of the OKB equations.

.

When we consider (6.1) in the comoving frame we have the resulting system of ODEs:

$$\begin{aligned} u' &= w; \\ w' &= -cw + \frac{1}{\epsilon}u(u-1)(u - \frac{b+v}{a}); \\ v' &= \frac{1}{c}(v - f(u)). \end{aligned} \tag{6.3}$$

This system has three equilibria of interest: $(0,0,0)$, $(b/a,0,0)$ and the equilibrium at the intersection of $f(u)$ and $au - b$. The essential observation is that by changing b we shift the $v = au - b$ nullcline, making $(0,0,0)$ a transcritical bifurcating equilibrium for $b = 0$.

Seeing that there is a transcritical bifurcation is easy since the center manifold can be calculated in the same straight forward as the scalar example. The linearization of

(6.3) is the following:

$$\begin{pmatrix} 0 & 1 & 0 \\ \frac{b}{\epsilon a} & -c & 0 \\ 0 & 0 & \frac{1}{c}. \end{pmatrix} \tag{6.4}$$

A cursory inspection of (6.4) shows that for $b = 0$ the v direction is unstable, the stable eigenspace is in the $u - w$ plane, and the center manifold is tangent to the u axis. Hence a returning homoclinic must be tangent to the $u - w$ plane. With this in mind we can calculate the center manifold easily:

$$u' = w = -\frac{1}{c}u^2 + \text{HOT}. \tag{6.5}$$

One should notice that the sign of the first term in the center manifold expansion has a negative coefficient, which is the opposite of the first term in the scalar example. This allows us to "guess" at the orientation of system (6.3) in terms of the conditions of Theorem 5. In fact, the strong stable eigenspace angles away from the unstable center direction as c increases. If we refer to figure 5.3 we see that this would indicate orientation-1 (recall that the scalar example was orientation-2.) Therefore we would guess that for $b = 0$ the trigger waves are unstable and the system is *anomalously dispersive* (see the next paragraph.) However, we do not know the behavior of the homoclinic orbit globally, and this local analysis only gives us a guess at the orientation; the homoclinic orbit could move faster than the strong stable eigenspace which would put the system in orientation-2.

6.2 Orientation, dispersion and inclination flips

We now wish to introduce some of the standard notions used to describe the stability of wave trains when viewed the concatenation of pulses, whose tails decay faster than their fronts. As is seen in the paper by Gardner [34] and elaborated by Sandstede and Scheel [30], wave trains are only stable with respect to perturbation if they are *repelling*. That is, when we consider the wave train as a concatenation of pulses, two such pulses should repel each other. Similarly, unstable wave trains are *attracting*. These notions are also described by *normal dispersion* when one is talking of stable wave trains and *anomalous dispersion* when one is referring to unstable wave trains.

The key observation in [2] (for our purposes at least) is that the equations 6.1 demonstrate both normal and anomalous dispersion for different values of ϵ. We believe that these different regimes can be interpreted in terms of our Theorem 5 and that the stability depends on whether the system is in orientation 1 or 2. In their paper, Or-Guil et. al. [2] hypothesize that change from normal to anomalous dispersion results from a change of dominance between the two stable eigenvectors of the equilibrium $(0, 0, 0)$. Using this change of dominance as an explanation for the change in stability is in accordance with our results if one recalls that Theorem 5 depends on the inner product of the asymptotic limit of the steep pulse at ∞ and that of the adjoint solution at $-\infty$.

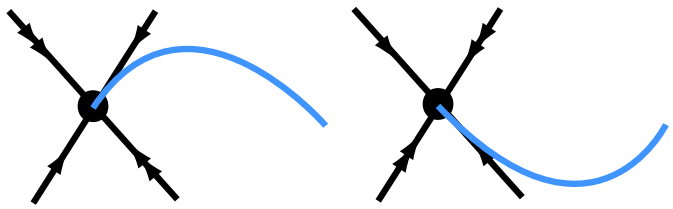

Figure 6.2: A change in dominance in the stable eigenspaces can change the asymptotics of the heteroclinic at ∞ substantially.

Unfortunately, ease of calculation in (6.1) ends with the center manifold. However, we can verify a number of the conditions for Theorem 5 numerical in a fairly convincing fashion. We used primarily the software MATCONT [39] to find and following homoclinic and periodic solutions to (6.3.) The steep pulse was found in a fairly convincing fashion for $b = 0$, $a = .84$, $\epsilon = .02$ and $c = .52$; see figure 6.3. A log-linear plot revealed that the front of the pulse has strong exponential decay while the back has a distinctly weak algebraic decay. We will take the spectral assumptions on the pulse for granted since there is a long history of studying the stability of FitzHugh-Nagumo pulses. Moreover, the existence (and hence stability) has been verified numerically [2].

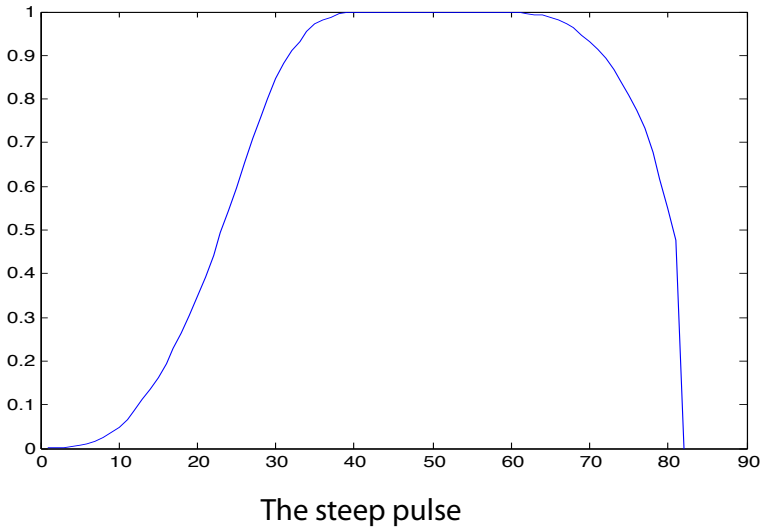

Figure 6.3: The steep pulse found numerically for $\epsilon = .02$, $a = .84$ and $b = 0$.

Or-Guil et. al. [2] report that the equations (6.1) exhibit normal or anomalous dispersive behavior depending on the choice of parameters. Specifically for $a = .84, b = .07$ and $\epsilon < .69$ the wave trains were attracting (normal dispersion), and for $\epsilon > .69$ the wave trains were repulsing (anomalous dispersion.) According to our theorem, we would predict that in the normal regime the trigger waves are slower than the pulses and the wave speed should increase with period as the periodic solutions (that correspond to the trigger waves) limit on the homoclinics (that correspond to the pulses.) Since the triggers waves are faster than the pulse in the anomalous regime, we would expect that wave speed should increase with period. This is in fact what was found numerically, as can be seen in figure 6.4.

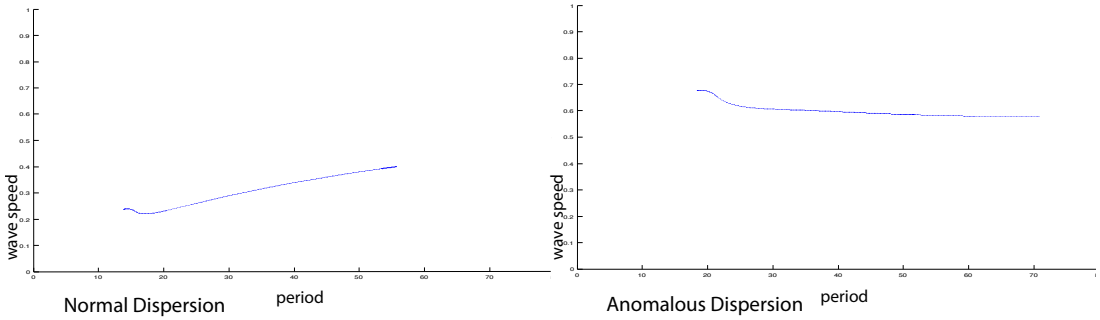

Figure 6.4: The figure to the left shows the dispersion curve under parameters $a = .84, b = .07, \epsilon = .02$ (normal dispersion). The figure to the right shows the dispersion curve under parameters $a = .84, b = .07, \epsilon = .11$ (anomalous dispersion.)

Chapter 7

Conclusion

We have presented a bifurcation and stability analysis for coherent structures at the boundary between excitable and oscillatory media. We argue that the simplest transition between the two types of media is organized around the steep pulse, which, in the traveling-wave ODE corresponds to an orbit-flip homoclinic to a saddle-node equilibrium. This study has produced a number of interesting results which we summarize below.

7.1 Discussion of the results

The excitation pulses could be continued as steep fronts after a saddle-node at a steep pulse, but without exchanging stability. The exchange of stability only happens in terms of the essential spectrum on $L^2(\mathbb{R}^N)$ and this instability can be shown to be transient when considered on appropriate exponentially weighted spaces.

It is important to consider in what sense the steep pulse, steep fronts and fast fronts are stable when we restrict to a weighted space. In most senses this sort of stability is sufficient since all compact perturbations are included. To fully interpret this kind of stability, we should ask ourselves what perturbations we are disallowing by restricting to the weighted space. In the exponentially weighted space we only consider perturbations that decay sufficiently in forward "space". Of course, the difference between any two fast fronts (or slow fronts for that matter) decays weakly in forward space and is therefore not in the weighted space. Thus by considering perturbations on weighted spaces we

are simply disallowing unbounded perturbations which are the difference of the fronts. Therefore the instability is truly "transient" in the sense of [13]

The trigger waves are only stable when they are slower than the excitation pulses. We can understand this through the following intuitive argument. Let wave A be followed by wave B on finite periodic boundary conditions. If B gets close to A, the tail of A effectively decreases the decay of the front of B. In orientation 1, this weaker decay causes the wave to move faster and hence closer to wave A; the waves are attracting and therefore unstable. In orientation 2, weaker decay means a slower wave and therefore they are repelling and stable.

The nearby trigger waves and phase waves share stability. Unfortunately we were not able to extend our stability result for a neighborhood of the steep pulse

Fast fronts are always stable, and slow fronts are always unstable. This is a consequence of the rather surprising observation that only two stability diagrams are possible. This adds evidence for the conjecture of van Saarloos ([15]) which states that only the fronts faster than the steep front will be stable. He states this conjecture in terms of "steep " and "pushed" fronts. As we saw from the previous spectral analysis, the fronts we consider connect a spectrally unstable equilibrium with a spectrally stable equilibrium. The linear instability of the unstable equilibrium dictates a linear propagation speed in terms of the spread of small perturbations referred to as the "linear spreading speed." Saarloos argues that nonlinear effects can only push the speed of a front beyond the linear spreading speed. His argument is easy and intuitive: if we imagine a front traveling at a speed less than the linear spreading speed, a small perturbation at the edge of the front will move at the faster linear spreading speed forcing the front to this faster speed. While this reasoning seems sound, there is no mathematical proof of this effect in general. Fronts that move at the linear spreading speed are called "pulled." Fronts that move faster than the linear spreading speed are called "pushed" since they are pushed by a nonlinear effect.

Using these categories, all of our fronts are "pushed." Saarloos further conjectures on the relation between "steep" pushed fronts (that is fronts that decay in a strong stable manifold) and slower pushed fronts. We refer to fronts that decay in a weaker fashion

than the steep front as "weak" fronts (though Saarloos does not use this terminology.) We may consider weakly decaying fronts as perturbations of the steep front. These

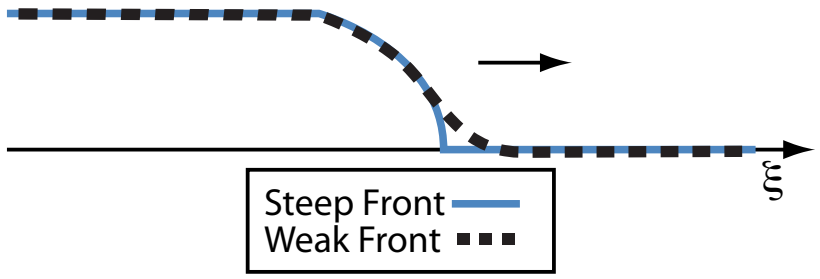

Figure 7.1: The weak front may be seen as a perturbation of the steep front. If the speed of the weak front is slower than the steep front, the steep front will eventually overtake the weak front. If the weak front is faster, then it will never be overtaken by the steep front.

perturbations by themselves only travel at the linear spreading speed which is necessarily less than the speed of the steep front. Therefore if the weak front can hope to stay ahead of the steep front it contains, it must depend on the nonlinearly pushed wave speed of the weak front itself. If the weak front is slower than the steep front, the steep edge will overtake the weak edge. This leads us to the conclusion that only the fronts faster than the steep front will be stable, which of course was what was observed.

7.2 Future Directions

Other nearby coherent structures. While the bifurcation diagram provided by Chow, Lin and Deng is exhaustive for a saddle-node bifurcation of a steep pulse, there are other nearby homoclinics we do not consider but are interesting none the less. Perhaps the most obvious is the "small front," that is the front that connect the equilibria through the bifurcating center manifold. These fronts are always stable and are in fact an example of fronts that travel at the linear spreading speed (or "pulled fronts" in Saarloos' terminology) as described above.

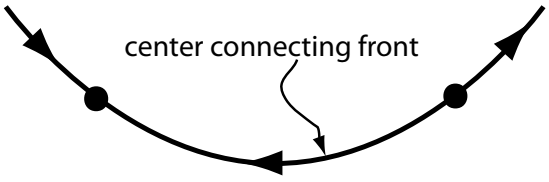

The other interesting group of structures are easily seen in the scalar example. If we continue to make μ increasingly negative, the node eventually becomes complex. We refer to this as the "spiral boundary." Clearly this is another important structure, and whether this is generic beyond the scalar model is an interesting question.

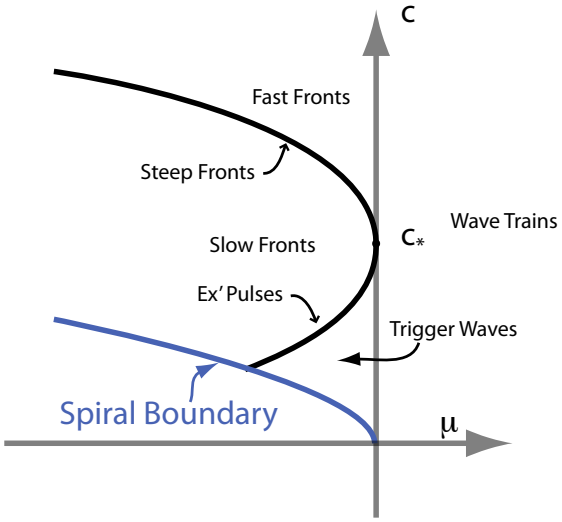

The primary unresolved question in this study is the stability of the trigger waves and phase waves in a full neighborhood of the steep pulse. The shared stability properties of the trigger-waves bordering the excitation pulses and the phase waves bordering the algebraic pulses suggests that the stability of the unknown waves

will follow similarly. This is also predicted by the easily analyzed scalar example. However, there are examples in the literature where phase waves do not share the stability properties of nearby trigger waves [40].

The investigation of other nonlinearities. We believe that the steep front associated with a saddle-node bifurcation is perhaps the most basic type of transition of an excitable regime to an oscillatory regime. However, there are numerous other nonlinearities that populate the literature describing oscillatory and excitable media. The most common case is that of the Hopf-type bifurcation.

The change from normal to anomalous dispersion. Our results give an explicit description of the difference between the normal and anomalously dispersive cases in terms of the orientations of the kernel and adjoint solutions. This explanation is compatible with that given by Or-Guil et. al. [2], where the change from normal to anomalous is attributed to an exchange of dominance in the unstable directions. While the conditions described in our theorem are often difficult to calculate analytically, they can often be reliably verified numerically using AUTO or other bifurcation software. We wonder if this sort of orientation flip in the related system of ODE's is responsible for the dispersion relation in other systems that support wave trains. Additionally, keeping this orientation condition in mind might allow for the construction of other examples that are anomalously dispersive.

References

[1] S.N. Chow and X.B. Lin. Bifurcation of a homoclinic orbit with a saddle-node equilibrium. *Diff. Int. Eqns.*, 3:435–46, 1990.

[2] M. Or-Guil, I.G. Kevrekidis, and M. Br. Stable bound states of pulses in an excitable medium. *Physica D*, 135:154–174, 2000.

[3] J. Moehlis. Canards in a surface oxidation reaction. *J. Nonlinear Sci.*, 12:319–345, 2002.

[4] R. Kollár and A. Scheel. Coherent structures generated by inhomogeneities in oscillatory media. *SIAM J. Appl. Dyn. Syst.*, 6:236–262, 2007.

[5] A. Doelman, B. Sandstede, A. Scheel, and G. Schneider. The dynamics of modulated wave trains. *Memoirs of the AMS, to appear.*

[6] B. Sandstede and A. Scheel. Defects in oscillatory media: toward a classification. *SIAM J. Appl. Dyn. Syst.*, 3:1–68, 2004.

[7] D.M. Rademacher and A. Scheel. Instabilities of wave trains and turing patterns in large domains. *Int. J. Bif. Chaos*, 16:2679–2691, 2007.

[8] D.M. Rademacher and A. Scheel. The saddle-node of nearly homogeneous wave trains in reaction-diffusion systems. *J. Dyn. Diff. Eqns.*, 19:479–496, 2007.

[9] B. Sandstede and A. Scheel. On the stability of periodic travelling waves with large spatial period. *J. Diff. Eqns.*, 172:134–188, 2001.

[10] M.J. ODonovan, A. Bonnot, P. Wenner, and G.Z. Mentis. Calcium imaging of network function in the developing spinal cord. *Cell Calcium*, 37.

[11] B. Kocsis, V. Varga, L. Dahan, and A. Sik. Serotonergic neuron diversity: Identification of raphe neurons with discharges time-locked to the hippocampal theta rhythm. *Proc. Natl. Acad. Sci. U.S.*, 103.

[12] G.B. Ermentrout and J. Rinzel. Waves in a simple excitable or oscillatory reaction-diffusion model. *J. Math. Biology*, 11:269–294, 1981.

[13] B. Sandstede and A. Scheel. Absolute and convective instabilities of waves on unbounded and large bounded domains. *Physica D*, 145:233–277, 2000.

[14] B. Deng. Homoclinic bifurcations with nonhyperbolic equilbria. *SIAM Journal on Mathematical Analysis*, 21:693–720, 1990.

[15] W. van Saarloos. Front propagation into unstable states. *Phys. Rep.*, 386:29–222, 2003.

[16] T. Kato. *Perturbation theory for linear operators*. Springer, 1976.

[17] D. Henry. *Geometric theory of semilinear parabolic equations*. Springer, 1981.

[18] A. Vanderbauwhede. Centre manifolds, normal forms and elementary bifurcation. *Dynamics Reported*, 2:89–169, 1989.

[19] N. Fenichel. Geometric singular perturbation theory for ordinary differential equations. *J. Diff. Eqns.*, 3:53–98, 1979.

[20] C.K.R.T. Jones. Geometric singular perturbation theory. In Johnson R, editor, *Dynamical Systems*, volume 1609, pages 44–120. Springer-Verlag, Berlin, 1995.

[21] A. Vanderbauwhede. Bifurcation of. degenerate. homoclinics. *Results Math.*, 21:211–223, 1992.

[22] J. Guckenheimer and P. Holmes. *Nonlinear oscillations, dynamical systems, and bifurcations of vector fields*. Springer-Verlag, 1990.

[23] S. Wiggins. *Global Bifurcations and Chaos: Analytical Methods*. Springer-Verlag New York, 1988.

[24] E.A. Coddington and N. Levinson. *Theory of ordinary differential equations.* McGraw-Hill New York, 1955.

[25] K. Yoshida. *Functional Analysis.* Springer Verlag, 1971.

[26] A. Scheel. Coarsening fronts. *Archive for Rational Mechanics and Analysis*, 181:505–534, 2006.

[27] D. Sattinger. Weighted norms for the stability of travelling waves. *Journal of Differential Equations*, 25:130–144, 1977.

[28] J.K. Hale and X.B Lin. Heteroclinic orbits for retarded functional differential equations. *J. Diff. Eq.*, 65:175–202, 1986.

[29] A. Scheel. Radially symmetric patterns of reaction-diffusion systems. *Mem. Amer. Math. Soc.*, 165:1–80, 2003.

[30] B. Sandstede and A. Scheel. On the stability of periodic travelling waves with large spatial period. *J. Diff. Eqns.*, 172:134–188, 2001.

[31] A. Lunardi. *Analytic Semigroups and Optimal Regularity in Parabolic Problems.* Birkhauser, 1995.

[32] K.J. Palmer. Transversal homoclinic points. *J. Diff Eqn.*, 55:225–256, 1984.

[33] P. Hartman. *Ordinary Differential Equations.* John Wiley and Sons Inc., 1964.

[34] R.A. Gardner. Spectral analysis of long wavelength periodic waves and applications. *J. Reine Angew. Math.*, 491:149–181, 1997.

[35] R. FitzHugh. Impulses and physiological states in theoretical models of nerve membrane. *Biophysical J.*, 1:445–466, 1962.

[36] A. Hodgkin and A. Huxley. A quantitative description of membrane current and its applications to conduction and excitation in nerve. *J. Physiol.*, 117:500–544, 1952.

[37] M. Bar, N. Gottschalk, M. Elswirth, and G. Ertl. Spiral waves ina surface reaction: Model calculations. *J. Chem. Phys.*, 100:1202–1215, 1994.

[38] D. Barkley. A model for fast computer simulation of waves in excitable media. *Physica D*, 49:61–70, 1991.

[39] M. Friedman, W. Govaerts, Yu.A. Kuznetsov, and B. Sautois. Continuation of homoclinic orbits in matlab. *Computational Science*, 3514:263–270, 2005.

[40] G. Bordiougov and H. Engel. From trigger to phase waves and back again. *Physica D*, 215:25–37, 2006.